

POLITECNICO DI TORINO

II Facoltà di Ingegneria

Corso di Laurea Magistrale in Ingegneria Energetica e Nucleare

Tesi di Laurea Magistrale

**A Power-to-Gas Case Study using High-Temperature  
Co-Electrolysis in California**



**Relatore:**

Prof. Massimo Santarelli

**Candidato:**

Rocco Castaldi

**Correlatore:**

Dott. Max Wei

© 2018

Rocco Castaldi

ALL RIGHTS RESERVED

# Abstract

Electrical energy storage is projected to be a critical component of the future California energy system, performing load-leveling operations to enable increased penetration of renewable and distributed generation. Currently the direct storage of electricity produced by wind turbines and solar photovoltaics is very challenging at the necessary scale, and a more promising approach seems to be energy storage in the form of chemicals. This research aims to investigate the potential of power-to-gas systems featuring high temperature co-electrolysis with subsequent syngas methanation. The first part focuses on the configuration and performances, while the second one on the costs for an economic assessment. Particular attention was paid to “integrated plant-design” considerations to ensure the lowest possible construction impact, trying to combine renewable energy and carbon dioxide sources, transmission lines, and natural gas supply infrastructure. A pilot power plant of 1 MWel-DC was taken as electricity input for the SOEC generator, based on real demonstration projects with methane output. The plant utilization factor was set to 20% by applying a forward-looking algorithm to the net load provided by the California Independent System Operator (CAISO). Thermal integration based on pinch analysis methodology was performed to determine the minimum external energy requirement. With these conditions, the electricity to SNG efficiency (LHV-based) was found to be greater than 80%. To evaluate the levelized cost of production, capital and operating costs were assessed following guidelines from the National Energy Technology Laboratory (1) (2) and the International Energy Agency GHG program (3) (4). A range of \$38.6 - \$54.9 per MBTU was calculated (2018 industrial and residential NG market prices in California are \$7.2 - \$12.8 per MBTU). Based on scenarios for in-state electricity generation, SNG production was compared with the total, industrial and residential future demand.

## Abstract (Italiano)

Lo stoccaggio di energia elettrica rappresenterà uno dei componenti critici per il futuro sistema energetico della California, eseguendo operazioni di livellamento del carico per consentire una maggiore penetrazione e generazione distribuita delle energie rinnovabili. Attualmente lo stoccaggio diretto di elettricità prodotta da turbine eoliche e solare fotovoltaico è molto impegnativo, e un approccio più promettente sembra essere lo stoccaggio sotto forma di energia chimica. Questa ricerca mira ad analizzare il potenziale dei sistemi power-to-gas caratterizzati da co-elettrolisi ad alta temperatura con successiva metanazione di syngas. La prima parte si concentra sulla configurazione e sulle prestazioni, mentre la seconda sui costi per una valutazione economica. Particolare attenzione è stata dedicata alla “progettazione integrata” dell’impianto, al fine garantire il minor impatto possibile sulla costruzione, cercando di combinare fonti di energia rinnovabile e anidride carbonica, linee di trasmissione e infrastrutture per la fornitura di gas naturale. Una potenza dimostrativa di 1 MWel-DC è stata presa come input elettrico per il generatore SOEC, sulla base di simili progetti esistenti per produzione di metano. Il fattore di utilizzazione dell’impianto è stato impostato al 20% dopo aver applicato un algoritmo previsionale al carico netto fornito dal California Independent System Operator (CAISO). È stata eseguita un’integrazione termica basata sulla metodologia di pinch analisi per determinare il minimo fabbisogno energetico esterno. Con queste condizioni, l’efficienza complessiva (basata sul PCI) è risultata superiore all’80%. Per valutare il costo di produzione livellato, i costi di capitale e i costi operativi sono stati analizzati seguendo le linee guida del National Energy Technology Laboratory (1) (2) e dell’International Energy Agency GHG program (3) (4). È stato calcolato un range di \$ 38,6 - \$ 54,9 per MBTU (i prezzi di mercato relativi al 2018 per NG industriale e residenziale in California sono \$ 7,2 - \$ 12,8 per MBTU). Infine, basandosi su scenari per la generazione di elettricità nello stato, la produzione di SNG è stata confrontata con la futura domanda totale, industriale e residenziale.

# Acknowledgments

First of all, I want to thank my parents Catia and Pierpaolo, to always sustain me during these five years, giving me a strong support in times of need and without which I would have no reached this important goal.

A dutiful thanks to Professor Massimo Santarelli and Max Wei, which gave me the possibility to elaborate my thesis in California at Lawrence Berkeley National Laboratory.

Finally, I would like to thank all those who have participated directly or indirectly to my university experience in Turin. I especially thank my classmates and my friends Alessandro, Edoardo, Fabio and Luca with whom I shared unbelievable moments.

Rocco Castaldi



*Figure 1 Sustainable Energy Systems Group, Lawrence Berkeley National Laboratory, California 2018*

# Index

Abstract .....	3
Abstract (Italiano) .....	4
Acknowledgments.....	5
List of Tables .....	8
List of Figures .....	10
1. Introduction.....	12
2. Synthetic hydrocarbons storage of RES .....	15
3. Solid Oxide Electrolyser Cell (SOEC): a brief technological review .....	20
3.1 Working principles and fundamental equations.....	21
3.2 Materials, components and configuration .....	24
3.3 Fabrication and scale-up.....	27
3.4 Performance degradations .....	28
4. Plant modeling.....	29
4.1 Utilization factor.....	34
4.2 Plant configuration .....	35
4.3 Model output .....	40
4.4 Thermal integration and energy performance .....	43
4.5 Economic analysis: evaluation of the capital cost.....	49
4.5.1 SOEC (stack, added systems, installation).....	55
4.5.2 Methanation line .....	57
4.5.3 Heat exchangers networks (HEN).....	58
4.5.4 Water pump.....	59
4.5.5 Zinc oxide guard bed.....	60
4.5.6 Compressors.....	60
4.5.7 Additional costs.....	62
4.5.8 Results – CAPEX.....	64
4.6 Economic analysis: evaluation of the operational cost .....	65
4.6.1 Fixed operating and maintenance costs .....	65
4.6.2 Variable operating and maintenance costs .....	66
4.6.3 Results – OPEX .....	69
4.7 Levelized cost of product .....	70

5. Power to SNG in California.....	75
5.1 In-state natural gas demand.....	75
6.2 California curtailments and RES penetration.....	76
5.3 Exploitation of oversupply for SNG generation.....	78
6. Conclusions.....	82
References.....	83

# List of Tables

Table 1 GHG emission targets set by AB 32 and Executive Order S-3-05.....	14
Table 2 Screening of grid storage technologies and technical attributes [Lenher et Al. 2014] .....	16
Table 3 Cement industries with relative CO <sub>2</sub> emissions in the area .....	32
Table 4 California prescriptions for natural gas feeding into distribution pipelines .....	36
Table 5 Plants modeling main assumptions .....	39
Table 6 Assumptions for isentropic and electro-mechanical efficiencies.....	39
Table 7 Gas composition at some key points.....	41
Table 8 Plant parameters.....	42
Table 9 Co-electrolysis + methanation: streams involved in pinch analysis. ....	43
Table 10 Pinch analysis main results .....	46
Table 11 Components DC power demand .....	47
Table 12 Plant results in terms of power input (electric) and output (chemical).....	48
Table 13 AACE Guidelines for Process Contingency .....	51
Table 14 TASC/TOC Factors. Investor Owned Utility (IOU) and Independent Power Producer (IPP) .....	52
Table 15 Main economic assumptions. Financing distribution between debt and equity and their interest rate for high risk investor owned utility projects. Distribution of total overnight capital over capital expenditure period for natural gas plant case (1) .....	54
Table 16 Main assumption for EPCC, TPC and TOC capital cost levels. For scenarios that adhere to the economic assumptions the multipliers 1.078 can be used to translate TOC to TASC to account for the impact of both escalation and interest during construction (1). ....	54
Table 17 Direct system cost with corporate markup and installation (32) .....	56
Table 18 Main constants and assumptions used for capital cost estimation for methanation line ....	57
Table 19 Main constants and assumptions used for capital cost estimation for methanation line ....	59
Table 20 Main constants and assumptions used for capital cost estimation for zinc oxide guard bed .....	60
Table 21 Main constants and assumptions used for capital cost estimation for CO <sub>2</sub> compressor.....	61
Table 22 Main constants and assumptions used for capital cost estimation for SNG compressor #1 .....	61
Table 23 Main constants and assumptions used for capital cost estimation for N <sub>2</sub> compressor #1...61	61
Table 24 Main constants and assumptions used for capital cost estimation for N <sub>2</sub> compressor #2...62	62
Table 25 Main constants and assumptions used for capital cost estimation for SNG compressor #2 .....	62
Table 26 Main constants and assumptions used for capital cost estimation for plant control system .....	62
Table 27 Main constants and assumptions used for capital cost estimation for additional costs for building and structures .....	63
Table 28 Main constants and assumptions used for capital cost estimation for land purchasing.....	63
Table 29 Main results of the economic analysis, CAPEX [SOEC total system cost 1058 \$/kW] ....	64
Table 30 Main constants and assumptions used for operational costs estimation for fixed costs .....	66
Table 31 Main constants and assumptions used for operational costs estimation for variable costs .....	68

Table 32 Main results of the economic analysis, OPEX..... 69  
Table 33 Main assumptions for scenario in 2050 ..... 79  
Table 34 Main output for scenario in 2050..... 79

# List of Figures

Figure 1 Sustainable Energy Systems Group, Lawrence Berkeley National Laboratory, California 2018.....	5
Figure 2 2017 Total System Electric Generation [data from <a href="http://www.energy.ca.gov/almanac/electricity_data/total_system_power.html">http://www.energy.ca.gov/almanac/electricity_data/total_system_power.html</a> ].....	13
Figure 3 Pie Chart, 2017 California Total System Electric Generation [data from <a href="http://www.energy.ca.gov/almanac/electricity_data/total_system_power.html">http://www.energy.ca.gov/almanac/electricity_data/total_system_power.html</a> ].....	13
Figure 4 Power to Gas Pathways (P2G) [Teaching Material, Polytechnic of Turin, Polygeneration and Advanced Energy Systems, 2017] .....	15
Figure 5 Ragone Plot-Energy Storage Technologies [ITM POWER 2014].....	17
Figure 6 General path for syngas production from high temperature electrolysis [Teaching Material, Polytechnic of Turin, Polygeneration and Advanced Energy Systems,2017] .....	17
Figure 7 CO <sub>2</sub> carbon capture sources for co-electrolysis.....	18
Figure 8 Syngas utilization pathways .....	19
Figure 9 Co-Electrolysis with SOEC [Menon et Al. 2015] .....	21
Figure 10 Flat plate (planar) solid oxide cell stack.....	26
Figure 11 Cement Plant with post-combustion CO <sub>2</sub> Capture (15).....	30
Figure 12 Cement plant without CO <sub>2</sub> Capture (15).....	30
Figure 13 Lehigh Hanson Southwest cement plant (Tehachapi), NG substations, transmission lines (16) (17) .....	31
Figure 14 Maps of the selected Area, visible Alta Wind Energy Center and Solar Star 1&2 (16) (17) .....	31
Figure 15 Maps of the selected Area - California.....	32
Figure 16 Cement industries in the area.....	33
Figure 17 Duck Curve, March 31, 2014,2021,2025,2030 .....	34
Figure 18 Model part 1.....	36
Figure 19 Model part 2.....	37
Figure 20 Model part 3.....	38
Figure 21 Model general overview .....	39
Figure 22 Results model part 1 .....	40
Figure 23 Results model part 2 .....	40
Figure 24 Results model part 3 .....	40
Figure 25 Gas composition at some key points .....	41
Figure 26 Range targets for Delta T <sub>min</sub> .....	44
Figure 27 Composite Curves.....	44
Figure 28 Grand composite curve.....	45
Figure 29 Thermal integration - external requirements .....	46
Figure 30 Capital Cost Levels and their Elements.....	49
Figure 31 a) Total direct costs (not including markup and installation costs) for systems as a function of system size and manufacturing volume (10,50,100,250 kWel), b), c) and d)	

Dependence of direct cost components as function of annual manufacturing volume for 10-kWe, 50-kWe, and 100-kWe system sizes. (32).....	55
Figure 32 Recommended HEN designs relative to the target provided by Aspen Energy Analyzer® .....	58
Figure 33 HEN economically optimized .....	59
Figure 34 Plant costs shared for each category [SOEC total system cost 1058 US\$/kW] .....	64
Figure 35 SOEC total system cost impact on TASC (1MWel Plant) .....	65
Figure 36 CAISO average hourly day-ahead energy market prices [ <a href="https://www.eia.gov/todayinenergy/detail.php?id=32172">https://www.eia.gov/todayinenergy/detail.php?id=32172</a> ] .....	67
Figure 37 CAISO average net electric load [ <a href="https://www.eia.gov/todayinenergy/detail.php?id=32172">https://www.eia.gov/todayinenergy/detail.php?id=32172</a> ] .....	67
Figure 38 Operational costs shared for each category (1MWel Plant, CF=20%).....	70
Figure 39 Levelized cost of product [\$/MBTU] as a function of the price of purchased electricity (for 50.000 SOEC systems/year) and 100 SOEC systems/year) .....	71
Figure 40 Levelized cost of product [\$/kg] as a function of the price of purchased electricity (for 50.000 SOEC systems/year) and 100 SOEC systems/year) .....	71
Figure 41 Cost of product shared for each category (case target SOEC annual manufacturing volume-50.000 systems/yr.).....	72
Figure 42 Cost of product shared for each category (case SOEC annual manufacturing volume-100 systems/yr.) .....	72
Figure 43 Sensitivity Analysis (CF=80%). Levelized cost of product [\$/MBTU] as a function of the price of purchased electricity (for 50.000 SOEC systems/year) and 100 SOEC systems/year) .....	73
Figure 44 Sensitivity Analysis (CF=80%). Levelized cost of product [\$/kg] as a function of the price of purchased electricity (for 50.000 SOEC systems/year) and 100 SOEC systems/year) .....	74
Figure 45 NG volumes delivered to consumers for each sector (2016) [Source: U.S. EIA].....	75
Figure 46 California natural gas consumption per 1997-2016, 1 m <sup>3</sup> = 35.3147 ft <sup>3</sup> [Source: U.S. EIA] .....	75
Figure 47 Curtailment totals by month (2016-2018) [CAISO].....	76
Figure 48 New clean and renewable energy capacity in California [Source: U.S. EIA].....	77
Figure 49 How increasing renewable penetration impacts wholesale electricity costs [Lawrence Berkeley National Laboratory] .....	77
Figure 50 California scenario for future energy generation in 2030 [Wei et Al.] .....	78
Figure 51 CO <sub>2</sub> availability in 2050.....	79
Figure 52 Main results for 2050 scenario, SNG offset of Total demand.....	80
Figure 53 Main results for 2050 scenario, SNG offset of Industrial demand [if all SNG production is dedicated to this sector].....	80
Figure 54 Main results for 2050 scenario, SNG offset of Residential demand [if all SNG production is dedicated to this sector].....	80
Figure 55 Shale gas as share of total dry NG production [Source: U.S. EIA].....	81
Figure 56 Water requirements: shale gas vs SNG .....	81

# 1. Introduction

This Master of Science Thesis has been developed at the [Lawrence Berkeley National Laboratory](#) (LBNL) commonly referred to as Berkeley Lab, under the supervision of Dr. Max Wei, a research scientist in the Energy Analysis and Environmental Impacts Division and Dr. Massimo Santarelli, Professor at Polytechnic of Turin. The Berkeley Lab is a United States national laboratory located in Berkeley, California that conducts scientific research on behalf of the United States Department of Energy. It is managed and operated by the University of California.

During my time at LBNL, I joined the Sustainable Energy Systems Group (SES). Its research activities include: energy, environmental and economic systems models, life-cycle analysis of products, heat resources use, local and regional air pollution, emissions measurements from energy production and manufacturing, transport and fate of pollutants, health risk assessment, and methods of mitigating climate change impacts. This research is also part of a project to support California Energy Commission (CEC) on “Long Term Energy Scenarios for 2050” and aims to provide a technical and economic description of a Power to Gas (PtG) system using Solid Oxide Electrolyzer System (SOEC) for electricity storage into Synthetic Natural Gas (SNG).

The state of California is the most populous in the United States and its energy demand is second only to Texas. Notwithstanding its high energy expenditure and even though it is the leader in many energy-intensive industries, California has the lowest per-capita energy consumption in the country, and the residential use energy demand is lower than that every other state except than Hawaii. Its efforts to increase energy efficiency, together with the application of aggressive policies for the diffusion of alternative clean technologies, has restrained its growth in energy demand. California accounts for an abundant supply of crude oil and is a leader for electricity production from hydroelectric, solar, geothermal and biomass. The transportation sector is critical, since more motor vehicles are registered than in any other state, dominating the energy consumption profile. California leads the United States in agricultural and manufacturing gross domestic product (GDP), and the industrial sector is the state's second-largest energy consumer. The state also accounts for one-fifth of the nation's jet fuel consumption (5).

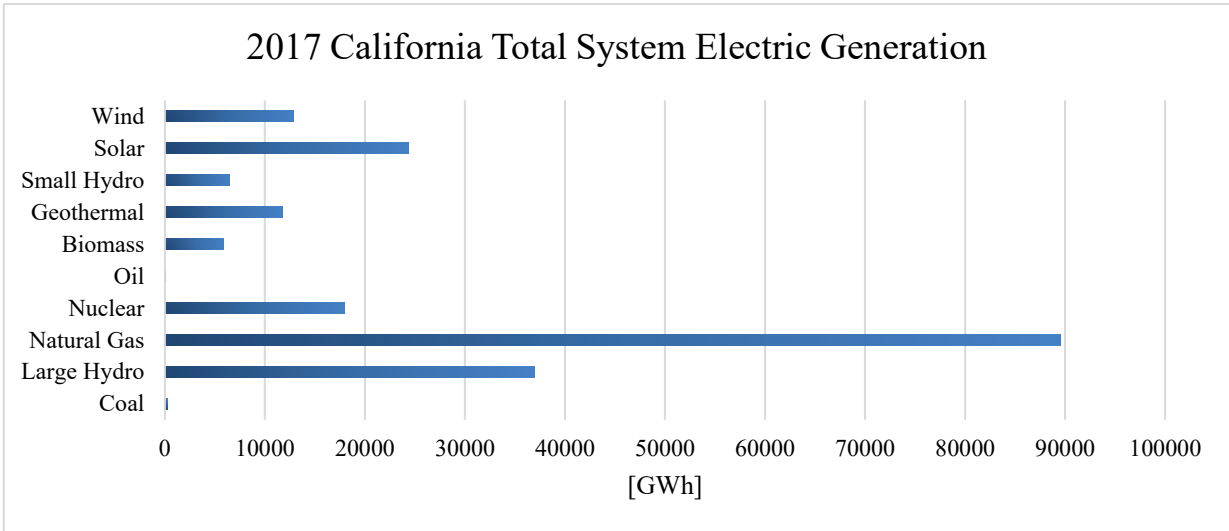


Figure 2 2017 Total System Electric Generation [data from [http://www.energy.ca.gov/almanac/electricity\\_data/total\\_system\\_power.html](http://www.energy.ca.gov/almanac/electricity_data/total_system_power.html)]

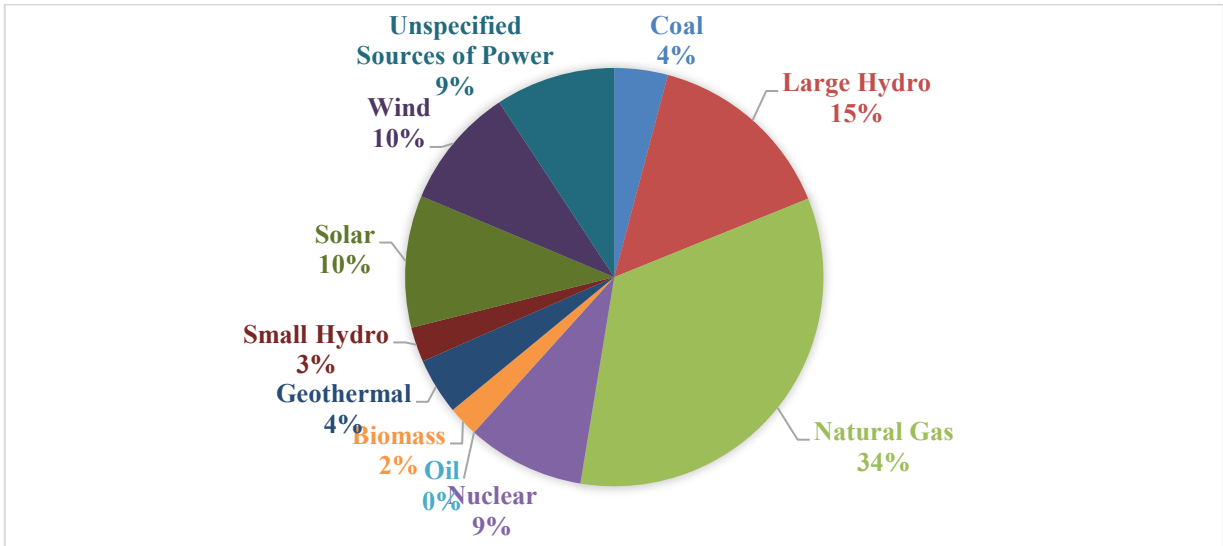


Figure 3 Pie Chart, 2017 California Total System Electric Generation [data from [http://www.energy.ca.gov/almanac/electricity\\_data/total\\_system\\_power.html](http://www.energy.ca.gov/almanac/electricity_data/total_system_power.html)]

As earlier emphasized, California has implemented very aggressive climate policies and regulations, among which the most relevant are:

1. Global Warming Solution Act (2006): known as Assembly Bill 32 (AB 32) sets economy-wide GHG emission targets for 2020 and the Executive Order S-3-05 signed in 2005 by Governor Arnold Schwarzenegger sets GHG emissions goals for 2050 as reported in Tab 1. The California Air Resources Board (CARB), the state agency for air quality preservation, has the authority to enforce the GHG reduction targets (6).

*Table 1 GHG emission targets set by AB 32 and Executive Order S-3-05.*

<b>Year</b>	<b>GHG Emission Target</b>
2020	Equal to 1990 emission level (AB 32)
2030	40% lower than 1990 GHG level (SB 32)
2050	Reduction of 80% compared to 1990 emission level

2. 2030 Senator Bill 32 (SB32) signed into law the Governor Jerry Brown in 2016 expands upon AB 32. SB32 sets a target of 40% reduction in GHG emission from 1990 levels by 2030 as an intermediate target before the 2050 80% goal.

Transportation electrification and cleaner fuels adoption could represent a solution for the emissions reduction. Another path to reduce GHG caused by transportation's sector might be the implementation of hydrogen vehicles. California is investing on this path, but we should to consider the various challenges posted by this technology: hydrogen distribution, storage, fuel cell technology, and costs. Another large contribution to the California's GHG emissions is given by the building energy demand. At present, most of building heating demand is satisfied through natural gas. Regulations that aim attention at improving natural gas heating or conventional internal combustion engine efficiency, without shifting away from fossil fuel, may be suitable for the short term but are not sufficient to meet long-term targets. In addition, the heating electrification will only be an effective measure if the electricity supply has zero GHG intensity (e.g. coming from solar, wind power etc.). As known, California spent great attention for RES. One enormous challenge is how to manage the intermittent nature of solar PV and wind generation, and how balance the energy supply and the end-user demand. The problem of the intermittent behavior of these sources can be solved implementing storage technologies (e.g. flywheels, batteries, super-capacitors), that permit storage of excessive electricity production and to re-use it when required (e.g. during times of peak demand). It is important to emphasize the difficulty to store large amounts of electrical energy, especially for long periods. Thus, alternative storage solutions can play an important role and need investigation. Among the various technological possibilities, chemical energy storage in the form of synthetic hydrocarbon fuels appears very attractive. Although this technique is still not mature, it represents one of the most efficient pathways for long term energy storage, like seasonal and yearly storage. Furthermore, it can be combined easily with heat, electricity and transportation sectors and fuels. Electrolysis units can be utilized to convert excess electricity into chemical energy via electrolysis of steam and/or carbon dioxide.



compressed-air energy storage (CAES) or batteries of any type (see Table 2). Chemical storage of electricity in the form of SNG looks even to be the most attractive technology when considering to long time-scale horizon storages, its versatility and its easy injection in the existing NG grids. Other advantages of PtG with respect to other conversion processes come from an easier plant management, controlling the electrodes potentials, the electrolyzer working temperature, and the modularity. PHS and CAES are strictly dependent on to the geographical landscape, limiting the collocation of these storages to few spots. Below are summarized the main storage technologies in terms of efficiency, capacity and time of discharge:

*Table 2 Screening of grid storage technologies and technical attributes [Lenher et Al. 2014]*

<i>Technology</i>	<i>Round-trip efficiency [%]</i>	<i>Capacity Rating [<math>MW_{el}</math>]</i>	<i>Energy Density [<math>kWh_{el} m^{-3}</math>]</i>	<i>Time Scale</i>
PHS	70-85	1-5000	0.23 for $\Delta h=100m$	Hours-months
Li-Ion Battery Pack	80-90	0.1-50	270	Minutes-days
Lead Acid Battery	70-80	0.05-40	75	Minutes-days
P2G	30-75	0.01-1000	$391^1-1200^2$	Minutes-months
CAES	70-75	50-300	6.9	Hours-months
Vanadium Redox Flow Battery	65-85	0.2-10	35	Hours-months
Sodium Sulfur Battery	75-85	0.05-34	150	Seconds-hours
Nickel Cadmium Battery	65-75	45	150	Minutes-days
Flywheel	85-95	0.1-20	-	Seconds-minutes

<sup>1</sup> Hydrogen storage at  $p=200$  bar and  $\eta_{el}=60\%$

<sup>2</sup> Methane storage at  $p=200$  bar and  $\eta_{el}=60\%$

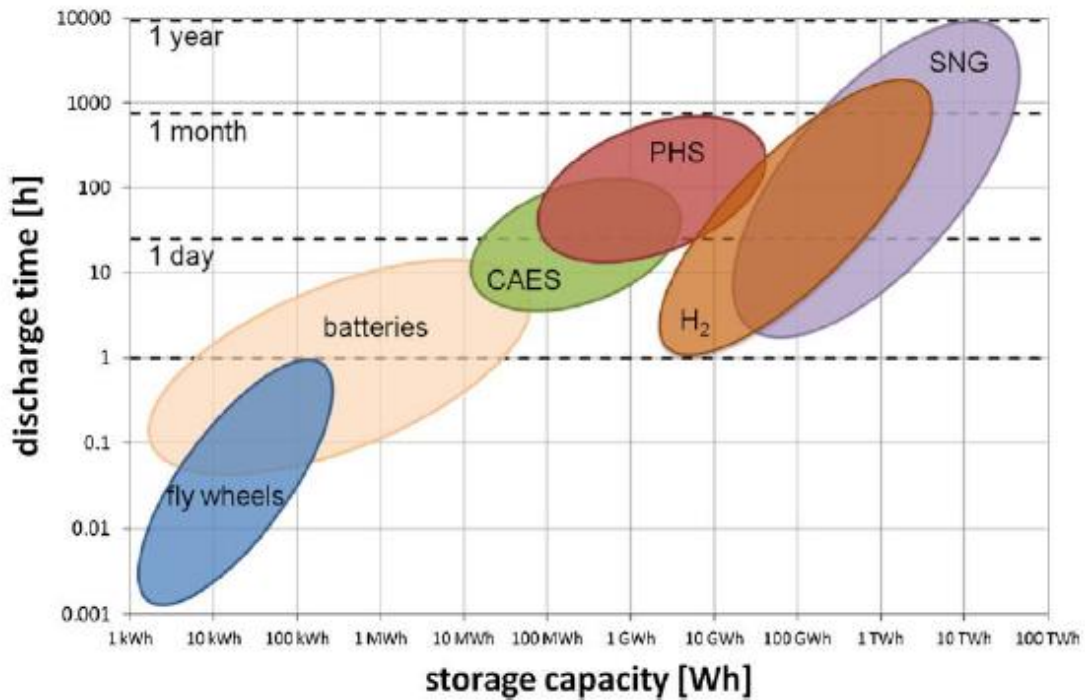


Figure 5 Ragone Plot-Energy Storage Technologies [ITM POWER 2014]

Figure 6 shows the high-temperature co-electrolysis route. The low-price or otherwise curtailed electricity can feed a solid oxide electrolyzer producing syngas, a mixture of  $H_2$  and  $CO$ , starting from  $H_2O$  and  $CO_2$  as feed reactants. A subsequent catalytic conversion with carbon dioxide leads to synthetic natural gas (SNG).

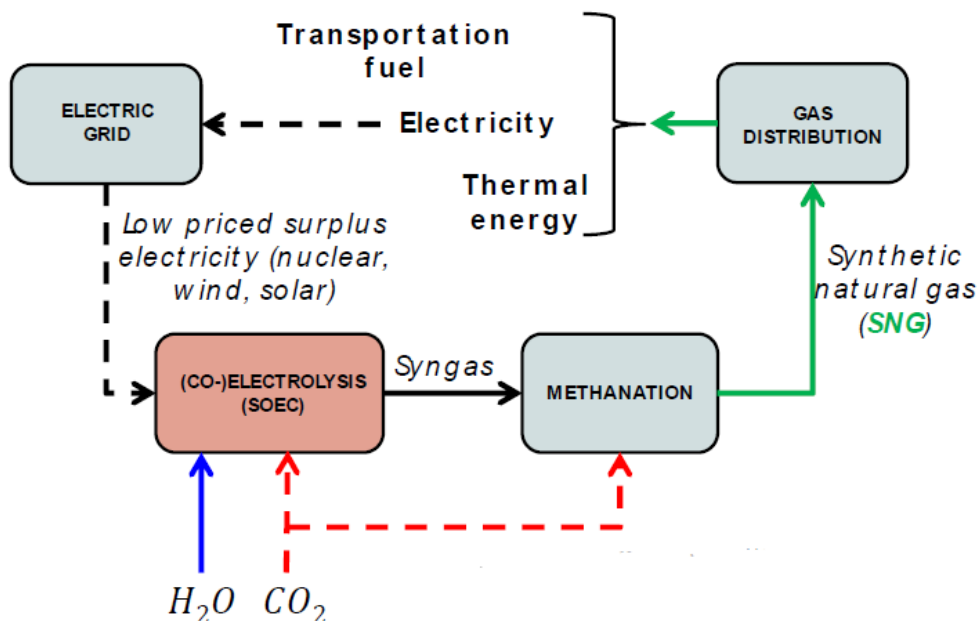
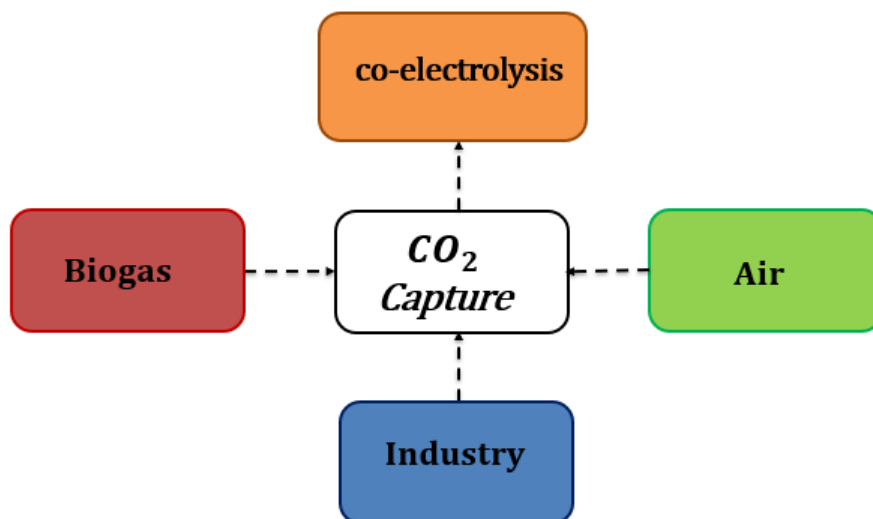


Figure 6 General path for syngas production from high temperature electrolysis [Teaching Material, Polytechnic of Turin, Polygeneration and Advanced Energy Systems,2017]

This path reduces the extra CO<sub>2</sub> emissions, enables large-scale energy conversion and facilitates the integration of renewable energies into the electric grid. Furthermore, the most encouraging method to achieve CO<sub>2</sub> reduction is the conversion of “exhaust carbon” into “working carbon”. The required CO<sub>2</sub> to enable the process can be captured from multiple sources:



*Figure 7 CO<sub>2</sub> carbon capture sources for co-electrolysis*

In the near term, the carbon capture from fossil fuels, e.g. by power plants or coal and chemical industries, might be the only viable solution for large synthetic fuel production.

On industrial scale carbon capture and sequestration (CCS) techniques are: pre-combustion capture, post-combustion capture and oxyfuel combustion capture. Chemical looping with metal oxidation seems also to be an attractive pathway for the fuel decarbonization. This essentially concerns a process in which a stream of fuel is decarbonized, removing CO<sub>2</sub> and maintaining the fuel capability to produce energy unchanged. It might be considered a process of substitution of carbon molecules with other molecules with relevant energy content.

The carbon source may be represented also by the CO<sub>2</sub> contained in anaerobic digested biogas or CO/CO<sub>2</sub> compounds in the bio-syngas, available from the thermo-chemical conversion of biomass and/or other bio-wastes. In the near future, CO<sub>2</sub> scrubbing directly from the atmosphere may also become economically feasible. If carbon dioxide is captured and used directly from the air, then the produced synthetic hydrocarbons can be considered as CO<sub>2</sub> neutral. The further exploration of these technologies is left to the reader since it would require an in-depth discussion. The syngas composition is highly dependent on the type of process (e.g. simple or co-electrolysis) and it is influenced by the thermodynamic conditions in which the electrochemical reactions take place.

Syngas is very versatile and can be implemented for transportation, electrification and thermal energy production.

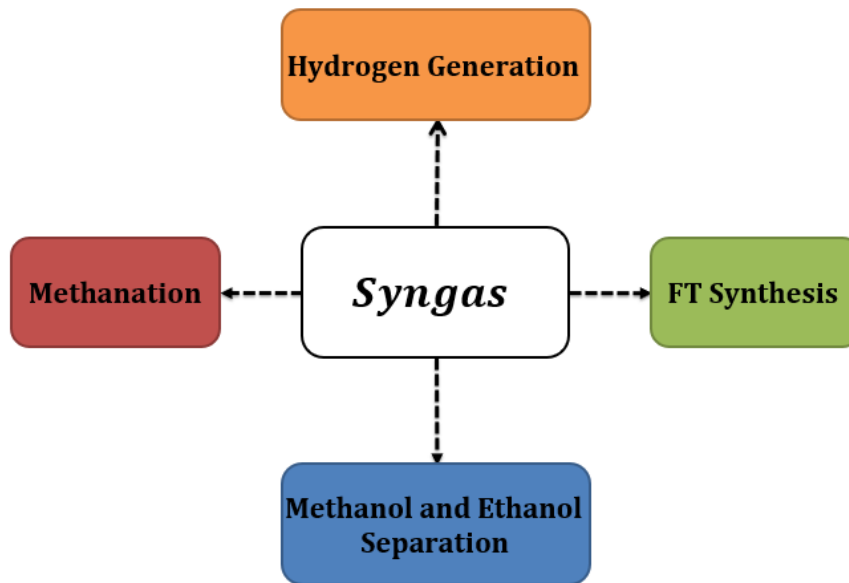


Figure 8 Syngas utilization pathways

More specifically (7) :

1. Syngas can be used to generate high pressure steam in a boiler and consequent expansion in a steam turbine with power generation.
2. It can feed gas turbine in combined cycles, fuel cells (e.g. SOFCs or DMFCs) or internal combustion engines (high H<sub>2</sub> content in syngas leads to a decrement of the combustion duration and thereby increases the efficiency of ICEs).
3. Subsequent methanation process of syngas produces synthetic natural gas (or substitute natural gas) with high content of methane (CH<sub>4</sub>), which can directly feed the existing infrastructures.
4. Hydrogen can be obtained from syngas (e.g. through a regenerative process) and can be implemented in refinery hydro treating, transportation fuels (hydrogen vehicles), fuel cells, chemicals and fertilizers.
5. Ethanol and Methanol may be achieved from syngas: di-methyl ether (DME) seems to be very attractive today since it can be used in diesel engines with few adjustments.
6. Fischer-Tropsch (FT) synthesis with syngas allow to obtain wax, diesel, gasoline or naphtha. FT could easily produce kerosene-type products, like RP-1, used as fuel in spacecraft rockets.

### **3. Solid Oxide Electrolyser Cell (SOEC): a brief technological review**

As already discussed, the simultaneous electrolysis of water and carbon dioxide is a promising way to store large quantities of energy into syngas, which can later be used as feedstock for several uses. A strength of this process is that the CO<sub>2</sub> utilized to feed the electrolyzer is the same of the following exploitation of the fuel, so that the entire “emission cycle” is neutral.

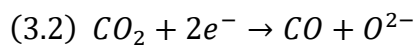
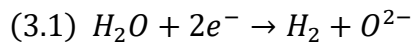
Splitting steam and carbon dioxide via co-electrolysis has these additional advantages:

1. The fast-overall electrochemical kinetics makes the process more energy efficient and potentially more cost-effective. The performance of the simultaneous electrolysis of water and carbon dioxide is close to the simple electrolysis (SE). The SE of carbon dioxide has a much higher activation energy demand due to the slow CO<sub>2</sub> splitting kinetics. Thus, co-electrolysis exhibits a lower polarization resistance and over-potential in comparison to sole CO<sub>2</sub> electrolysis.
2. The majority of CO<sub>2</sub> conversion to CO in the co-electrolysis operation moves in a reverse water gas shift (RWGS) chemical reaction which results in a remarkable reduction of the total electrical consumption to produce syngas.
3. Introducing steam (H<sub>2</sub>O) during the process allows to avoid the carbon deposition’s problem, whereas in case of dry CO<sub>2</sub> electrolysis, CO<sub>2</sub> could be deeply split to carbon, causing severe coking and loss of cell function.
4. High temperature leads to high efficiency with lower cost.

Nonetheless, the high operating temperature can be also a disadvantage, since results in long start-up times and break-in times. The high operating temperature also leads to mechanical compatibility issues such as thermal expansion mismatch and chemical stability issues such as diffusion between layers of material in the cell.

### 3.1 Working principles and fundamental equations

During operation a stream composed mainly of  $H_2O$  and  $CO_2$  is provided to the cathode, where the reactants receive electrons supplied from the external power ( $W_{el}$ ) to produce syngas as well as the oxygen ions:



The negative ions ( $O^{2-}$ ) are carried across the dense electrolyte from the cathode to the anode side under the driving force of applied voltage ( $V$ ). They are subsequently oxidized to oxygen gas ( $O_2$ ), releasing the electrons as the following reaction:

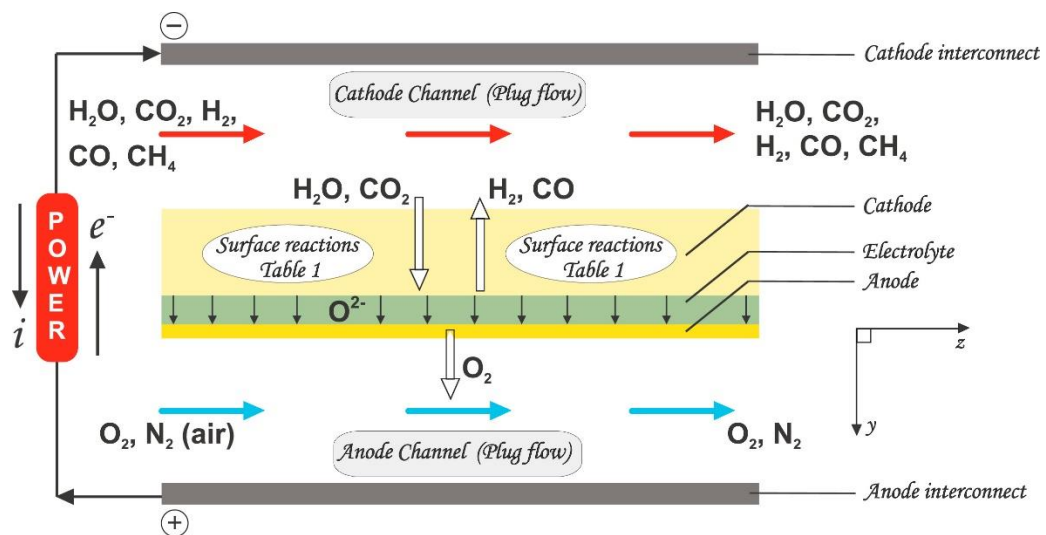
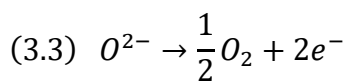
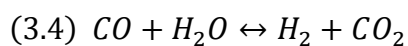
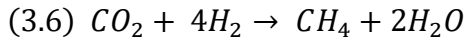
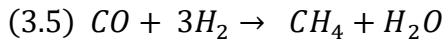


Figure 9 Co-Electrolysis with SOEC [Menon et Al. 2015]

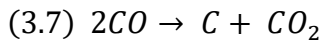
It has been proved that the best part of CO content of cathode outlet is produced from reversed water gas shift reaction (RWGS). The RWGS is endothermic and hence favored at higher operating temperatures.



Pressurizing the system favors the shifting of equilibrium towards the products (methane formation):



Methanation reactions are highly exothermic and enhanced at high pressures and low temperatures. This condition would result in lower amount of syngas (hydrogen/carbon monoxide) in the cathode exhaust. This could be unwanted for the FT synthesis and therefore can result in lower performance of the whole system. High operating pressures of the system brings also to easier carbon deposition:



The correlation that expresses the reactant consumption rate in a cell is the Faraday's law. The molar flowrate consumption is proportional to the flowing current (Faraday current):

$$(3.8) n_r = \frac{I_f}{n_e * F} = \frac{j * A}{n_e * F}$$

where  $n_r$  is the reactant consumption [mol/s],  $I_f$  is the Faraday current [A],  $n_e$  is the number of electrons involved in the reaction and  $F$  is the Faraday constant [96.485 s\*A/mol]. The Faraday current can be also expressed as the product between the current density  $j$  [A\*cm<sup>-2</sup>] and the active surface  $A$  (cm<sup>2</sup>). The reversible voltage (or Nernst potential) [V] can be expressed as:

$$(3.9) V_{rev} = -\frac{\Delta g}{2 * F}$$

Where  $\Delta g$  is the molar Gibbs free energy of the reaction [J/mol] ( $\Delta G = \Delta H - \Delta(T * S)$ ).

Since two electrons are involved both for steam and carbon dioxide reduction reactions is possible to substitute  $n_e$  with 2. The inlet molar flow that is effectively undertaking electrochemical reactions ( $n_r$ ) is related to the total inlet mole flow  $n_{in}$  through the following equation:

$$(3.10) n_r = n_{in} * RR * RU$$

Where RU (reactant utilization) is the fraction of reactant which effectively reacts in the stack, and RR (reactant ratio) is the reactant fraction of the inlet molar flow rate. The reactant ratio considers that the inlet feed stream to the SOEC must contain some fraction of H<sub>2</sub> to avoid re-oxidation of the ‘fuel’ electrode and generally this is accomplished by recirculating a fraction of the cathode exhaust to the inlet. The polarization curve (expressing the relation between voltage and current) is affected by non-linear transport phenomena as charge transfer, charge conduction and mass transport. For the next considerations linear simplified relationship between voltage and current density will be adopted. The Area Specific Resistance (ASR) [ $\Omega \cdot \text{m}^2$ ], is the angular coefficient of the current-voltage characteristic.

$$(3.11) \quad ASR = \frac{V_{op} - V_{rev}}{j}$$

Where  $V_{op}$  and  $V_{rev}$  are the stack operating and the reversible voltage [V], respectively. It is possible directly to infer the expression of  $V_{op}$  as a function of  $j$ :

$$(3.12) \quad V_{op}(j) = V_{rev} + ASR(T, p) * j$$

The Area Specific Resistance (ASR) depends on electrodes or electrolyte materials, geometrical features and the thermodynamic conditions. The working principle of an electrolyzer is different respect to a fuel cell, aside from the obvious change in the direction of the electrochemical reaction. From the thermal management point of view, the galvanic cell operation mode typically needs an excess of air flow rate with respect of stoichiometric amount, to prevent overheating of the stack. Indeed, the exothermic behavior of the reactions and the heating released for irreversibility phenomena makes possible the exploitation of the heat generated, especially in high temperature devices (SOFCs). In the electrolysis mode, the steam and/or carbon dioxide reduction reaction is endothermic. Therefore, depending on the operating voltage, net heat generation within the stack may be negative, zero, or positive. The produced heat flux [ $\text{W}/\text{cm}^2$ ] produced by the cell is:

$$(3.13) \quad \varphi_{gen} = j^2 * ASR = j * (V_{op} - V_{rev})$$

Using the Faraday’s law, the heat requirement can be expressed as:

$$(3.14) \quad \varphi_r = \frac{j}{2 * F} * T * \Delta s$$

During electrolysis, the net heat flux is negative for low operating voltages (endothermic) and positive (exothermic) at higher voltages and current densities. The thermal-neutral voltage (null neat heat flux) can be obtained as:

$$(3.15) V_{tn} = \frac{\Delta h}{2 * F}$$

Where  $\Delta h$  represents the molar enthalpy variation of the reaction [J/mol].

The current density  $j$ , referring to the thermo-neutral voltage, can be expressed taking advantage of the previous relations:

$$(3.16) j_{tn} = \frac{V_{tn} - V_{rev}}{ASR} = \frac{\Delta h - \Delta g}{ASR * 2 * F} = \frac{T * \Delta s}{ASR * 2 * F}$$

With reference to the previous equations, heat requirement  $\varphi_r$ , can be written as:

$$(3.17) \varphi_r = \frac{1}{2 * F} * T * \Delta s = \frac{j}{2 * F} * T * (\Delta h - \Delta g) = j * (V_{tn} - V_{rev})$$

During fuel cell operation, the heat flux is always positive and increases with the current density  $j$ . As already mentioned, during electrolysis operation, the heat flux can assume positive and negative values depending on the operating voltage. Working in thermo-neutral conditions, the heat fluxes ( $\varphi_r$ ) and ( $\varphi_{gen}$ ) have same expression and opposite sign, making the overall heat requirement equal to zero.

## 3.2 Materials, components and configuration

The solid oxide electrolysis cell mainly consists of a fuel electrode (cathode), an oxygen electrode (anode) and a dense electrolyte. One of the most common configurations of a SOEC is the Ni-YSZ|YSZ|LSM-YSZ configuration. During SOEC operation, the electrode materials are used for electrochemical reactions like the O<sub>2</sub> oxidation and the reduction of H<sub>2</sub>O and CO<sub>2</sub>. They also provide pathways for transport of electrons, ions, reactants and products. Electrolyte has a major impact on electrolysis cell performance since its contribution to the ohmic internal resistance. The

interconnect offers electrical connection between the oxygen electrode of one individual cell to the fuel electrode of the neighboring one in SOEC mode. It provides a physical barrier to protect the oxygen electrode material from the reducing atmosphere of the fuel electrode side and the fuel electrode from the oxidizing environment. Gaskets provide correct compression and act as a barrier for potential fuel leaks maximizing the highest possible efficiency. The most used materials are silicon, Teflon and fiberglass. Interconnect and cell sealing represent fundamental components especially for multiple cell stack. The high temperature characterizing the SOECs functioning leads to important limitations with the necessity to respect several requirements:

- The dense electrolyte should have poor electronic conduction, excellent ionic conductivity, and chemical stability.
- The dense electrolyte should be as thin as possible to lower ohmic over-potential, but also possess a gastight structure to separate the syngas and the O<sub>2</sub>.
- The porosity should be designed to not only support gas transportation but also provide sufficient triple phase boundary (TPB, the interface of the electrolyte/electrode/gas).
- Electrodes and electrolyte should have compatible thermal expansion coefficients (TECs) to prevent material failure.
- The interconnect materials should be chemically stable in both reducing and oxidizing atmospheres since they have contact with CO (g), H<sub>2</sub>O (g), CO<sub>2</sub> (g), and O<sub>2</sub> (g) simultaneously.
- The manufacturing cost and raw materials should be as cheap as possible.

To reach high electrolytic efficiency, the microstructure and porosity of electrode materials is very important, and an increment of the electrodes active surface area should be performed. Porous fuel electrodes are used to provide reaction active sites for the decomposition of H<sub>2</sub>O and CO<sub>2</sub>, allowing the reactants to be transported and the products to be removed from the reaction active sites at the surface. They also guarantee a path for the electrons, to move from the interconnect to the reaction sites on the electrolyte/electrode. Ni-YSZ (Nickel-yttrium stabilized zirconia) is widely used due to its reasonable electro-catalytic activity, low cost, excellent chemical stability, and appropriate thermal expansion coefficient. A fuel electrode that permits to enhance cell electrochemical efficiency by limiting the ionic losses, is composed of a porous Ni-YSZ substrate (also called a support layer or a current collecting layer), a functional layer (also called a catalyst layer) and a thin electrolyte. At the current state of technology there is still no single compound or composite material that can meet all requirements such as stability, activity, flexibility and low cost in SOEC

operation simultaneously. In general, the electrode materials can be classified into three large categories: metal electrodes, ceramic electrodes and composite electrodes.

1. Metal Electrodes: Nickel and platinum may be applied as fuel electrodes and only noble metals such as platinum or gold can be used as oxygen electrodes in SOECs. Obviously, the noble metals used as electrode materials are too costly for commercial SOECs. Nickel has a significant thermal expansion mismatch to stabilized zirconia, and it may aggregate by grain growth especially at high temperatures.
2. Ceramic Electrodes: SFM, LSV, LSCM, LSM are generally chosen due to their good ionic and/or electronic conductivities, although it seems that their catalytic properties and stabilities are not optimal.
3. Composite Electrodes: Developed to enhance the reactive areas and thus the electrode activity and even the stability. The composite electrodes can be generally classified into two groups including metal–ceramic electrodes (e.g. Ni–YSZ, Ni–SDC, LSCM–Cu etc.) and ceramic–ceramic electrodes (e.g., LSC–YSZ, LSM–YSZ, LSM– GDC etc.). Aside from the enhancement of activity, a closer overall thermal expansion matching with the electrolyte can also be achieved for composite electrodes.

The main configurations for this technology include planar, tubular or flat tubular SOCs. Tubular configuration allows to reach higher mechanical and thermal stability respect than that the flat-plate. The sealing of the cell is also much easier in tubular configurations. Anyway, planar designs have still been widely adopted due to their much shorter current collection paths and significantly higher volumetric density.

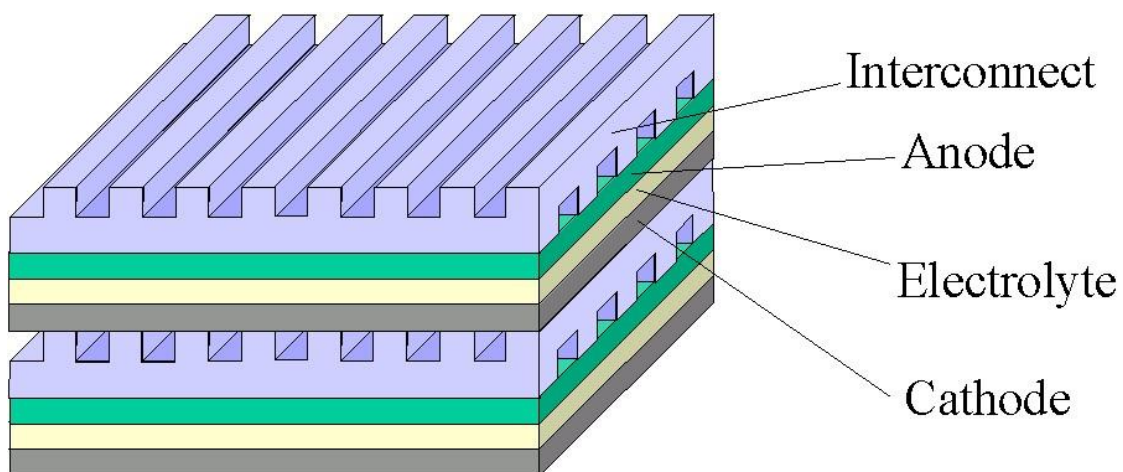


*Figure 10 Flat plate (planar) solid oxide cell stack*

### 3.3 Fabrication and scale-up

The two main approaches to fabrication are the particulate and the deposition method. The particulate method involves the compaction of ceramic powder into the components of SOEC cells and then densification at high temperatures, such as tape casting and tape calendaring. The deposition method for manufacturing of cell components on a support involves processes such as plasma spraying, chemical vapor deposition (CVD) or spray pyrolysis. There are currently three main particulate processes for the fabrication of SOECs: tape casting, tape calendaring and extrusion. The first two processes are often used in the fabrication of planar SOECs whereas the third one is used for tubular SOECs. The deposition techniques are widely used for the fabrication of both planar and tubular SOECs and the main processes include: sputtering, dip coating, spray pyrolysis and plasma spraying.

Other deposition processes are electrophoretic deposition and vapor phase electrolytic deposition.

For the scale-up, normally, modular designs arrange single cells in a uniform size together to form a SOEC stack. After that, several of these stacks can be assembled to make a basic module.

In general, as the number of modules increases, larger is the surface area which can result in higher production capacity. SOEC stacks are the key components for high temperature electrolysis. However, similar to fuel cell systems, high temperature electrolysis systems also include many subsystems besides the SOEC stack itself. These include heat management subsystems, power management subsystems, steam management subsystems, gas transfer/purification subsystems, data acquisition and control subsystems and security subsystems. Efficient heat management can improve the overall efficiency of high temperature electrolysis processes by reducing energy consumption and recovering some heat contained in the outlet products of the electrolysis. The chemical production rate of SOEC systems can be flexibly changed with power supply management. SOEC systems are more complex as compared to SOFC systems. The main reason is steam condensation, which will result in SOEC stack cracking as well as fluctuations in operating conditions. Steam management subsystems therefore can guarantee the effective use and accurate control of steam. The main function of gas transfer/purification subsystems is to control the composition of the inlet gas, and to purify the product. Data acquisition and control subsystems can monitor and control the SOEC modules. In a high temperature electrolysis system, safety precautions are essential to handle high temperature H<sub>2</sub> and O<sub>2</sub> effectively.

### 3.4 Performance degradations

For solid oxide cells long term degradation represent the main issue. The durability for syngas production is significantly related to the components, the configuration, the fuel gas compositions and the operating conditions (temperature and current). Observed degradation mechanisms in SOCs include: impurities poisoning, microstructural damage, and thermal stress. Other degradation mechanisms specific for solid oxide co-electrolysis cells resulted from the deep electrolysis at high current densities and high humid conditions. The durability of solid oxide co-electrolysis cells results in a degradation rate  $< 5\%/1000$  h under a constant electrolysis current lower than  $1 \text{ A/cm}^2$  (8).

However, more severe degradation phenomena occur increasing current densities and operating temperatures (9). At low current, degradation at the Ni/YSZ electrode is dominant, whereas at higher current densities the Ni/YSZ electrode continues to degrade but degradation at the LSM electrode has major influence on the overall loss in cell performance. Compared to sole  $\text{CO}_2$  electrolysis, carbon deposition has been largely suppressed in co-electrolysis with the addition of steam. Nonetheless, at high current density and high  $\text{CO}_2$  conversion, the local concentration of CO and  $\text{H}_2$  at the Ni-YSZ/YSZ interface are possibly high enough to contribute a reducing condition, inducing carbon deposition. Reference (10) analyzed the SOEC degradation under high currents observing hole/pore formation along the grain boundaries of the YSZ electrolyte close to the LSM/YSZ oxygen electrode. The performance cell degradation was related to the nucleation and growth of oxygen clusters in the YSZ. The failure mechanism of LSM oxygen electrode can be attributed to the formation of nanoparticles within the contact rings on the electrolyte surface, due to the migration of oxygen ions from the electrolyte to the LSM grains. It results in the shrinkage of LSM lattice, with further generation of local tensile strains and micro cracks at the electrode/electrolyte interface (11). Other cases of analyzed case of degradation, may be related to the impurities poisoning originated from the inlet gases, the seals and interconnect materials. Since the feed gases of hydrogen and carbon dioxide is generally produced from natural gas or coal gasification, hydrogen and carbon dioxide may contain trace amounts of  $\text{H}_2\text{S}$ . Because of the limited tolerance of nickel-based to  $\text{H}_2\text{S}$ , severe catalyst poisoning may occur.  $\text{H}_2\text{S}$  can quickly dissociate into hydrogen and sulfur, which strongly absorbs on the nickel surface and blocks the active sites for the reduction of steam, leading to degradation of the electrochemical performance. Hydrogen sulfide poisoning, normally irreparable, may only be avoided by cleaning the inlet gases for the Ni-based electrodes or developing new electrode materials with higher tolerance to  $\text{H}_2\text{S}$  (12) (13).

## 4. Plant modeling

In this chapter the SNG production through an integrated plant featuring high temperature co-electrolysis is examined. The modeling and the process simulation has been developed with Aspen Plus®, a widely used software in chemical engineering to model and size industrial processes. An input of 1 MWe<sub>el</sub> (Pilot Plant) has been chosen as DC electricity for the solid oxide cell, based on Power to Gas demonstration projects like Jupiter 1000 (France), Falkenhagen-D (Germany) (14). The plant is envisioned to be located in Tehachapi, Kern County (California). This County accounts for the 52.4% and 21.4% of the total 2017 wind and solar in-state electricity generation. In particular, is worth emphasizing the proximity of two huge power stations: Alta Wind Energy Center and Solar Star. The Alta Wind Energy Center (Alta windfarm) is the nation's largest wind facility and second in the world. It is located in the wind resource area at the Tehachapi Pass in Kern County. The Alta windfarm supplies 1.548 megawatts (MW) of renewable energy to Southern California Edison (SCE) customers and will continue through 2040 under a 3.000 MW wind power development initiative, producing enough electricity to power 450.000 homes. The Solar Star projects are two distinct projects, Solar Star 1 and Solar Star 2, co-located in Kern and Los Angeles counties. They represent the world's largest utility-scale solar projects. Installed across 3.230 acres, they are comprised of 1.7 million Sun-Power monocrystalline silicon PV panels with a combined generating capacity of 579 megawatts. The presence of large number of renewables fit well with Power to Gas systems, since low-price or otherwise curtailed electricity would be an ideal input of the SOEC generator. The selection of the site (Tehachapi) is also linked to the CO<sub>2</sub> source: the Lehigh Hanson Southwest cement plant. The CO<sub>2</sub> measured emission in 2017 by the California Air Resource Board from this plant is almost 600.000 metric tons. Research (15) show the possibility to reuse the carbon captured from the process of mineral decomposition of cement industry through post-combustion amine scrubbing using monoethanolamine (MEA), with limited modification to the already existing plant and CO<sub>2</sub> capture up to 74%.

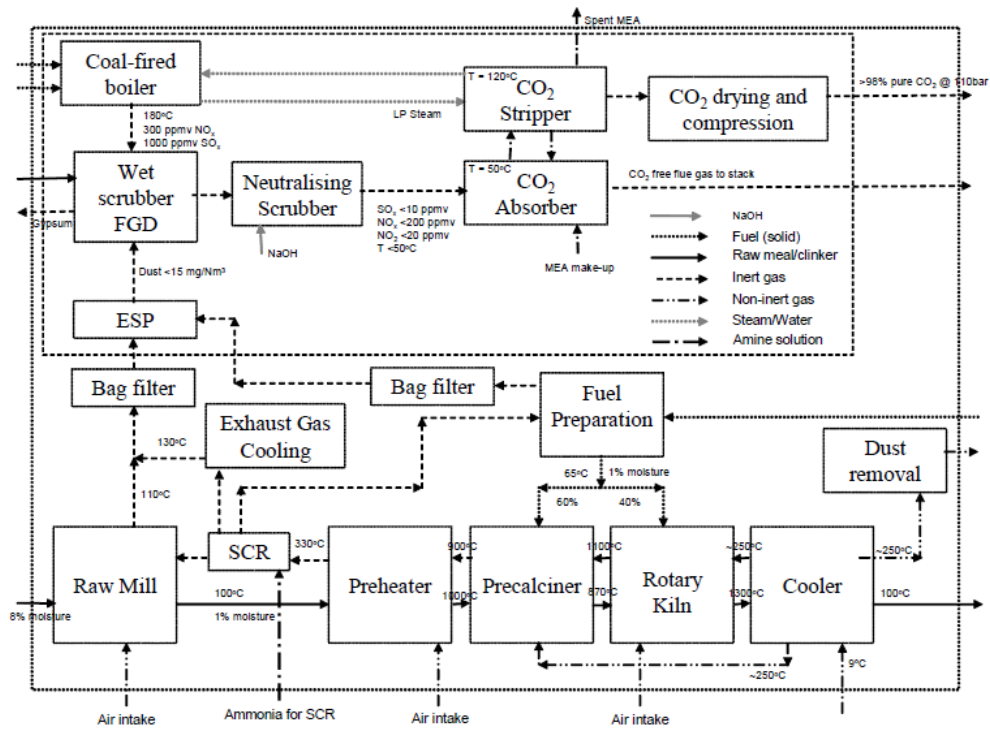


Figure 11 Cement Plant with post-combustion CO<sub>2</sub> Capture (15)

A brief description of the cement plant with post-combustion CO<sub>2</sub> capture follows below. A Selective Catalytic Reduction (SCR) unit is interposed between the raw mill and the pre-heater to reduce the amount of NO<sub>x</sub>. A wet limestone Flue Gas Desulfurization (FGD) unit is used to remove the sulfur oxides (SO<sub>x</sub>) from the gas stream and the MEA amine solvent-based capture equipment is installed. In order to generate low pressure steam for the MEA stripping and provide the additional request power for the compressor and the amine absorption, a coal-fired CHP plant can be added. The carbon dioxide coming from this process is also captured and mixed with the cement plant flue gas before the limestone flue-gas desulfurization unit. The net CO<sub>2</sub> produced is compressed and dried. Figure 12 shows the process flow arrangement for a typical modern cement plant without CO<sub>2</sub> capture as used as the base case in this study.

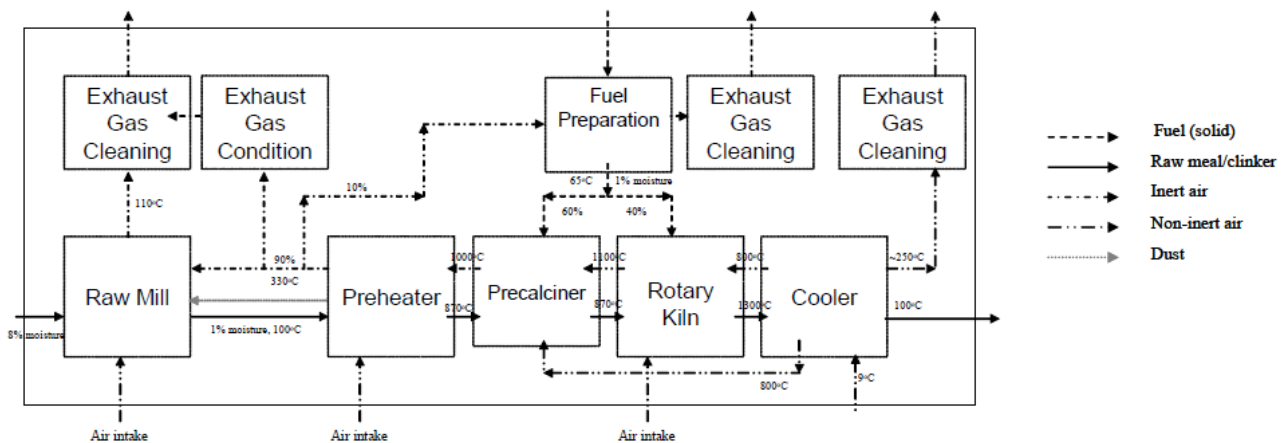


Figure 12 Cement plant without CO<sub>2</sub> Capture (15)

Furthermore, the proximity to NG infrastructures and transmissions lines was verified, for the direct grid injection of the SNG and RES exploitation (16) (17).



Figure 13 Lehigh Hanson Southwest cement plant (Tehachapi), NG substations, transmission lines (16) (17)

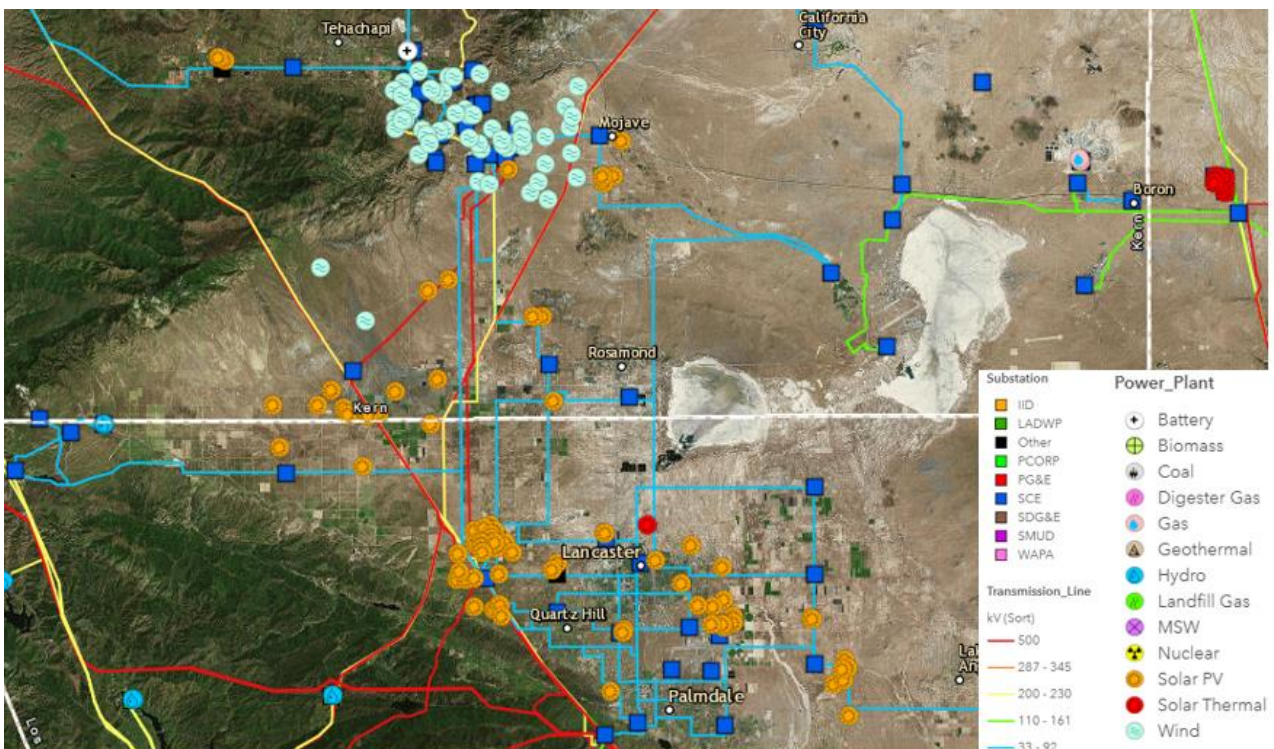


Figure 14 Maps of the selected Area, visible Alta Wind Energy Center and Solar Star 1&2 (16) (17)

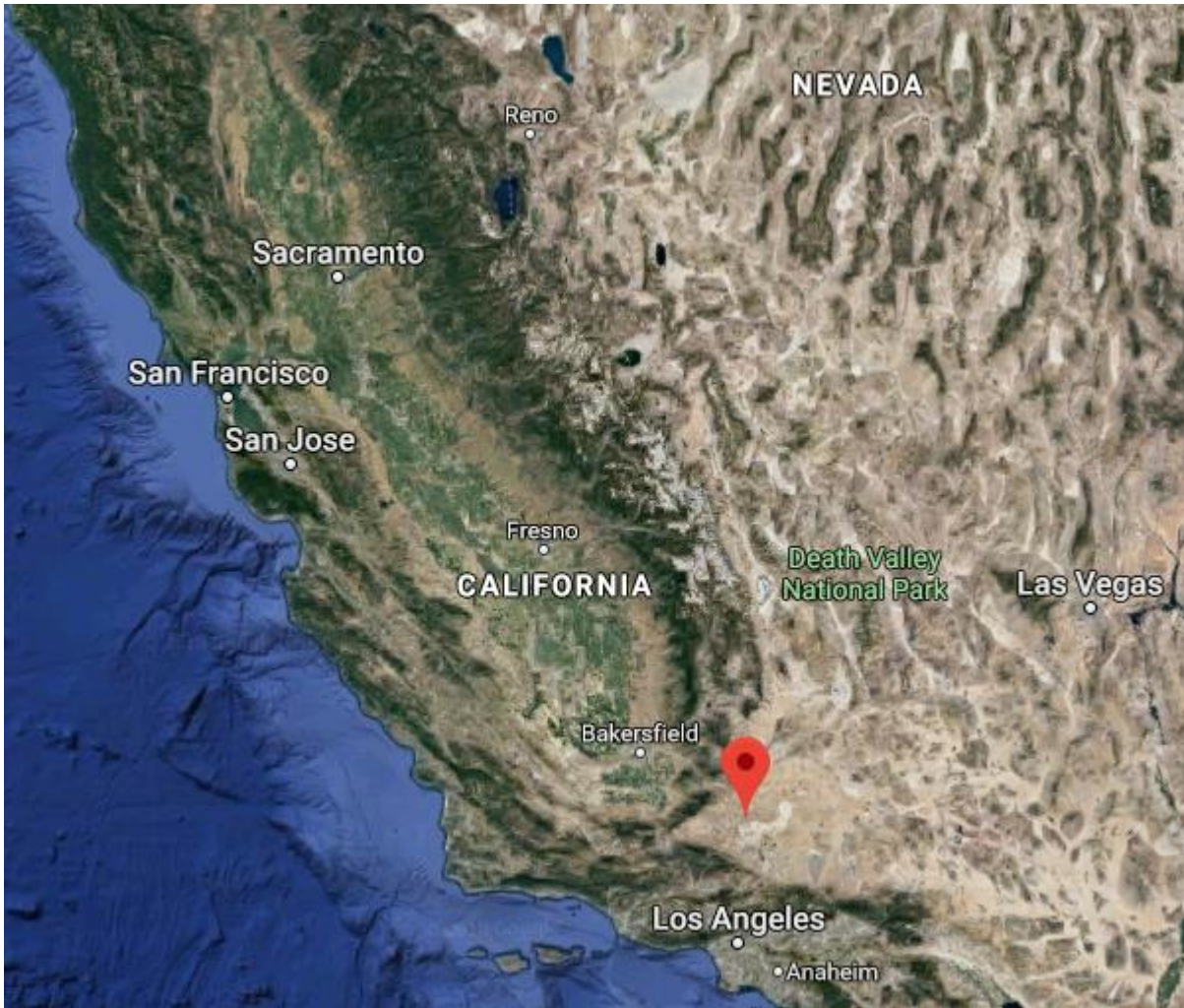


Figure 15 Maps of the selected Area - California

Table 3 contains other cement industries (and their relative emissions) in the area:

Table 3 Cement industries with relative CO<sub>2</sub> emissions in the area

Name	CO <sub>2</sub> Emissions [tons]	Distance [miles]
Lehigh Southwest Cement Co - Tehachapi	596.515	12
National Cement Company - Lebec	711.525	54
Cemex Construction Materials Pacific LLC - Victorville Plant	2.156.578	100

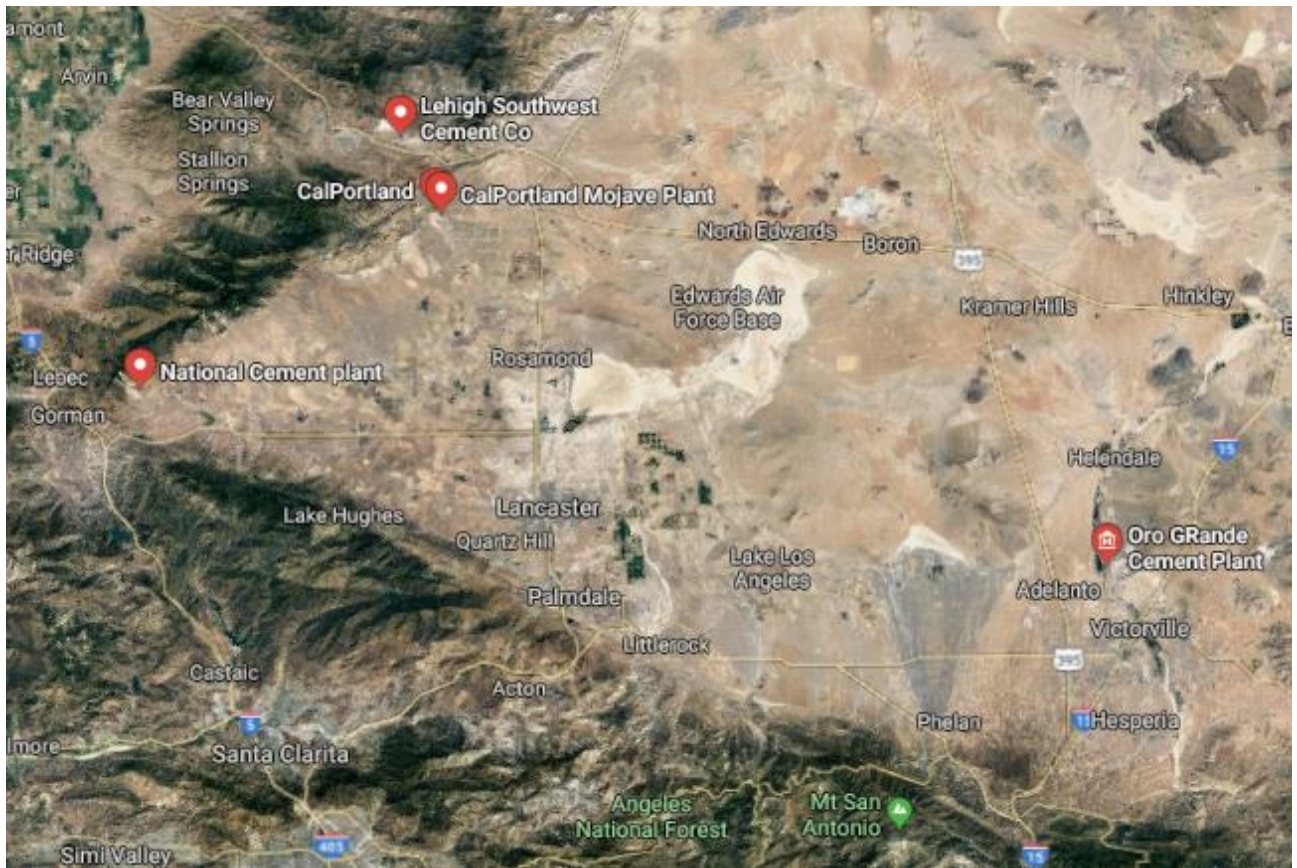


Figure 16 Cement industries in the area

## 4.1 Utilization factor

To determine a reasonable number of plant operating hours, the state net load was considered. The System Operator (CAISO) net load is defined for each time step  $t$  as:

$$(4.1) \text{ Net Load } (t) = \text{Load } (t) - \text{Solar Generation } (t) - \text{Wind Generation } (t)$$

Other renewable energy sources such as geothermal and biomass are not included since their output is not as intermittent as solar and wind resources. Forecasts for 2025 and 2030 have been performed (18). In this work, hourly projections among 2014 to 2021 are linearly interpolated from data for 2014 and 2021, while for each hour  $t$  within each forecast year  $N$ , the projections beyond 2021 are extrapolated following the same linear trend:

$$(4.2) \text{ Net Load } (t, N) = \text{Net Load } (t, 2014) + \left( \frac{\text{Net Load}(t, 2021) - \text{Net Load}(t, 2014)}{2021 - 2014} \right) * (N - 2014)$$

The figure below shows the net load of a particular day (March 31) for 2014, 2021, 2025 and 2030. Is worth emphasizing that a significant drop of the net load occurs during the central hours of the day, mainly from the solar power contribution.

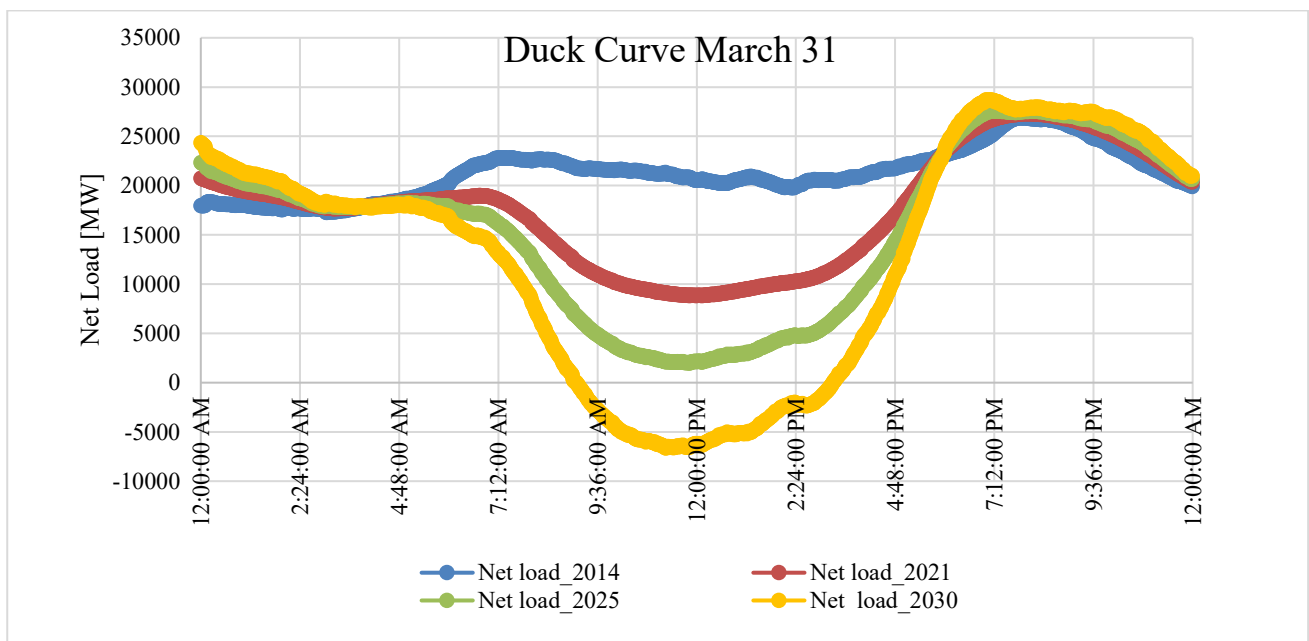


Figure 17 Duck Curve, March 31, 2014,2021,2025,2030

For 2030, 1089 hours per year were calculated under the threshold value of 10.000 MW. Extending the reasoning also for 2040 and 2050, 1870 and 2345 h/yr. respectively were founded. Naturally, is necessary to consider that the assumption of linearity described above is losing of accuracy for 2040 and 2050. On the basis of such considerations, a reasonable capacity factor of 20 % has been assumed (1752 h/y).

## 4.2 Plant configuration

In the following paragraph the configuration and the main characteristics of the developed model, featuring high temperature co-electrolysis and subsequent methanation, will be discussed.

The process can be essentially divided in three parts: the conversion of the products (water and carbon dioxide) into syngas, the methanation and the compression. Eventually a blending with an inert gas can be performed to meet the prescribed quality requirements. Aspen Plus® does not contain a prebuilt electrolyzer component and we model it here as a design with combination of prebuilt units.

The process simulation with Aspen Plus® has been performed in Peng-Robinson equation of state property model (PENG-ROB).

An elevated purity of reactants is necessary for durable and stable operation of the Ni catalyst and electro-catalyst contained in methanation and SOEC reactors. Thus, demineralized water has been selected for the SOEC. As regards to CO<sub>2</sub>, different contaminants that must be removed could be present depending on the carbon source considered. In our scenario, with carbon capture and recovery (CCR) in the cement industry, CO<sub>2</sub> from pipelines should already meet stringent quality criteria being almost ready to feed the SOEC (19). The PtG plant is designed to achieve a stream of almost pure methane and meeting the NG grid injection criteria of California (in term of heating value [Btu/scf] and Wobbe index [Btu/scf]) (20) (21).

$$(4.3) \quad WI = \frac{HHV}{\sqrt{G_s}}$$

where the specific gravity ( $G_s$ ) is a dimensionless quantity calculated as:

$$(4.4) \quad G_s = \frac{MW_{gas}}{MW_{air}}$$

Where MW is the molecular weight of the substance.

Table 4 California prescriptions for natural gas feeding into distribution pipelines

Higher heating value (HHV) [ Btu/scf ]	Wobbe index (WI) [ Btu/scf ]
950 - 1235	1279 -1385

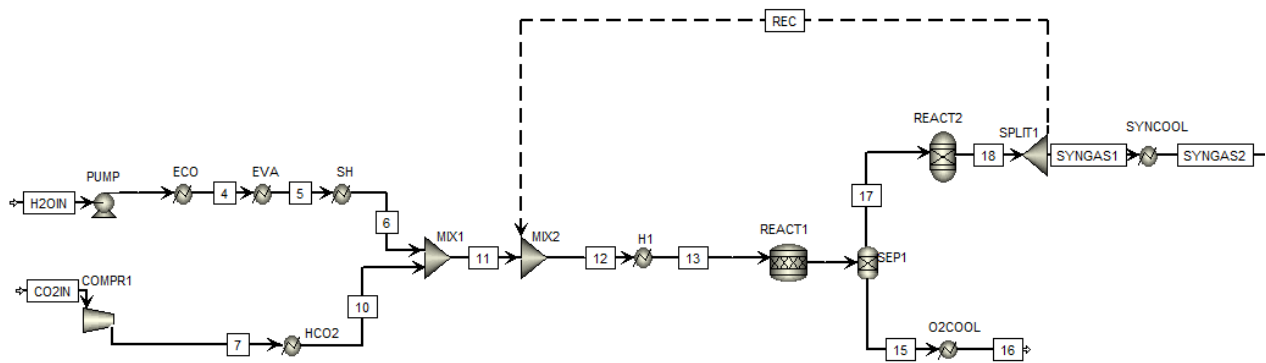


Figure 18 Model part 1

We assume that the solid oxide electrolyzer cell operates at high pressure (30 bar) and temperature of 1472 °F/800°C. For simplification, we assume thermo-neutral conditions ( $V_{op} = V_{tn}$ ,  $j = j_{tn}$ ). Pressurized stack operation was implemented since methanation is favored at high pressure. A pressurized SOEC is beneficial also because an atmospheric SOEC would require bigger syngas work compression upstream of methanation in comparison to the water pumping in the pressurized option. Atmospheric electrolyzer would require cooling far below the 220°C at the first methanation reactor. Finally, high pressures allow a reduction to the volume sizes and are mostly used in commercial reactors.

The water (68°F/20°C and 1 atm) is pumped and heated up through a steam generator composed of an economizer (ECO), an evaporator (EVA) and a super heater (SH). The carbon dioxide (68°F/20°C and 1 atm) is compressed and heated up to the cell operating temperature where it co-feeds to the electrolyser with the steam. A mixture consisting of H<sub>2</sub> and CO (syngas) is obtained for downstream methanation. A hydrogen mole fraction of 10% was reached with a design specification, by varying iteratively the recirculation rate of cathode outlet, to avoid Ni re-oxidation

in the electrode. To achieve SNG with the greatest amount methane is important that the feed for the methanation section has a particular feed ratio of reactants defined as following (22):

$$(4.5) \text{ SYNGAS\_COMP} = \frac{[H_2] - [CO_2]}{[CO] + [CO_2]} = 3$$

A proper design specification was implemented to achieve syngas\_comp=3 changing carbon dioxide mole flowrate in an iterative way. The syngas is cooled to the methanation inlet temperature of 428 °F/220°C and anode outlet (pure oxygen) to 95°F/35°C. To reach high methane concentrations (95–98%) in the final gas stream, it is necessary to connect several methanation reactors in series with intercooler in between (23).

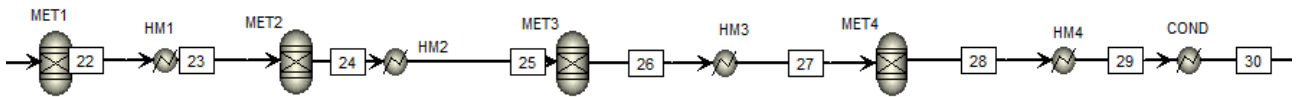


*Figure 19 Model part 2*

The carbon monoxide and the carbon dioxide are hydrogenated according to the methanation reactions (3.5) and (3.6), favored by low water content and high pressure. The final gas stream is chilled to condense the mixture (“COND” brings to mixture to 95°F/35°C) and the separate water (H2OREC) can be recycled back to the SOEC. Dry SNG is further cleaned by passing it through a molecular sieve that removes residual H<sub>2</sub>O and CO<sub>2</sub> (SEP2).

The SNG is compressed to 60 bar and eventually blended with an inert stream (for this model N<sub>2</sub> has been chosen) to meet pipeline prescriptions. An additional heat exchanger (POSTCOOL) can be installed to meet temperature requirements (95°F/35°C)

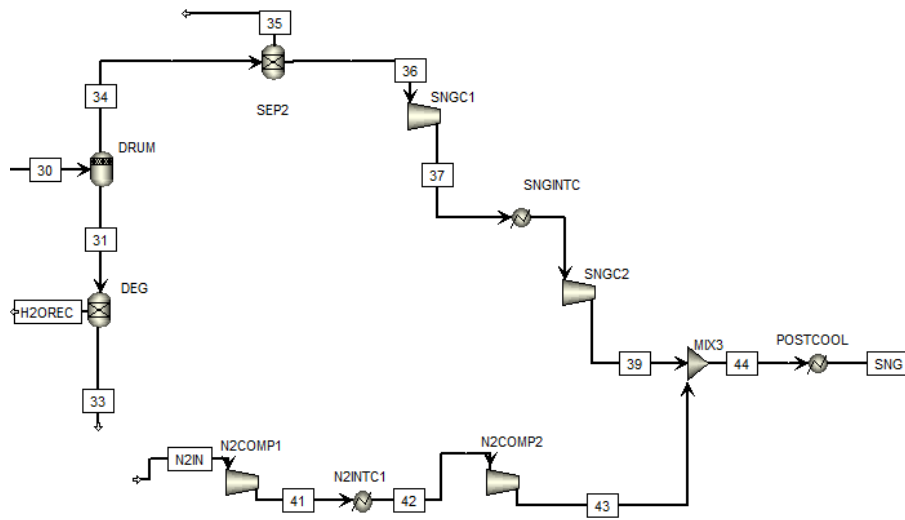


Figure 20 Model part 3

Other design specifications were adopted to model the plant size and the reactant utilization (RU). The selected value of 1 MW<sub>el</sub> was fixed adjusting the external water molar flowrate:

$$(4.6) W_{el} = n_{out} * h_{out} - n_{in} * h_{in} = n_{out,an} * h_{out,an} + n_{out,cat} * h_{out,cat} - n_{in} * h_{in} = 1 \text{ MW}$$

Where:

- n is the molar flowrate expressed in [kmol/s].
- h is the enthalpy expressed in [kJ/kmol].

The reactant utilization (RU) was fixed to 0.7 for the model, varying the fractional conversion of “REACT1”, where the split of H<sub>2</sub>O and CO<sub>2</sub> occur.

$$(4.7) RU = \frac{n_{in} - n_{out}}{n_{in}} = \frac{n_{H2Oin} + n_{CO2in} - n_{H2Oout} - n_{CO2out}}{n_{H2Oin} + n_{CO2in}} = 0.7$$

Pressure drops have been attributed to the main components in the integrated plant. The pressure drop for water vaporization and subsequent steam superheating was set as of 6% of the total inlet pressure (24). For methanation reactors, an average pressure drop value of 0.7 bar was chosen (25). Other equipment like compressors and pumps are characterized by isentropic and electro-mechanic

efficiencies. Isentropic efficiency was assumed 0.75 for compressors and to 0.8 for pumps. Electro-mechanic efficiency was assumed 0.95 for compressors and 0.9 for pumps.

Table 5 Plants modeling main assumptions

Stack pressure (bar)	Stack temperature	[H <sub>2</sub> ] at the cathode inlet	Electrolysis power [kW]	Reactant Utilization (RU)	Methanators inlet temperature
30	800°C-1472°F	10%	1000	0.7	220°C-428°F

Table 6 Assumptions for isentropic and electro-mechanical efficiencies

Component	Isentropic efficiency	Electro-mechanical efficiency
PUMP (H <sub>2</sub> O)	0.75	0.9
COMPR1 (CO <sub>2</sub> )	0.8	0.95
SNGC1 (SNG)	0.8	0.95
SNGC2 (SNG)	0.8	0.95
N2COMP1 (N <sub>2</sub> )	0.8	0.95
N2COMP2 (N <sub>2</sub> )	0.8	0.95

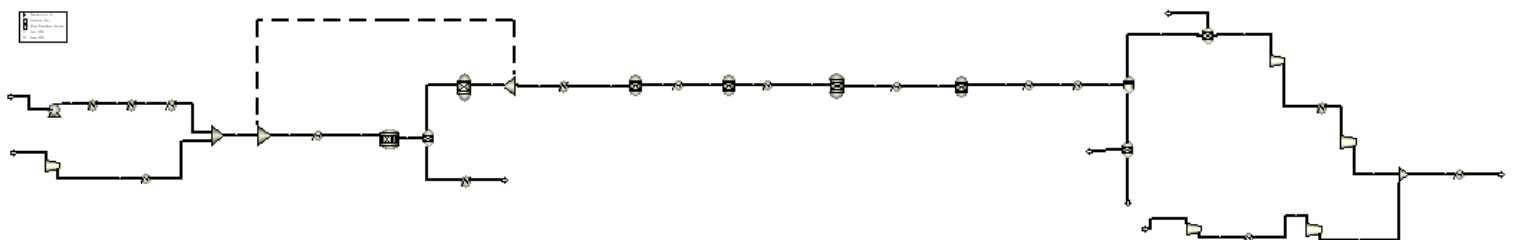


Figure 21 Model general overview

### 4.3 Model output

The results of process simulation are following reported: temperature (°C), pressure (bar), flowrate (kg/s), work (kW) and cooling/heat requirements (kW):

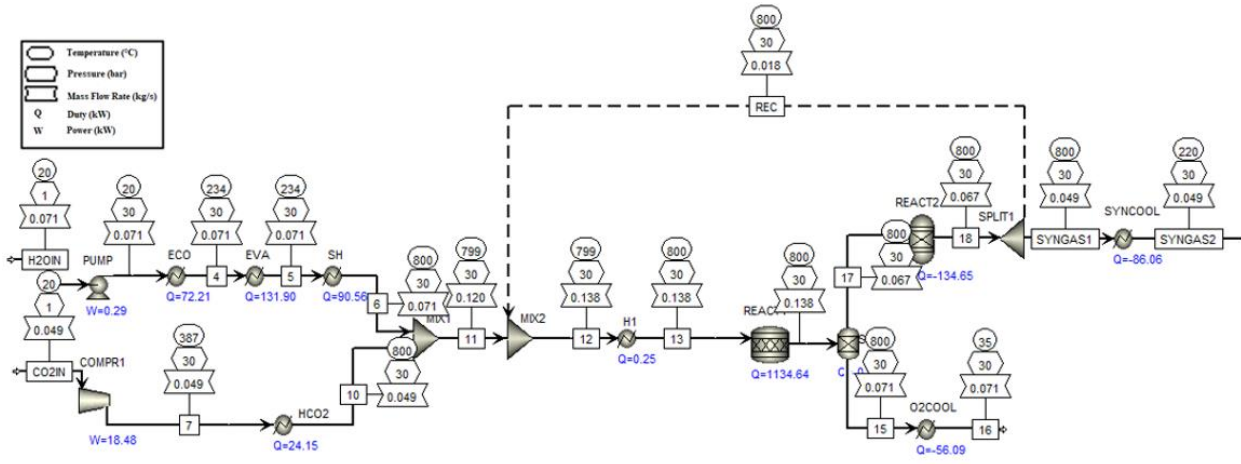


Figure 22 Results model part 1

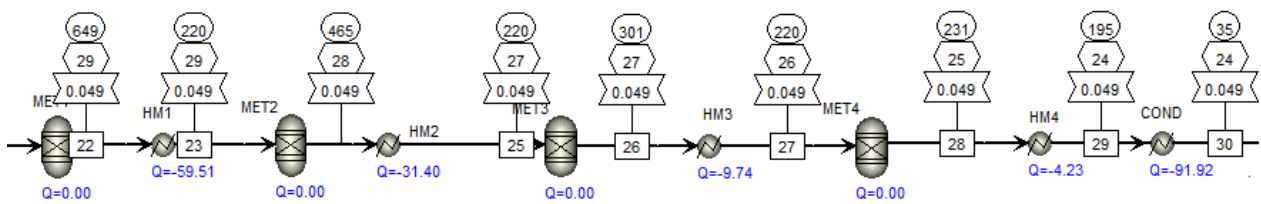


Figure 23 Results model part 2

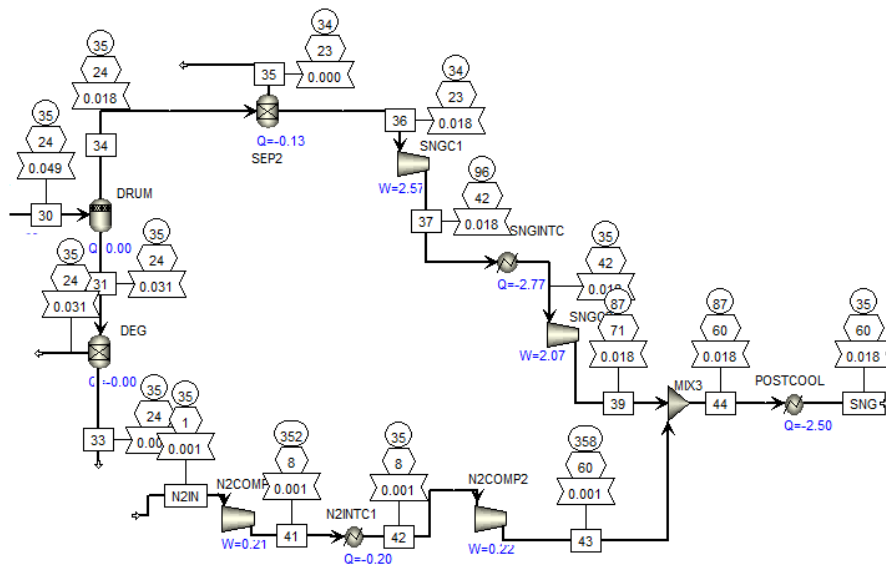


Figure 24 Results model part 3

The table below shows the gas composition at some key points in the analyzed plant:

Table 7 Gas composition at some key points

Component	Cathode inlet (before the SOEC)	Cathode outlet (after the SOEC)	Methanation inlet	Methanation outlet	SNG outlet
H <sub>2</sub> O	66.4%	26.1%	26.1%	60.1%	-
CO <sub>2</sub>	18.3%	5.1%	5.1%	0.2%	60 ppm
H <sub>2</sub>	10%	45%	45%	0.6%	1.6%
CO	1.8%	8.2%	8.2%	0.2 ppm	0.4 ppm
O <sub>2</sub>	-	-	-	-	0
CH <sub>4</sub>	3.5%	15.6%	15.6%	39.1%	96.5%
N <sub>2</sub>	-	-	-	-	2.2%

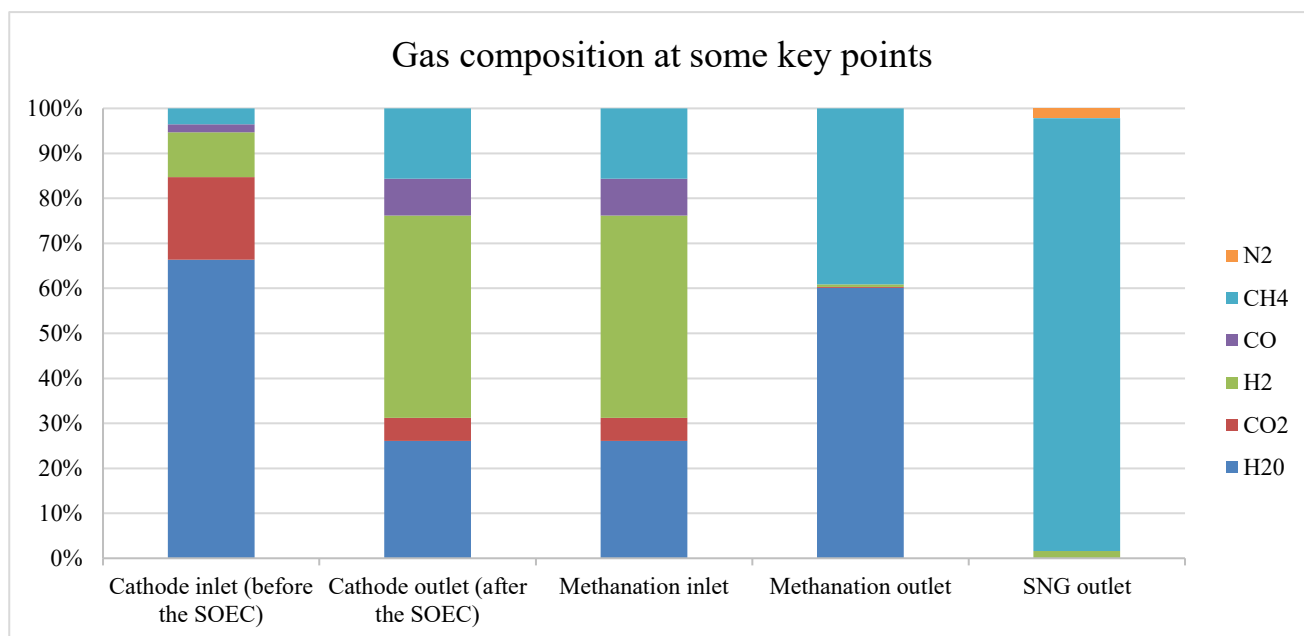


Figure 25 Gas composition at some key points

The cathode outlet is composed of hydrogen, water, carbon dioxide, carbon monoxide and methane. The molar fractions of hydrogen and steam are respectively higher than carbon monoxide and carbon dioxide. This is because of the larger quantity of H<sub>2</sub>O involved in co-electrolysis with

respect to CO<sub>2</sub>, to respect the defined syngas composition entering in the methanation section. The concentration of methane is quite high due to the operating pressure of the stack. The recirculated stream (REC) is 26.9 % of the total exiting from the SOEC cathode. The model has been developed with the cathode outlet gas feeding the methanation inlet. The stoichiometric relationship between hydrogen, carbon monoxide and carbon dioxide, is verified substituting the concentration reported in the table above with the “SYNGAS\_COMP=3” respected. At the methanation section outlet there is an elevated water content due to the reactions stoichiometry (considering the methanation section as control volume, the hydrogen utilization is around 99%). The reactant ratio (RR) (the fraction of water and carbon dioxide feeding the cathode) is 84.7%. The recirculated water, useful to avoid excessive consumption, is recovered by condensation of the syngas flowing out from the methanation section and is 43.7% of the water inlet. Furthermore, it has been verified that Wobbe index (WI) and the High Heating Value (HHV) meet the prescribed quality standards for the state (950 Btu/scf < HHV < 1235 Btu/scf and 1279 Btu/scf < WI < 1385 Btu/scf).

*Table 8 Plant parameters*

<b>Wobbe Index (WI)</b>	981 Btu/scf
<b>Higher Heating Value (HHV)</b>	1320 Btu/scf
<b>SNG production</b>	66.2 kg/h
<b>H<sub>2</sub>O recovered</b>	43.7 %
<b>H<sub>2</sub>O requirement</b>	252.3 ton/yr.
<b>CO<sub>2</sub> requirement</b>	309.1 ton/yr.
<b>Recirculated mixture at cathode inlet</b>	26.9%
<b>Reactant Ratio (RR)</b>	84.7%
<b>Heating requirement</b>	318.82 kW
<b>Cooling requirement</b>	344.42 kW

## 4.4 Thermal integration and energy performance

The methanation section makes available a large quantity of heat, because of the exothermic behavior of the involved reactions, which can be used for reactants pre-heating. In this chapter mass and energy streams are thermally integrated in a heat exchanger network (HEN) able to minimize the cooling and heating requirements. The heat-feed of inlet water was divided in three parts (economization, evaporation and superheating steps) because of the different specific heat ratio taken by the stream. The same consideration holds for syngas cooling after the last methanator. The water condensation takes place in a heat-exchanger section separated from the previous one with gas phase only. Aspen Energy Analyzer® was used to obtain target values performing the pinch analysis.

Table 9 Co-electrolysis + methanation: streams involved in pinch analysis.

NAME	TYPE	INLET T[°C]	OUTLET T[°C]	Gc [kW/K]	ENTHALPY [kW]
1	C	20	233.1	0.339	72.21
2	C	233.1	234.1	131.9	131.90
3	C	234.1	800	0.160	90.56
4	C	387	800	0.059	24.15
5	H	800	35	0.073	56.09
6	H	800	220	0.148	86.06
7	H	649	220	0.139	59.51
8	H	465	220	0.128	31.40
9	H	301	220	0.120	9.74
10	H	231	195	0.118	4.23
11	H	195	35	0.575	91.92
12	H	96	35	0.045	2.77
13	H	87	35	0.048	2.50
14	H	352	35	6.31E-04	0.2

The letter “C” means cold fluid and the letter “H” hot fluid. The  $\Delta T_{\min}$  was set to 15°C comparing the total heat exchanger (HE) target area (shell and tube HEs have been selected) and the hot utility target. The analyzed interval is between  $\Delta T_{\min}=10$  °C and  $\Delta T_{\min}=20$ °C. The heat transfer coefficients necessary to compute the HEN area were derived from literature data according to

fluids involved and their physical state (liquid, gas at different pressures, condensing or evaporating fluid, etc.) (26).

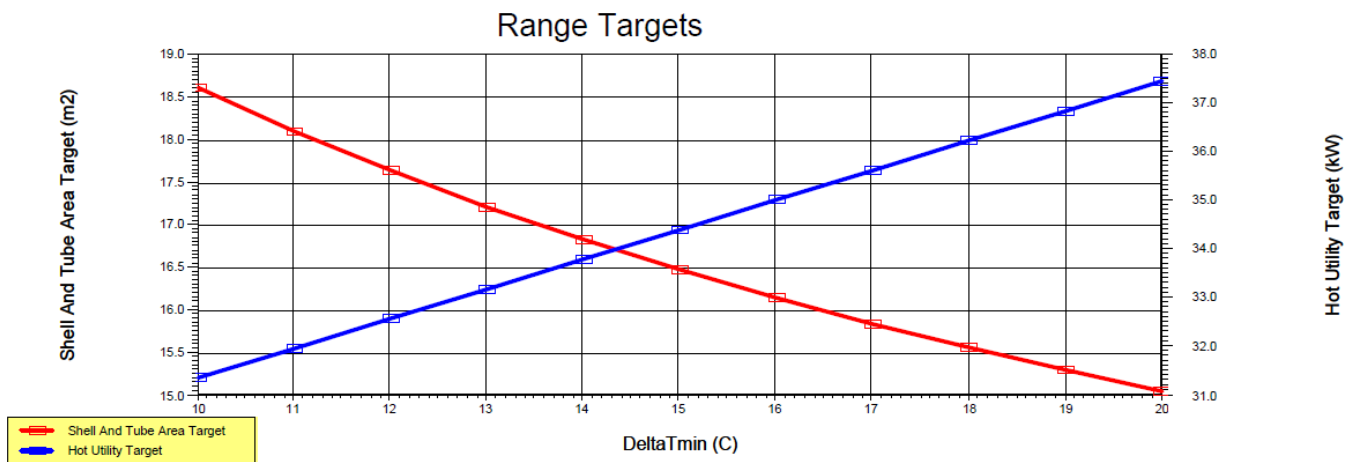


Figure 26 Range targets for Delta T<sub>min</sub>

Figure 24 shows the curves built by evaluating the enthalpy balance for each temperature interval.

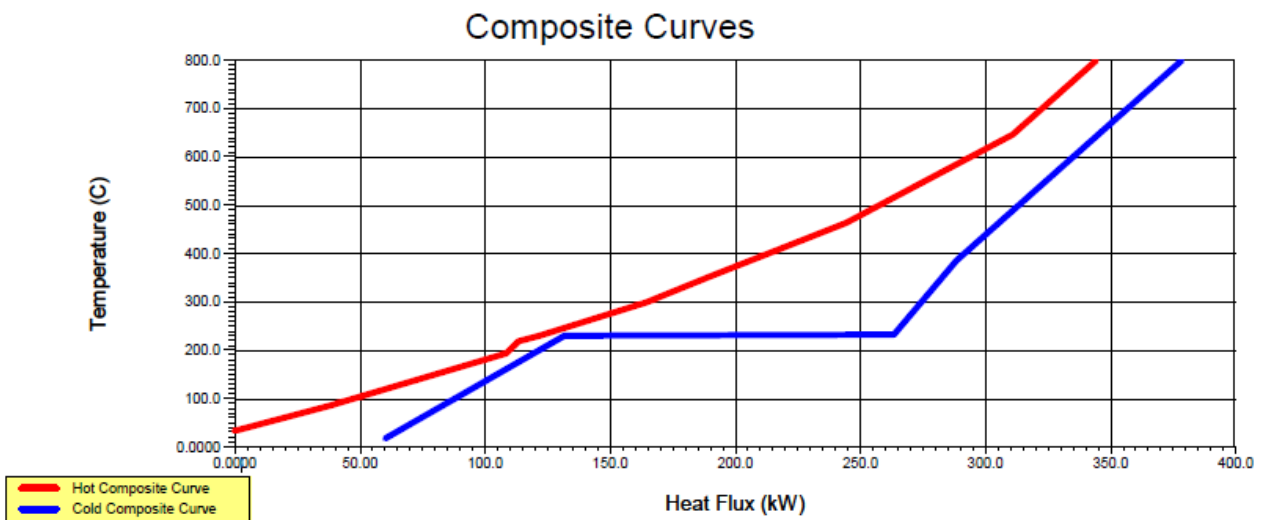


Figure 27 Composite Curves

In theory, when hot and cold composite curve are overlaid, it means that in a certain zone of the system cold fluid temperature is higher than hot fluid. The cold composite curve must be right shifted until the minimum difference between hot and cold curves is equal to  $\Delta T_{min}$  defined. According to composite curves construction methodology three zones should be highlighted:

- “Pinch point”, in which minimum temperature difference between hot and cold fluids occurs.

- External heat requirements represented by the difference between hot and cold composite curves in the right side of the chart.
- Waste heat represented by the difference between hot and cold composite curves in the left side of the chart.

A “plateau” appears corresponding to the evaporation of reactant pressurized water. “Pinch” occurs when water is at saturated liquid condition. In these systems an external energy input is necessary. This conclusion could be guessed also considering that the highest temperature of a cold fluid coincides with that of a hot fluid (800 °C). Since  $\Delta T_{\min}$  is not equal to 0, it is impossible to realize a complete heat exchange without external source. Results show also that  $T_{pp,HOT}=248.1$  °C and  $T_{pp,COLD}=233.1$ °C with minimum heating and cold needs of 34.42 kW and 60.02 kW.

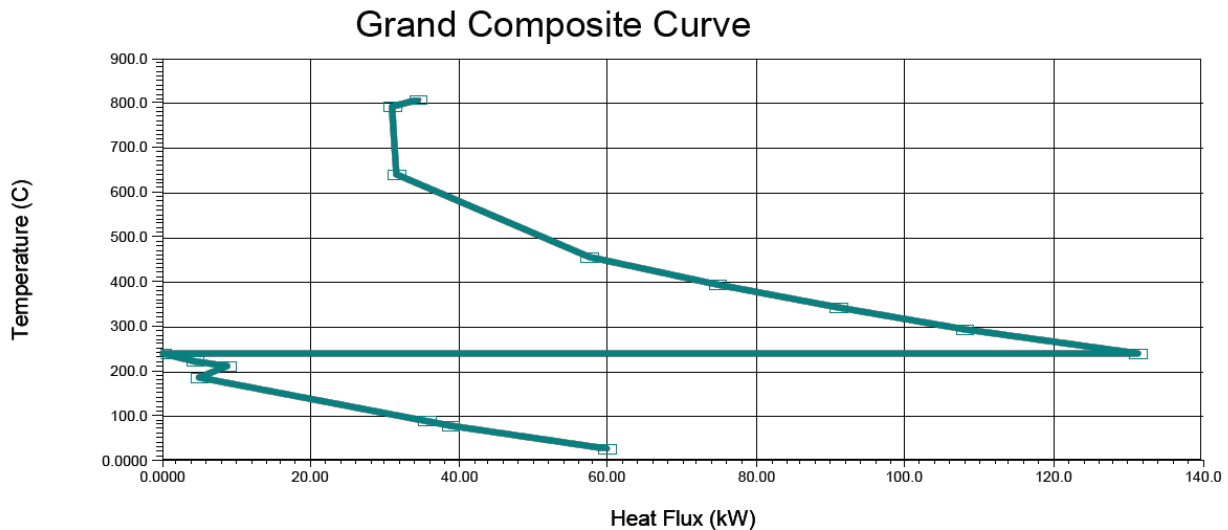


Figure 28 Grand composite curve

Figure 27 shows the grand composite curve (GCC) for the constructed problem using the data given in Table 9. The curve indicates not only the cold and the hot utility target, but also provides an opportunity to find at what level of temperature they are needed. Thus, there is no need to supply all the utility heating at the highest temperature interval. Instead, a considerable amount of heat can be supplied at lower temperatures bringing down the utility cost. In GCC the pinch is also easily identified as the point where net heat flow is 0. At this point the GCC touches the temperature axis. Thermal integration plays a key role in the performance optimization. As remarked in Tab.8, without thermal integration the external heating and cooling requirements would be 319 kW and 345 kW.

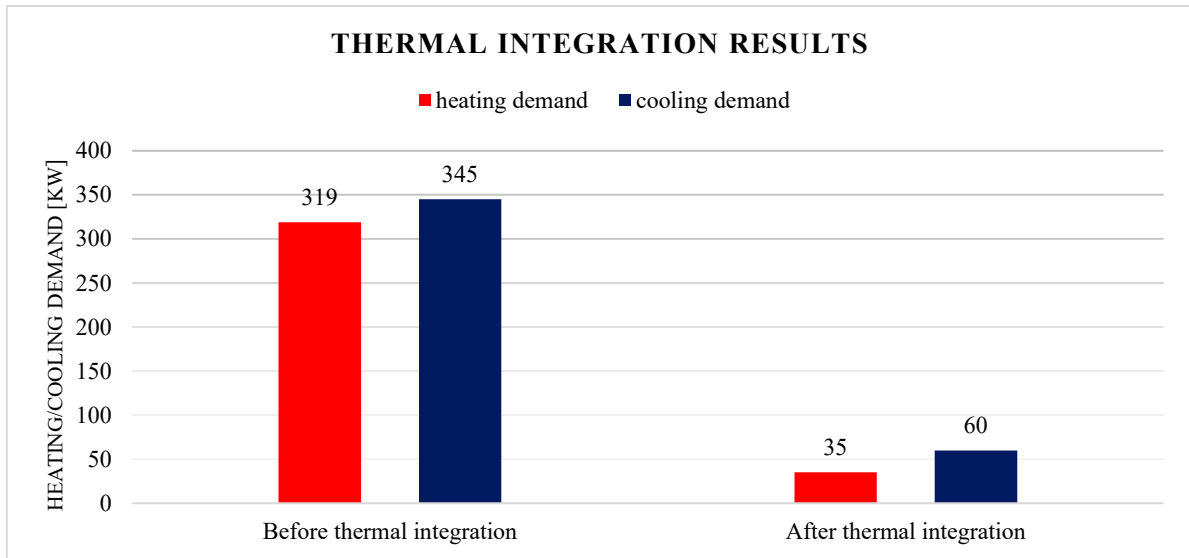


Figure 29 Thermal integration - external requirements

A well-designed thermal integration seems to be essential for this type of system. Considering the configuration for the minimum energy requirement (MER), the 89% and the 82.5% of the heating and cooling demand might be saved. The main results of the pinch analysis are reported in the table below:

Table 10 Pinch analysis main results

Plant Design	Value
$\Delta T_{\min}$	15 °C - 59 °F
$T_{pp,hot}$	248.1°C - 478.6 °F
$T_{pp,cold}$	233.1 °C - 451.6 °F
External heating requirement	35 kW
External cooling requirement	60 kW
Energy savings	85.7 %
Number of units for MER	20

At this point, the overall efficiency of the plant can be calculated as the ratio between the chemical power associated with generated synthetic natural gas and total power input [kW].

$$(4.8) \eta_{plant} = \frac{W_{ch,SNG}}{W_{el} + Q_{ext}} = \frac{LHV_{SNG} * G_{SNG}}{W_{el} + Q_{ext}}$$

The LHV [kJ/kg] of SNG was calculated considering its composition after the blending with the inert stream (N<sub>2</sub>) considering both methane and hydrogen as fuel. G<sub>SNG</sub> is the mass flowrate expressed in [kg/s]. The total electrical power input includes electricity fed to the SOEC, the power to drive pump and compressors. We assume that the external heating requirement (35 kW) is electrically provided while the cooling one is satisfied using an external utility (cooling water from 15 °C to 20°C). Furthermore, since the electricity is usually available from the grid, AC–DC loss of 2% is considered.

*Table 11 Components DC power demand*

<b>Component</b>	<b>DC power demand [kW]</b>
<b>SOEC</b>	1000
<b>Water Pump</b>	0.29
<b>CO<sub>2</sub> Compressor</b>	18.48
<b>SNG Compressor 1</b>	2.57
<b>SNG Compressor 2</b>	2.07
<b>N<sub>2</sub> Compressor 1</b>	0.22
<b>N<sub>2</sub> Compressor 2</b>	0.21
<b>External Heating Requirement</b>	35

The energy requirement (in terms of kWhel/kgSNG) for the analyzed systems can be evaluated as:

$$(4.9) \quad ER = \frac{W_{el(AC)}}{G_{SNG}}$$

Where G<sub>SNG</sub> is the synthetic natural gas mass flowrate [kg/h] and W<sub>el</sub> the total AC power input [kW]. The main results are synthetized in the following table:

Table 12 Plant results in terms of power input (electric) and output (chemical)

<b>Plant Design</b>	<b>Value</b>
<b>DC input</b>	1059 kW
<b>CO<sub>2</sub> compression</b>	19 kW
<b>Other compressions</b>	5 kW
<b>AC total input</b>	1081 kW
<b>LHV SNG</b>	21505 Btu/lb. - 50 MJ/kg
<b>SNG mass flow rate</b>	0.0184 kg/s
<b>Energy Requirement</b>	16.3 kWh/kgSNG
<b>SNG chemical power</b>	920 kW
<b>Overall plant efficiency (LHV basis)</b>	80.6 %

An increasing interest in PtG with electrolysis and synthetic fuels production was found especially in Europe, where electricity from wind and solar is exploited. In the Audi 6 MWel PtG plant in Werlte (Germany), a chemical-catalytic process under high pressure and high temperature alkaline electrolysis takes place. For the Audi plant an efficiency of 70% (on HHV basis) is reported (27). Assuming a SNG final composition equal to our model, an energy requirement of 19.8 kWh/kgSNG was calculated. The PEM electrolysis takes usually about 66 kWh/kgH<sub>2</sub> including the hydrogen compression (28). The developed model based on SOEC co-electrolysis 16.3 kWh/kgSNG. The LHV of H<sub>2</sub> is usually around 2.5 times the LHV of methane (29), making our process 35-40 % more efficient. Further research studies (30) provide an estimation to assess the PtG process efficiency for PEM/AEL electrolysis with subsequent methanation. Here too, an overall efficiency around 70% (adopting a thermal recovery) is reported. In both cases the efficiencies of these models are significantly lower than ours (80.6%). It is worth emphasizing that the overall efficiency is highly dependent on how the thermal integration is performed. In most cases is preferred to set aside the minimum energy requirement target, since reducing the heat exchangers surface results more economic convenient, despite a subsequent decrement of the overall plant efficiency.

## 4.5 Economic analysis: evaluation of the capital cost

In this section the plant capital costs for each item is evaluated. The thermal integration and is further extended to design the heat exchanger network (HEN), which will represent an important investment cost of the whole plant. Solid oxide cells degradation was also considered since implies the installation of additional active area with consequent impact on economics. The methodology used was developed by National Energy Technology Laboratory (NETL) (1) (2).

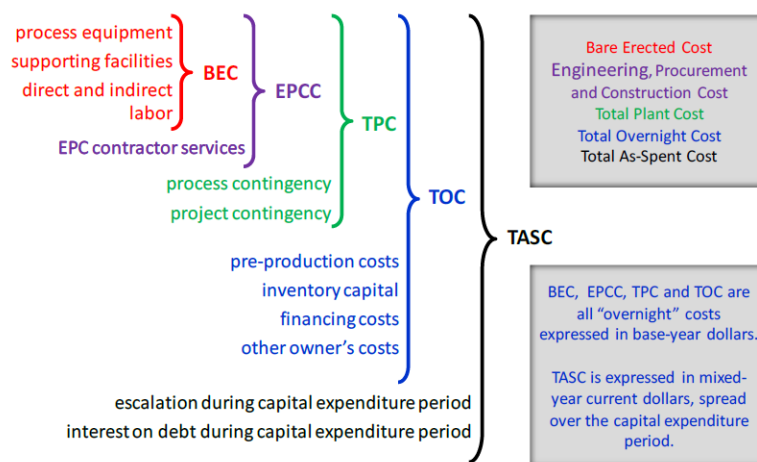


Figure 30 Capital Cost Levels and their Elements

As illustrated by Figure 28, this methodology defines capital cost at five levels: BEC, EPCC, TPC, TOC and TASC. BEC, EPCC, TPC and TOC are “overnight” costs and are expressed in “base-year” dollars. The base year is the first year of capital expenditure. TASC is expressed in mixed, current-year dollars over the entire capital expenditure period, which is assumed in most NETL studies to last five years for coal plants and three years for natural gas plants.

### Bare Erected Cost (BEC)

BEC comprises the cost of process equipment, on-site facilities and infrastructure that support the plant (e.g., shops, offices, labs, road), and the direct and indirect labor required for its construction and/or installation (1) (2). The cost of EPC services and contingencies are not included in BEC.

## **Engineering, Procurement and Construction Cost (EPCC)**

EPCC comprises the BEC plus the cost of services provided by the engineering, procurement and construction (EPC) contractor (1) (2). EPC services include: detailed design, contractor permitting (i.e., those permits that individual contractors must obtain to perform their scopes of work, as opposed to project permitting, which is not included here), and project/construction management costs.. EPCM contractor services are estimated at 8 to 10 % of BEC.

## **Total Plant Cost (TPC)**

TPC comprises the EPCC plus project and process contingencies (1) (2). Process and project contingencies are included in estimates to account for unknown costs that are omitted or unforeseen due to a lack of complete project definition and engineering. Contingencies are added because experience has shown that such costs are likely, and expected, to be incurred even though they cannot be explicitly determined at the time the estimate is prepared. Capital cost contingencies do not cover uncertainties or risks associated with: scope changes, changes in labor availability or productivity, delays in equipment deliveries, changes in regulatory requirements, unexpected cost escalation and performance of the plant after startup (e.g., availability, efficiency). Process contingency is intended to compensate for uncertainty in cost estimates caused by performance uncertainties associated with the development status of a technology. Process contingencies are applied to each plant section based on its current technology status. As shown in Table 13, International Recommended Practice 16R-90 provides guidelines for estimating process contingency. They are typically not applied to costs that are set equal to a research goal or programmatic target since these values presume to reflect the total cost. AACE 16R-90 states that project contingency for a “budget-type” estimate (AACE Class 4 or 5) should be 15% to 30% of the sum of BEC.

Table 13 AACE Guidelines for Process Contingency

Technology Status	Process Contingency (% of Associated Process Capital)
New concept with limited data	40+
Concept with bench-scale data	30-70
Small pilot plant data	20-35
Full-sized modules have been operated	5-20
Process is used commercially	0-10

### Total Overnight Capital (TOC)

TOC comprises the TPC plus all other overnight costs, including owner's costs (1) (2). It considers the following items:

- Pre-production costs, including waste disposal cost for one month and an additional term (2% of TPC).
- Inventory capital estimated at 0.5% of TPC for spare parts.
- Land cost.
- Financing cost assessed at 2.7% of TPC, which covers the cost of securing financing (excluding interest during construction).
- Other owner's costs, estimated at 15% of TPC, including preliminary feasibility studies, local economic development, construction or improvement of infrastructures outside of site boundaries, legal fees, permitting costs and owner's engineering (staff for a third-party advice helping the owner).

### The Total As-Spent Capital (TASC)

TASC is the sum of all capital expenditures as they are incurred during the capital expenditure period including their escalation (1) (2). TASC also includes interest during construction. For

scenarios that adhere to the global economic assumptions and utilize one of the finances (1), the multipliers shown in Table 14 can be used to translate TOC to TASC to account for the impact of both escalation and interest during construction.

Table 14 TASC/TOC Factors. Investor Owned Utility (IOU) and Independent Power Producer (IPP)

<b>Finance Structure</b>	<b>High Risk IOU</b>		<b>Low Risk IOU</b>	
Capital Expenditure Period	Three Years	Five Years	Three Years	Five Years
TASC/TOC	1.078	1.140	1.075	1.134
<b>Finance Structure</b>	<b>High Risk IPP</b>		<b>Low Risk IPP</b>	
Capital Expenditure Period	Three Years	Five Years	Three Years	Five Years
TASC/TOC	1.114	1.211	1.107	1.196

Cost estimates in most NETL studies have an expected accuracy range of -15%/+30%. Purchasing costs of equipment (PEC) are usually available from the literature. Typically happens that a price is known for a different size than what modeled. In order to scale each equipment price according to its size (or its capacity) the following equation can be adopted (31):

$$(4.10) \frac{PEC_1}{PEC_2} = \left(\frac{C_1}{C_2}\right)^\gamma$$

C represents the equipment cost attribute (size or capacity) and  $\gamma$  is a cost scaling factor ( $<1$ ). The cost attribute can be the power for compressors, reactor volume for vessels and heat exchange area for heat exchangers. The scaling factor or cost exponent depends on the specific equipment type. It is generally set to a default value of 0.6 giving the “six-tenths-rule” (31). When reference costs for particular sizes are not available, mathematical expressions (for various type of equipment) that link the purchasing cost of equipment to its cost attribute. The general equation used in this report is (31):

$$(4.11) \log_{10} PEC_0 = k1 + k2 * \log_{10}(C) + k3 * [\log_{10}(C)]^2$$

where k1, k2 and k3 are constant values depending on the specific equipment type. Equation 4.10 gives the PEC for components operating at atmospheric pressure and a defined temperature level. Pressure effects are considered through the pressure factor  $F_P$ . The equation to evaluate  $F_P$  is (31) :

$$(4.12) \log_{10} F_P = z_1 + z_2 * \log_{10}(p) + z_3 * [\log_{10}(p)]^2$$

$z_1$ ,  $z_2$  and  $z_3$  are constant values depending on the equipment type and  $p$  is pressure expressed in bar. The effect of the temperature (and the material choice), is influenced by a material factor  $F_M$ , which can be obtained from diagrams and tables. In conclusion, the general formula to calculate the BEC can be expressed:

$$(4.13) BEC = PEC_0 * F_{BM} = PEC_0 * (B_1 + B_2 * F_M * F_P)$$

The value  $F_{BM}$  is called “bare module factor”. In general, the value of  $F_P$  and  $F_M$  is larger or equal than 1.  $B_1$  and  $B_2$  is given for different components. For some types of equipment, the bare module factor  $F_{BM}$  is directly provided, and the calculation of  $F_P$  and  $F_M$  can be avoided.

Sometimes equipment costs refer to a specific year. All the costs reported by (31) are expressed in 2007\$. To escalate them to 2017\$, a scaling can be applied:

$$(4.14) \frac{PEC_a}{PEC_b} = \frac{CI_a}{CI_b}$$

$a$  and  $b$  refer to the time when the cost is known and the base year, respectively.  $CI$  is the Chemical Engineering Plant Cost Index (CEPCI), a time-dependent parameter. CEPCI for 2007 is 525.4, CEPCI for 2017 is 567.5.

*Table 15 Main economic assumptions. Financing distribution between debt and equity and their interest rate for high risk investor owned utility projects. Distribution of total overnight capital over capital expenditure period for natural gas plant case (1)*

<b>Debt/equity share</b>	45-55%
<b>Debt/equity interest rate</b>	5.5-12%
<b>Capital cost escalation during capital expenditure period</b>	3.6%
<b>Distribution of TOC over capital expenditure period</b>	3 years period: 10%, 60%, 30%
<b>Income tax rate</b>	38% Effective (34% State, 6% Federal)
<b>Capital Depreciation</b>	20 years, 150 declining balance
<b>Repayment term of debt</b>	15 years
<b>Escalation of COE (revenue), O&amp;M Costs, Fuel Costs (nominal annual rate)</b>	3.0%
<b>Operational period</b>	30 years

*Table 16 Main assumption for EPCC, TPC and TOC capital cost levels. For scenarios that adhere to the economic assumptions the multipliers 1.078 can be used to translate TOC to TASC to account for the impact of both escalation and interest during construction (1).*

<b>EPCC</b>	+9%BEC
<b>TPC</b>	+20%EPCC
<b>TOC</b>	+20.2%TPC
<b>TASC</b>	+10.78%TOC

### 4.5.1 SOEC (stack, added systems, installation)

The SOEC stack cost is one of the most critical for our plant. The high CAPEX is currently the greatest impediment to the successful diffusion of stationary systems. Researches (32) show that increasing system size has a larger impact on the total cost than increasing manufacturing volume for the same annual cumulative production increase in MWe. This is driven by the BOP costs per kWel being more favorable in moving to a higher system power vs. a higher volume at the same system power, whereas the reduction in stack costs are comparable in moving to either higher power or higher volume.

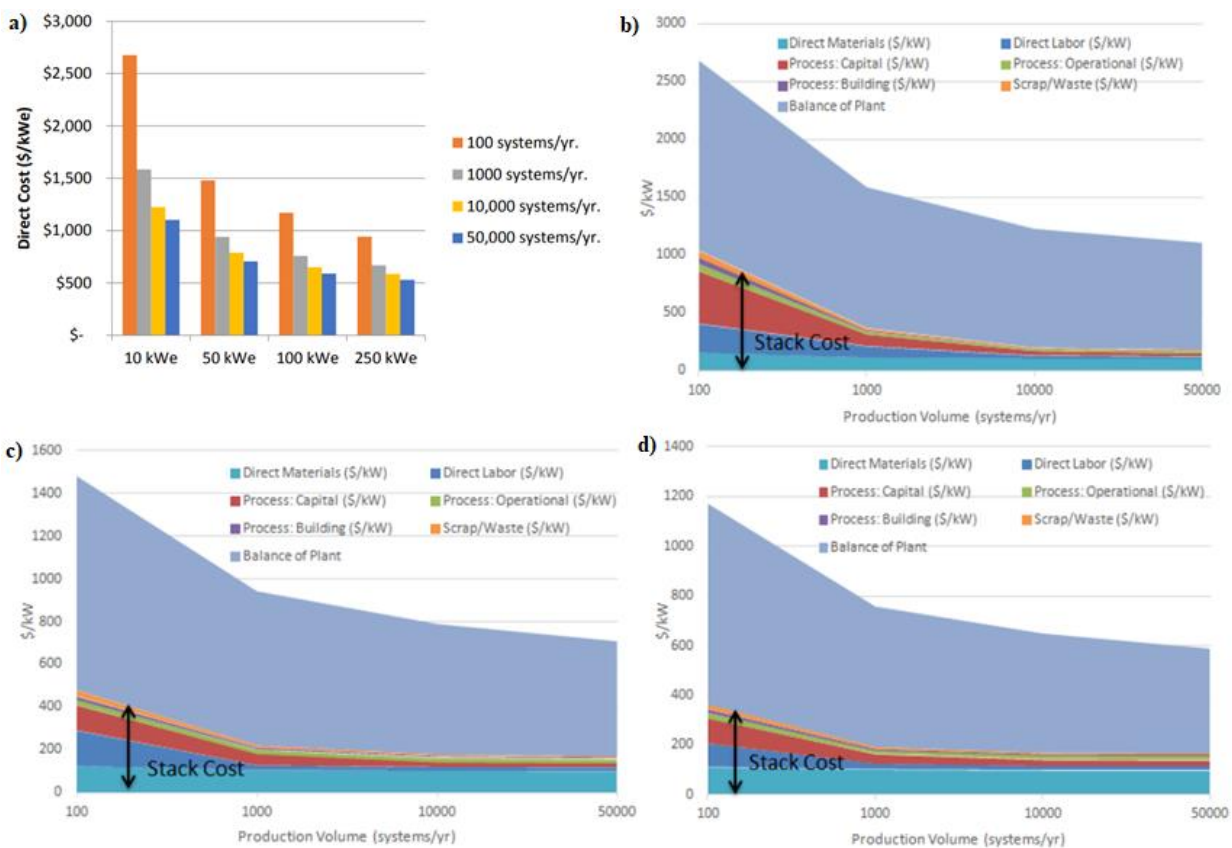


Figure 31 a) Total direct costs (not including markup and installation costs) for systems as a function of system size and manufacturing volume (10,50,100,250 kWe), b), c) and d) Dependence of direct cost components as function of annual manufacturing volume for 10-kWe, 50-kWe, and 100-kWe system sizes. (32).

It can be observed that the BOP cost fraction of the overall direct system cost is in all cases greater than 60% of the system cost. In general, at the lower system sizes, the BOP becomes a greater portion of overall cost as manufacturing volume increases, due to large reduction in stack cost which far outstrip reductions in BOP cost. At the higher system sizes (100kWe and 250kWe), the BOP fraction is roughly stable at 70% of overall costs since reductions in BOP cost as a function of

volume are similar to reductions in the stack cost. The largest stack cost reduction is observed at lower stack size and lower annual volumes, due large increases in tool utilization as volume is increased. Note that the stack costs leveling off once a certain level of annual volume has been reached, e.g., the stack reduction in cost is very small in moving from 100kWe, 10,000 systems per year to 50,000 systems per year, or from 1GWe to 5GWe. Total direct costs including corporate markup and installation costs, were estimated assuming a corporate markup of 50% and an installed cost adder of 33%, following the report by Wei et al. (2014).

Table 17 Direct system cost with corporate markup and installation (32)

<b>Total direct cost with corporate markup and installation [US\$/kW<sub>e</sub>]</b>				
	<b>Annual manufacturing volume [systems/year]</b>			
<b>System size [kW<sub>e</sub>]</b>	<b>100</b>	<b>1.000</b>	<b>10.000</b>	<b>50.000</b>
1	29.290	16.584	12.976	11.471
10	5.341	3.160	2.441	2.201
50	2.952	1.877	1.572	1.410
100	2.337	1.514	1.297	1.176
250	1.879	1.334	1.170	1.058

In this work the installation of four systems of 250 kW<sub>e</sub> was assumed, considering initially a target value of 1.058 \$/kW<sub>e</sub> (50.000 systems/year). The system impact on capital cost is after assessed varying the cost from 1.879 US\$/kW<sub>e</sub> to 1.058 US\$/kW<sub>e</sub>.

$$TPC_{SOEC} = \text{specific cost} * \text{size} = 1058 \frac{\text{US\$}}{\text{kW}_e} * 1000 \text{ kW}_e = 1.058.000 \text{ US\$}$$

## 4.5.2 Methanation line

All the reactors in the methanation line are packed bed reactors with thermal insulation. The initial catalyst fill (expressed in m<sup>3</sup>) has been estimated from a document of NETL (33) through a linear interpolation between catalyst volume and CH<sub>4</sub> production rate. The overall catalyst volume was divided for 4, which represents the number of reactors in our model, assuming the same volume for each methanation reactor. Furthermore, this value has been increased by 50% to account for the volume of the pressurized vessel containing the catalyst. The reactor volume (V) represents the equipment cost attribute for vertical process vessels in equation 4.11. For this case, the pressure factor (F<sub>P</sub>) is given by the following formula (31):

$$(4.15) \quad F_P = \frac{(p + 1) * \left(\frac{D}{2}\right) * (850 - 0.6 * (p + 1)) + 0.00315}{0.0063}$$

P is pressure in [bar] and D is the diameter [m]. The diameter (D) of the reactor is unknown. To allow the diameter calculation starting from volume, an L/D factor of 5 (where L is the length of the reactor) was chosen. Material factor (F<sub>M</sub>), and constant values B<sub>1</sub> and B<sub>2</sub> for vertical vessels were taken from (31). In general, the material factor changes with the temperature involved, since different materials should be implemented.

- If T < 350 °C carbon steel is used (CS) [i.e. used in this case]
- If T > 350 °C and T < 550 °C stainless steel is used (SS)
- If T > 550 °C Ni-alloy is used (Ni)

Catalyst fill is usually entirely replaced every four years. In this work it was not considered among the capital costs, but like an operational and maintenance cost in the next part.

*Table 18 Main constants and assumptions used for capital cost estimation for methanation line*

L/D	K1	K2	K3	F <sub>M</sub>	B1	B2
				CS		
5	3.4974	0.4485	0.1074	1	2.25	1.82

The BEC can be consequently calculated with equations 4.11 and 4.13. It is furthermore reported in 2017 US\$ using equation 4.14.

$$BEC_{2017US\$} = 18.316 \text{ US\$}$$

### 4.5.3 Heat exchangers networks (HEN)

As it has been stated, most of the time the heat exchangers network adopted by the designers does not meet the minimum energy requirement, while it results in a compromise between energy savings and capital expenditure. A criterion of this type was adopted in this work taking advantage of the tool “recommended designs” provided by Aspen Energy Analyzer®. The CAPEX in terms of TPC is calculated by default with the input data for the pinch analysis (temperatures, enthalpy changes, HTC and external utilities). The software generates automatically several designs. It is possible to compare all the generated layouts in relative terms with respect than the target one.

Design	Total Cost Index [%]	Area [%]	Units [%]	Shells [%]	Cap. Cost Index [%]	Heating [%]	Cooling [%]
A_Design5	99.5	107.3	100.0	78.3	99.5	208.6	162.3
A_Design9	98.0	86.0	100.0	66.7	98.0	258.6	190.9
A_Design4	92.1	68.6	95.0	53.3	92.1	208.6	162.3
A_Design6	87.9	72.7	90.0	55.0	87.9	208.6	162.3
A_Design8	87.7	71.8	90.0	55.0	87.7	208.6	162.3
A_Design10	83.1	70.8	85.0	51.7	83.1	208.6	162.3
A_Design3	82.7	66.1	85.0	45.0	82.7	333.3	233.8
A_Design2	82.2	59.9	85.0	45.0	82.2	333.3	233.8
A_Design1	82.2	58.4	85.0	45.0	82.2	333.3	233.8

Figure 32 Recommended HEN designs relative to the target provided by Aspen Energy Analyzer®

The design 10, provides almost 20% of economic savings. The heating and cooling requirements are now 72 kW and 97 kW (against the 35 kW and 60 kW of MER). The number of installed units decreases from 20 to 17. The area and the shells are respectively the 85% and the 52 % of the MER. The new overall efficiency would amount to 75.7 % (-4.9%).

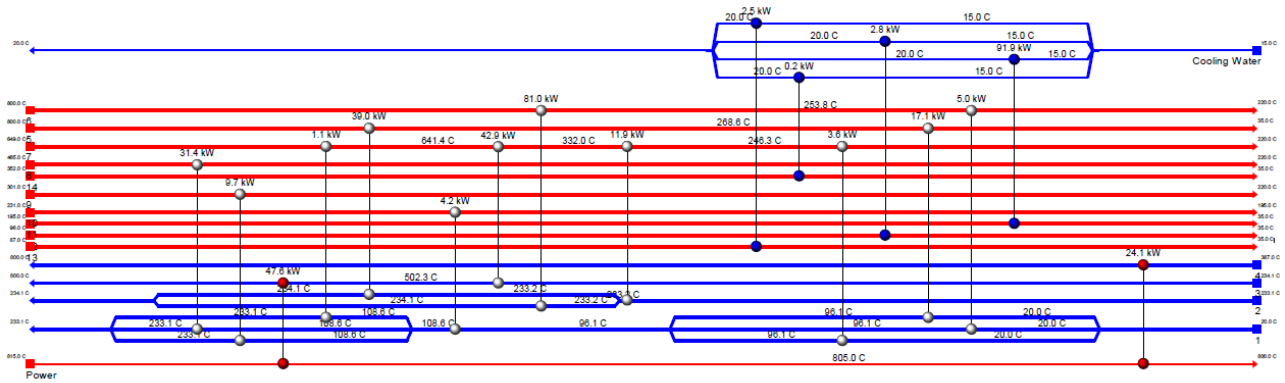


Figure 33 HEN economically optimized

$$TPC_{HEN} = 180.561 \text{ US\$}$$

#### 4.5.4 Water pump

To calculate the cost of the water pump, equations 4.11-4.14 were considered. The data are available for centrifugal pumps (31). The shaft power (in kW) is the equipment cost attribute.  $F_M$  used is equal to 1, whereas the pressure factor was estimated by using equation 4.12. BEC is obtainable by using equation 4.13 with suggested values for  $B_1$  and  $B_2$ . The BEC is reported in 2017 US\$ using equation 4.14.

Table 19 Main constants and assumptions used for capital cost estimation for methanation line

Size [kWel]	K1	K2	K3	Z1	Z2	Z3	FM	B1	B2
							CS		
0.3	3.3892	0.0536	0.1558	-0.3935	0.3957	0.00226	1	1.89	1.35

$$BEC_{2017US\$} = 10.844 \text{ US\$}$$

### 4.5.5 Zinc oxide guard bed

To protect both SOEC and methanation Ni-based catalysts from sulfur poisoning, a zinc oxide guard bed (ZOGB) was implemented. The purchase equipment cost was estimated through Eq. 4.10 and 4.14. The capacity is represented by the CO<sub>2</sub> volume flow rate in Nm<sup>3</sup>/min. Base capacity and cost, are taken from (33) and are equal to 450 Nm<sup>3</sup>/min and 793,000 \$, respectively. “Six-tenths-rule” is applied and the cost was escalated to 2017 US\$. F<sub>BM</sub> was derived from (33) and is equal to 1.18.

Table 20 Main constants and assumptions used for capital cost estimation for zinc oxide guard bed

<b>PEC<sub>1</sub></b> <b>[2011\$]</b>	<b>C<sub>1</sub></b> <b>[Nm<sup>3</sup>/min]</b>	<b>C<sub>2</sub></b> <b>[Nm<sup>3</sup>/min]</b>	<b>F<sub>BM</sub></b>
793.000	450	1.593	1.18

$$BEC_{2017US\$} = 34.206 \text{ US\$}$$

### 4.5.6 Compressors

In this part the cost for CO<sub>2</sub>, SNG and N<sub>2</sub> compression was calculated, respectively. The BEC for both carbon dioxide compression was estimated through the equations 4.11 – 4.14 with data from (31). According to the defined validity range the correlation for rotary compressors was used. The minimum size allowing for the use of rotary compressor values is 18 kW; For the other compressors the PEC<sub>0</sub> was estimated through equation 4.10 where power (kW<sub>el</sub>) is the equipment cost attribute in equation 4.10 and by setting the cost scaling factor  $\gamma$  equal to 0.84 (31). The bare module factor (F<sub>BM</sub>) is provided (assuming a value of 2.4) (31) and BEC is calculated. The BEC also in this case was expressed in 2017 US\$.

## CO<sub>2</sub> Compressor

Table 21 Main constants and assumptions used for capital cost estimation for CO<sub>2</sub> compressor

Size [kWel]	K1	K2	K3	F <sub>BM</sub>
19	5.0355	-1.8002	0.8253	2.4

$$\text{BEC}_{2017\text{US\$}} = 31.385 \text{ US\$}$$

## SNG Compressor #1

Table 22 Main constants and assumptions used for capital cost estimation for SNG compressor #1

Size [kWel]	K1	K2	K3	F <sub>BM</sub>	$\gamma$
3	5.0355	-1.8002	0.8253	2.4	0.84

$$\text{BEC}_{2017\text{US\$}} = 6.859 \text{ US\$}$$

## N<sub>2</sub> Compressor #1

Table 23 Main constants and assumptions used for capital cost estimation for N<sub>2</sub> compressor #1

Size [kWel]	K1	K2	K3	F <sub>BM</sub>	$\gamma$
1	5.0355	-1.8002	0.8253	2.4	0.84

$$\text{BEC}_{2017\text{US\$}} = 6.859 \text{ US\$}$$

## N<sub>2</sub> Compressor #2

Table 24 Main constants and assumptions used for capital cost estimation for N<sub>2</sub> compressor #2

Size [kWel]	K1	K2	K3	FBM	$\gamma$
1	5.0355	-1.8002	0.8253	2.4	0.84

$$BEC_{2017US\$} = 1.052 \text{ US\$}$$

## SNG Compressor #2

Table 25 Main constants and assumptions used for capital cost estimation for SNG compressor #2

Size [kWel]	K1	K2	K3	FBM	$\gamma$
1	5.0355	-1.8002	0.8253	2.4	0.84

$$BEC_{2017US\$} = 1.052 \text{ US\$}$$

## 4.5.7 Additional costs

Table 26 Main constants and assumptions used for capital cost estimation for plant control system

MICRO-PROCESSOR BASED PLANT CONTROL SYSTEM	Cost [2007\$/kWel]
Monitors, keyboards and other instrumentation	50 (34)

$$TPC_{2017US\$} = 54.006 \text{ US\$}$$

*Table 27 Main constants and assumptions used for capital cost estimation for additional costs for building and structures*

<b>ADDITIONAL STRUCTURES</b>	<b>Cost [2007\$/kWel]</b>
Buildings and structures inside the site boundary	25 (34)

$$\text{TPC}_{2017\text{US\$}} = 27.003 \text{ US\$}$$

*Table 28 Main constants and assumptions used for capital cost estimation for land purchasing*

<b>LAND [acre]</b>	<b>Cost [\$/acre]</b>
2	3000 (34)

$$\text{TPC} = 6.000 \text{ US\$}$$

## 4.5.8 Results – CAPEX

Table 29 Main results of the economic analysis, CAPEX [SOEC total system cost 1058 \$/kW]

COMPONENT	BEC [US\$]	EPCC [US\$]	TPC [US\$]	TOC [US\$]	TASC [US\$]
SOEC	-	-	1.058.000	1.271.716	1.408.807
METHANATION LINE	18.316	19.964	23.957	28.797	31.901
HEN	-	-	180.561	217034	240431
H <sub>2</sub> O PUMP	10.844	11.820	14.184	17.049	18.887
Zn OXIDE GUARD BED	34.206	37.285	44.741	53.779	59.577
CO <sub>2</sub> COMPRESSOR	31.385	34.210	41.052	49.344	54.663
SNG COMPRESSOR #1	6.859	7.476	8.972	10.784	11.946
SNG COMPRESSOR #2	6.859	7.476	8.972	10.784	11.946
N <sub>2</sub> COMPRESSOR #1	1.052	1.147	1.376	1.654	1.832
N <sub>2</sub> COMPRESSOR #2	1.052	1.147	1.376	1.654	1.832
PLANT CONTROL SYSTEMS	-	-	54.006	64.915	71.913
ADDITIONAL STRUCTURES	-	-	27.003	32.458	35.957
LAND PURCHASING	-	-	6.000	7.212	7.989
<b>TOTAL</b>			<b>1.470.199</b>	<b>1.767.180</b>	<b>1.957.682</b>

### Plant costs shared for each category



Figure 34 Plant costs shared for each category [SOEC total system cost 1058 US\$/kW]

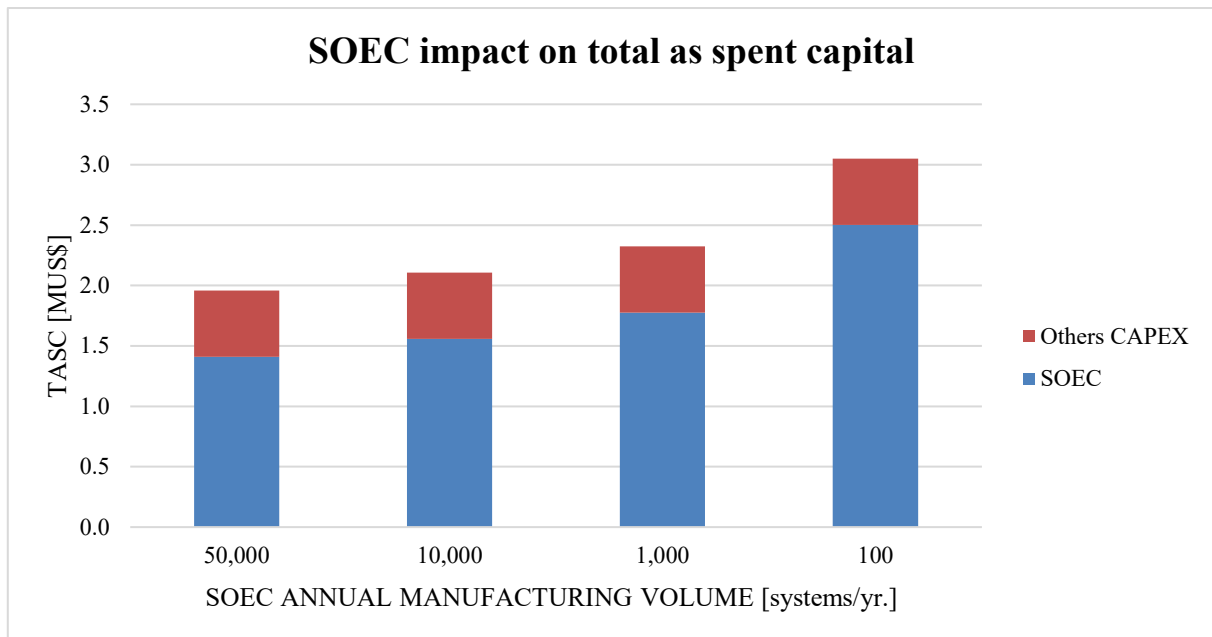


Figure 35 SOEC total system cost impact on TASC (1MWel Plant)

Figure 33 displays as the capital cost is highly dependent on the price of the SOEC system. TASC goes from 1.958 M\$ to 3.051 M\$ (+55.8%), increasing the cost of SOEC system (with corporate markup and installation) from 1058 US\$/kWel to 1879 US\$/kWel. An increase of the SOEC cost makes the CAPEX more and more dependent by the cost of this technology, strengthening what Figure 32 already displays with the target value (1058 US\$/kWel).

## 4.6 Economic analysis: evaluation of the operational cost

To evaluate the OPEX the utilization factor (or capacity factor) of the plant plays a crucial role. In general, the lower the capacity factor the higher will be the cost of product (COP), with a hyperbolic trend varying yearly operating hours, as shown in previous studies (35) (36).

### 4.6.1 Fixed operating and maintenance costs

The fixed costs are independent on plant utilization and are usually expressed in US\$/year. Operating labor, maintenance, administrative and insurance costs are considered in this section. The methodology developed by IEA Greenhouse Gas R&D Program was followed in this study (3) (4).

Table 30 Main constants and assumptions used for operational costs estimation for fixed costs

<b>Operating</b> (1-person half of the time, highly automated plant)	75.000 US\$/person/year
<b>Maintenance</b> (Labor 40%, Material 60%)	2% TPC (4)
<b>Administrative and support labor</b>	30% Operating + Maintenance Labor (3) (4)
<b>Insurance</b>	1% TPC (3) (4)

#### 4.6.2 Variable operating and maintenance costs

The variable costs are related to the plant utilization and can be expressed in US\$/h or US\$/yr. To maintain a constant SNG output with a decaying SOEC performance, spare capacity must be installed to compensate for the power density loss of operating stacks. The spare capacity is considered as a variable cost, since cell degradation is correlated to the yearly amount of plant operational hours. The CO<sub>2</sub> market pricing was analyzed more in detail, since its cost might be extremely variable. The price for pipelined CO<sub>2</sub> has historically been in the range of US\$9-US\$26 per ton, which incorporates the cost of the pipeline infrastructure (capital and operational costs). The Dakota Gasification Company's Great Plains Synfuels Plant pipes CO<sub>2</sub> 205 miles to Canada. In 2009 they sold US\$53.2m worth of CO<sub>2</sub>, whilst it produced 2.8Mton/y, suggesting a price of US\$19/ton produced (37) (38). For the catalyst consumption and Zinc oxide guard bed (ZOGB) sorbent replacement, a linear correlation with CH<sub>4</sub> production rate and the CO<sub>2</sub> consumption was assumed, scaling all the cost items (33). Waste disposal and demi-water costs were also considered in this section with costs from literature (33) (35) (39). The price of electricity is assumed as a variable (from 0 \$/MWh to 30 \$/MWh) observing the trend of the net load from CAISO from January 1 through June 30 of each year.

**California Independent System Operator average hourly day-ahead energy market prices**  
 January through June average  
 dollars per megawatthour

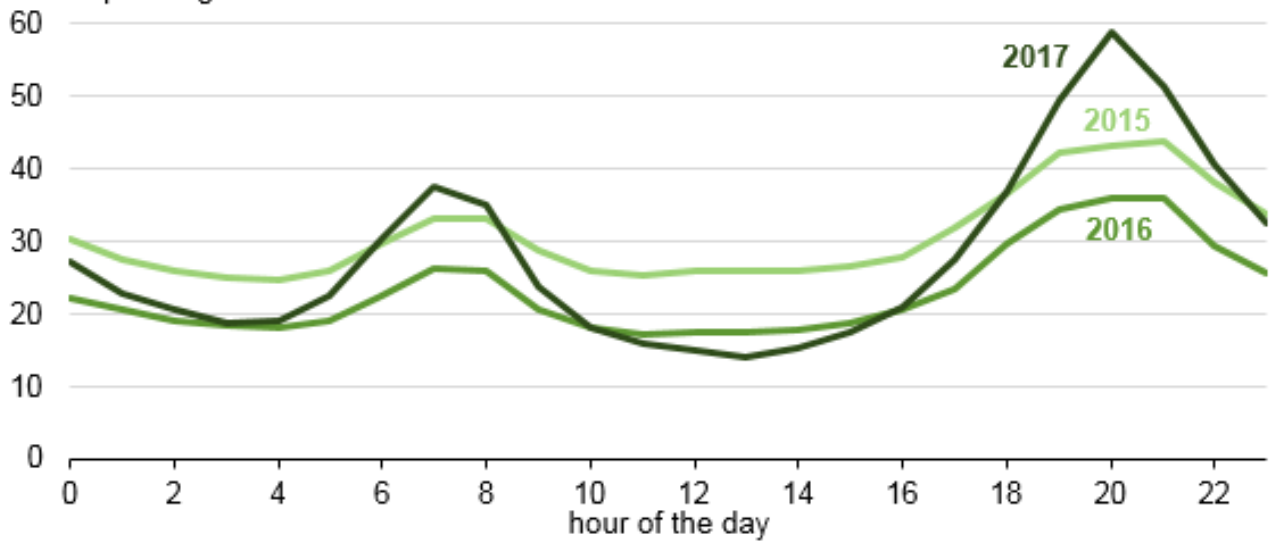


Figure 36 CAISO average hourly day-ahead energy market prices  
 [https://www.eia.gov/todayinenergy/detail.php?id=32172]

**California Independent System Operator (CAISO) average net electric load**  
 last week of March  
 gigawatts

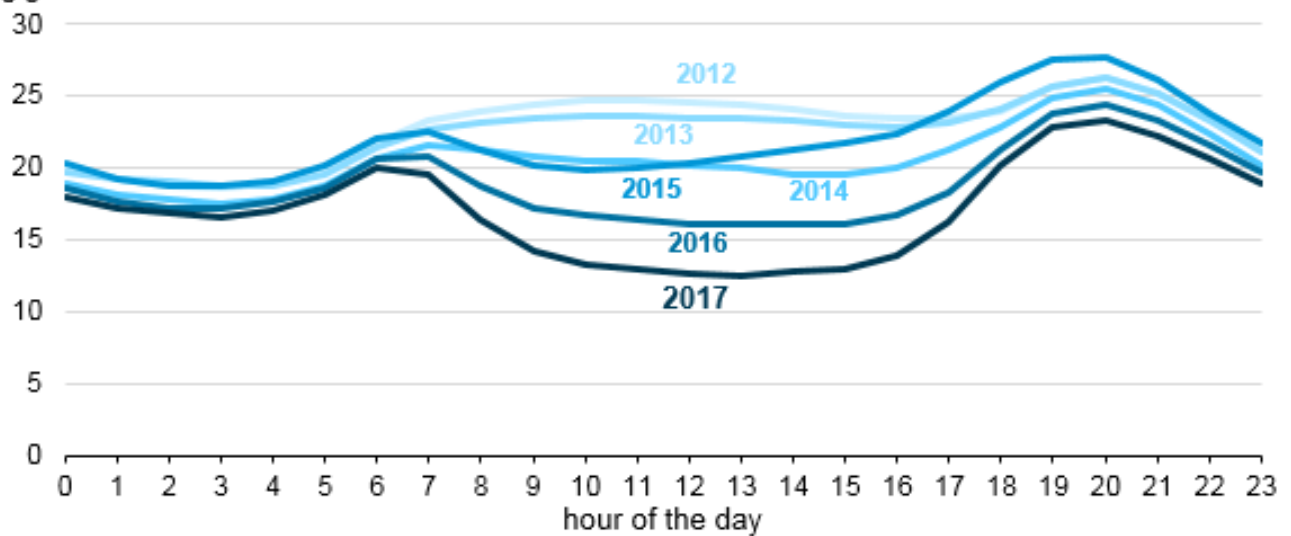


Figure 37 CAISO average net electric load [https://www.eia.gov/todayinenergy/detail.php?id=32172]

*Table 31 Main constants and assumptions used for operational costs estimation for variable costs*

<b>Operating hours</b>	1752 h/y
<b>Methanation Catalyst Cost</b>	\$440 /scf (33)
<b>ZOGB sorbent replacement</b>	12.5 \$/kg (33)
<b>Demineralized Water</b>	1 \$/ton (39)
<b>Nitrogen</b>	8 \$/ton (35)
<b>Average price of electricity</b>	0-30 \$/MWh (Variable)
<b>Carbon dioxide</b>	19 \$/ton (37) (38)
<b>Waste disposal</b>	16.23 \$/ton (33)
<b>SOEC substitution/spare parts</b>	2%/1000h (40)

### 4.6.3 Results – OPEX

Table 32 Main results of the economic analysis, OPEX

<b>Operational Expenditures</b>	<b>Costs [US\$/y]</b>
Operating labor	37.500
Maintenance	15.025
Administration	13.053
Insurance	7.513
FOM	73.091
Catalyst replacement	246
ZnO sorbent replacement	246
Demineralized water	252
Nitrogen	31
Carbon dioxide feedstock	5.872
SOEC substitutions/spare parts	11.880
Electricity	0-52.560
VOM	53.567
FOM+VOM	91.618-144.178

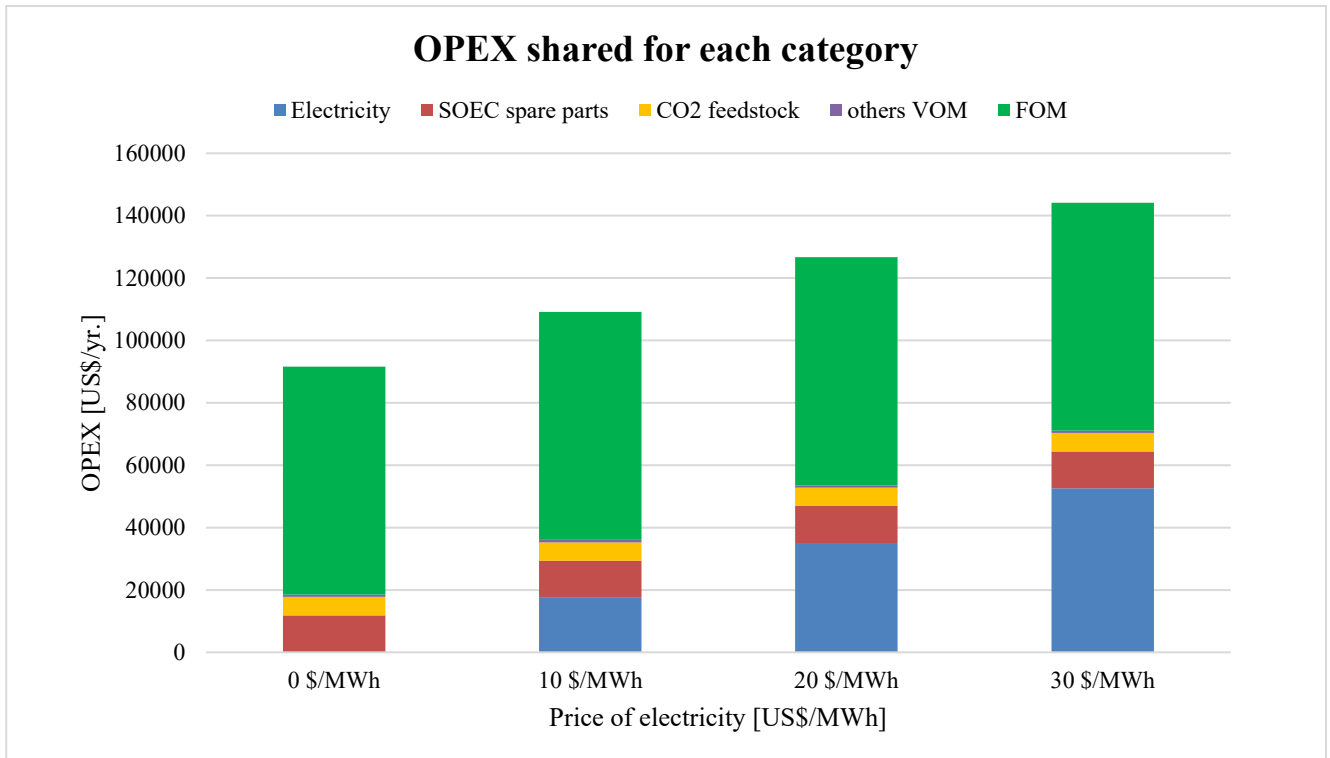


Figure 38 Operational costs shared for each category (1MWel Plant, CF=20%)

The operational expenditures go from 91.6 k\$/yr. (for 0 \$/MWh) to 144 k\$/yr. (for 30 \$/MWh) with an increment of 57.2%. The electricity contribution to OPEX can reach the 36% (worst case). Fixed and operating maintenance costs (labor, maintenance, administration & insurance) cover the majority of OPEX (from 80 to 51 %). This result is naturally linked to the plant operating hours. In fact, increasing the utilization factor would bring the price of electricity to have much more influence of on the OPEX.

## 4.7 Levelized cost of product

A simple investment analysis was performed in this section. With the previous assumptions the levelized cost of product (LCOP) was calculated as the value making the net present value equal to 0 after the operational period, maintaining the SNG price constant. An average annual inflation rate of 3.0% was assumed. This rate is equivalent to the average annual escalation rate between 1947 and 2008 for the U.S. Department of Labor's Producer Price Index for Finished Goods.

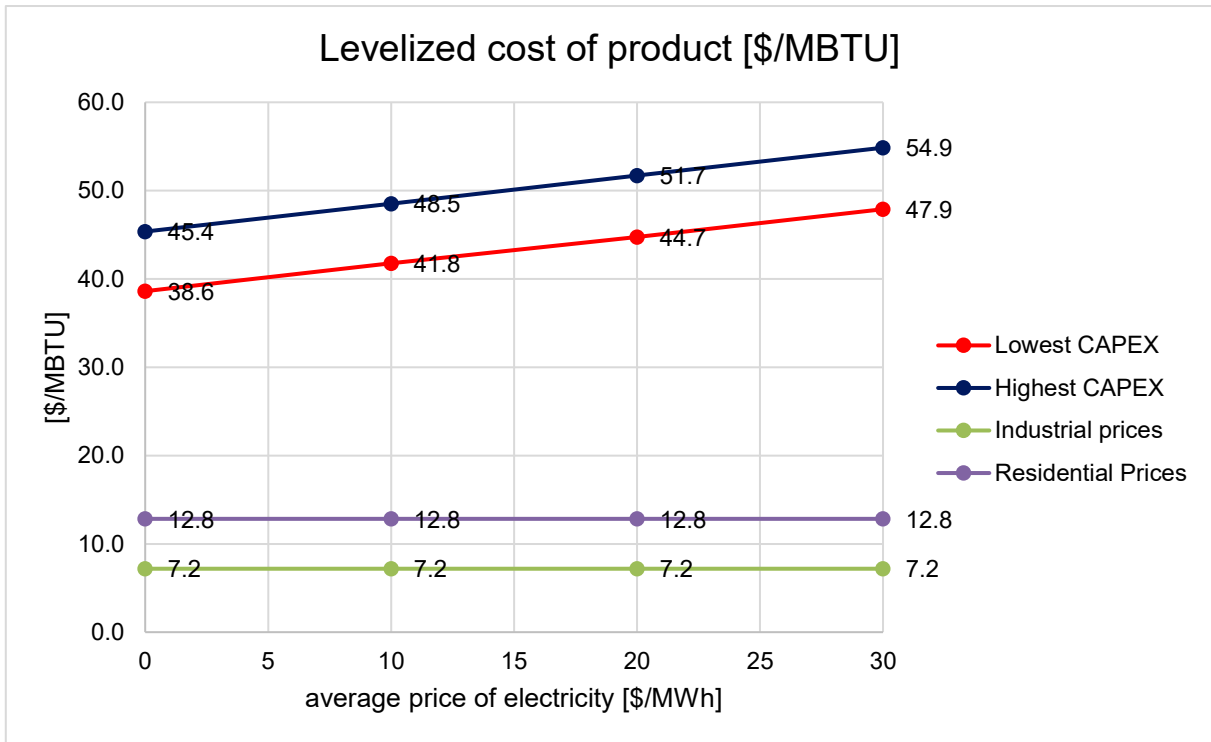


Figure 39 Levelized cost of product [\$/MBTU] as a function of the price of purchased electricity (for 50.000 SOEC systems/year) and 100 SOEC systems/year)

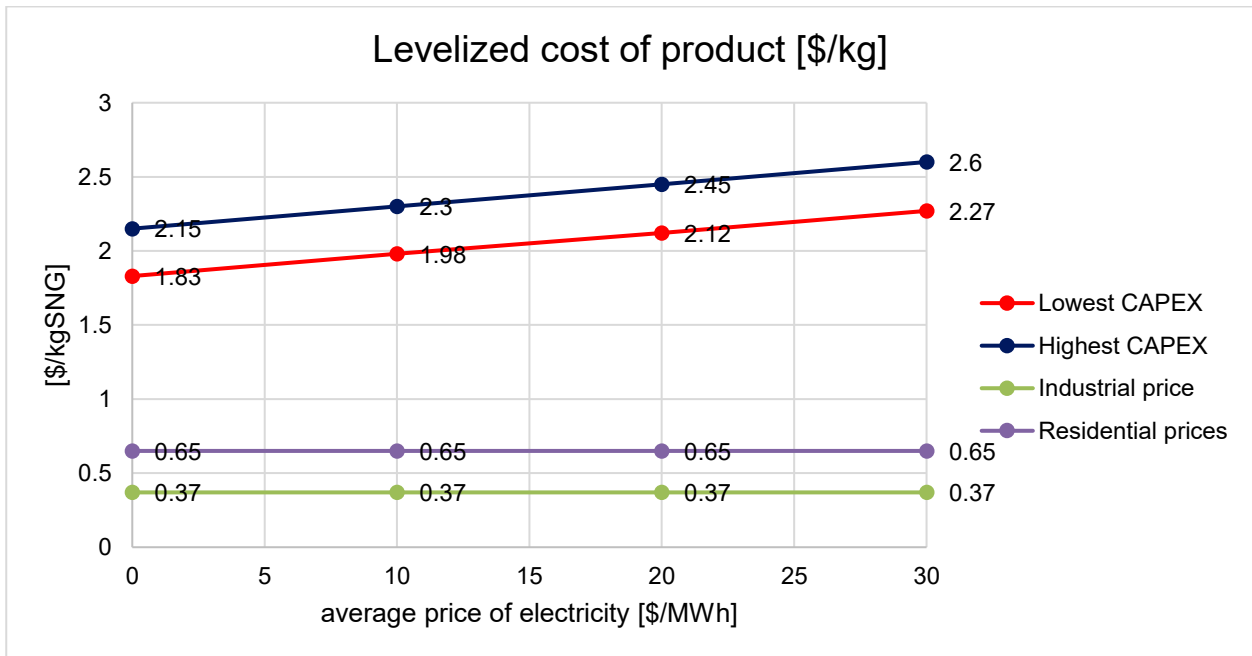


Figure 40 Levelized cost of product [\$/kg] as a function of the price of purchased electricity (for 50.000 SOEC systems/year) and 100 SOEC systems/year)

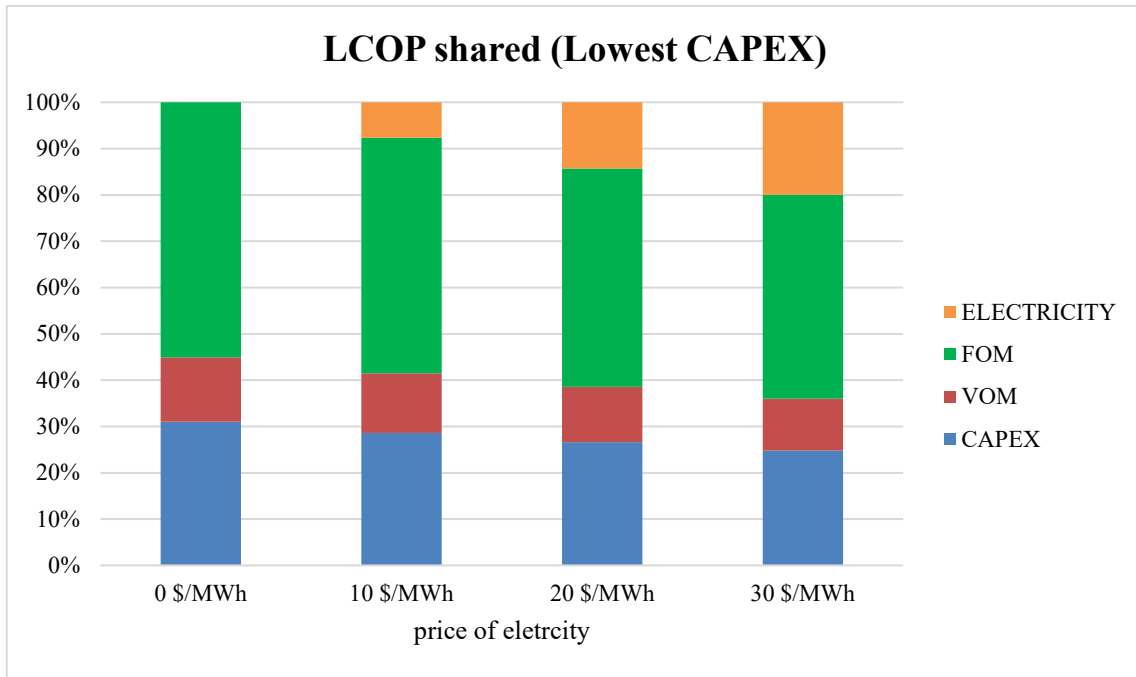


Figure 41 Cost of product shared for each category (case target SOEC annual manufacturing volume-50.000 systems/yr.)

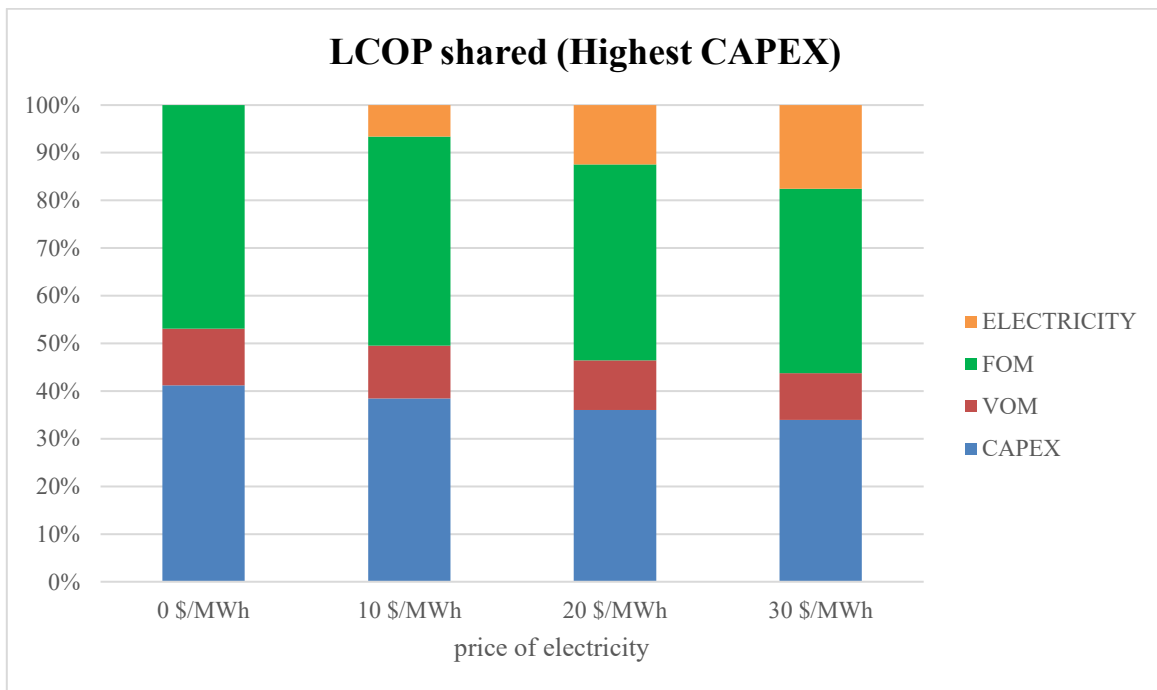


Figure 42 Cost of product shared for each category (case SOEC annual manufacturing volume-100 systems/yr.)

The Levelized Cost of Product (LCOP) is highly dependent on the price of the purchased electricity and the plant utilization factor. Increasing the working hours and/or the price of the electricity, the operational expenses keep growing depending more and more by the energy needs. At the same

time an increment of the capacity factor brings to higher production and respectively higher gains. If we want our plant be competitive in the market, an increment of the utilization factor together with a decrement in energy expenditure is necessary. Figure 39 displays the levelized cost of product as function of the average price of purchased electricity (0 \$/MWh – 30 \$/MWh). The plot shows also as LCOP changes as function of the initial investment. “Lowest CAPEX” is the capital cost assuming a SOEC volume of 50.000 systems/yr. while “ Highest CAPEX “ 100 systems/yr. Analyzing the price for NG in California, we observed a flat trend during the past years. The industrial and residential NG prices for 2017 (41) are respectively 7.2 \$/MBTU and 12.8 \$/MBTU, highlighting as to compete with the fossil NG, government incentives and further cost reductions (beyond the target values) are necessary.

A sensitivity analysis shows that a very high capacity factor (80%, 7008 h/yr.) and free electricity, are necessary to make the LCOP competitive with residential NG market prices in California. Otherwise, a CF higher than 80% together with very cheap prices of electricity would be needed.

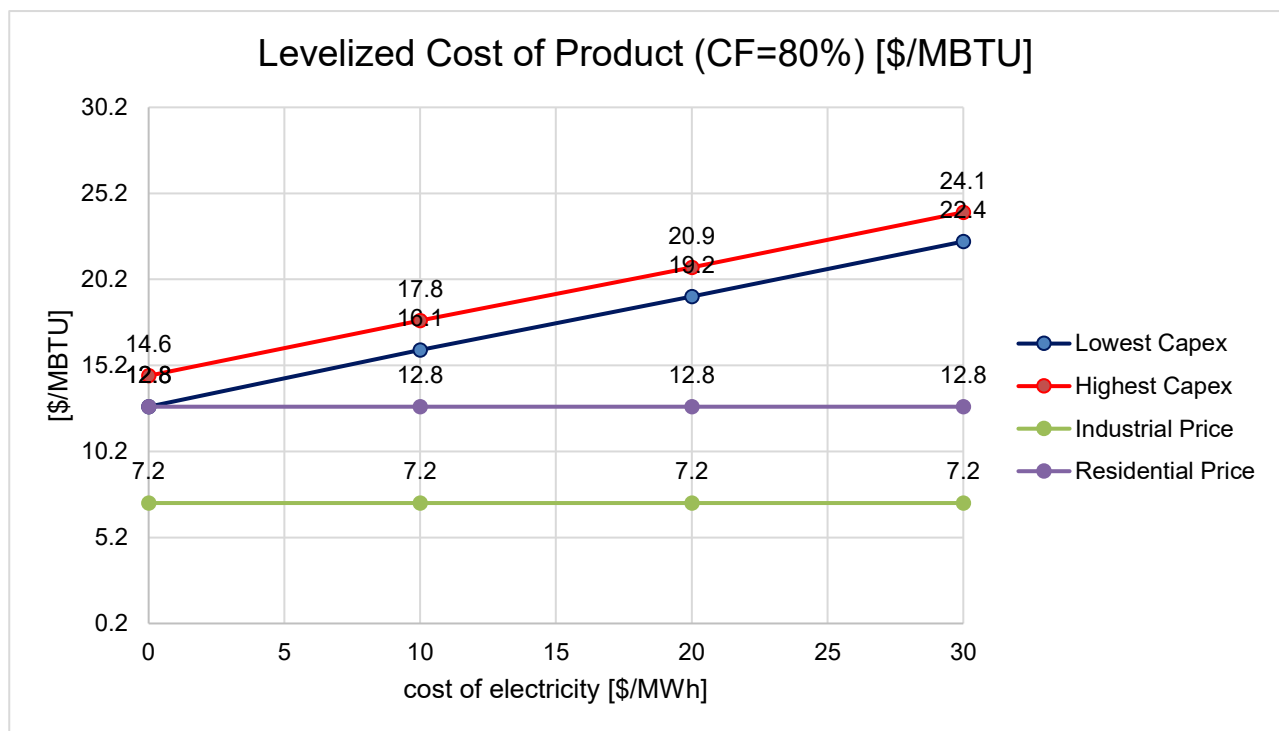


Figure 43 Sensitivity Analysis (CF=80%). Levelized cost of product [\$/MBTU] as a function of the price of purchased electricity (for 50.000 SOEC systems/year) and 100 SOEC systems/year)

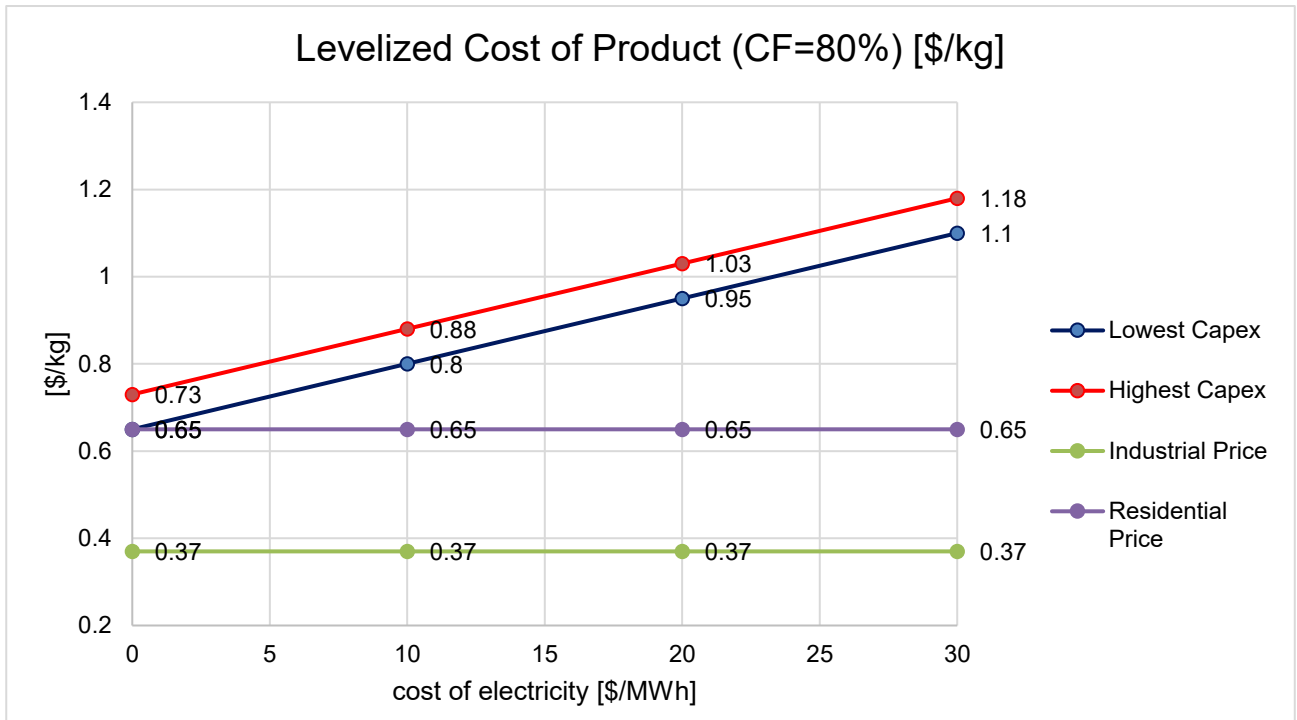


Figure 44 Sensitivity Analysis (CF=80%). Levelized cost of product [\$/kg] as a function of the price of purchased electricity (for 50,000 SOEC systems/year) and 100 SOEC systems/year)

## 5. Power to SNG in California

### 5.1 In-state natural gas demand

Although the considerable efforts of California for the implementation of clean technologies to meet the future climate targets, a highly dependence from natural gas has still been highlighted. In fact, one third of energy commodities consumed in California is NG. The market continues to evolve, and service options expand. Residential, commercial, industrial, and power generation sectors represent most of consumption. In addition, natural gas is a viable alternative to petroleum for use in cars, trucks, and buses. Alternative transportation-related vehicles are growing on consumers as well as the development of a safe, reliable refueling infrastructure.

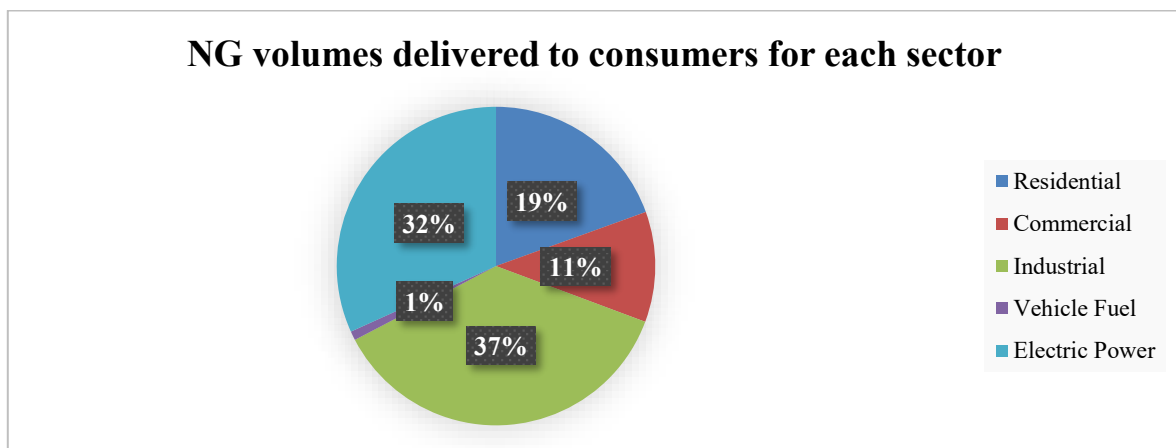


Figure 45 NG volumes delivered to consumers for each sector (2016) [Source: U.S. EIA]

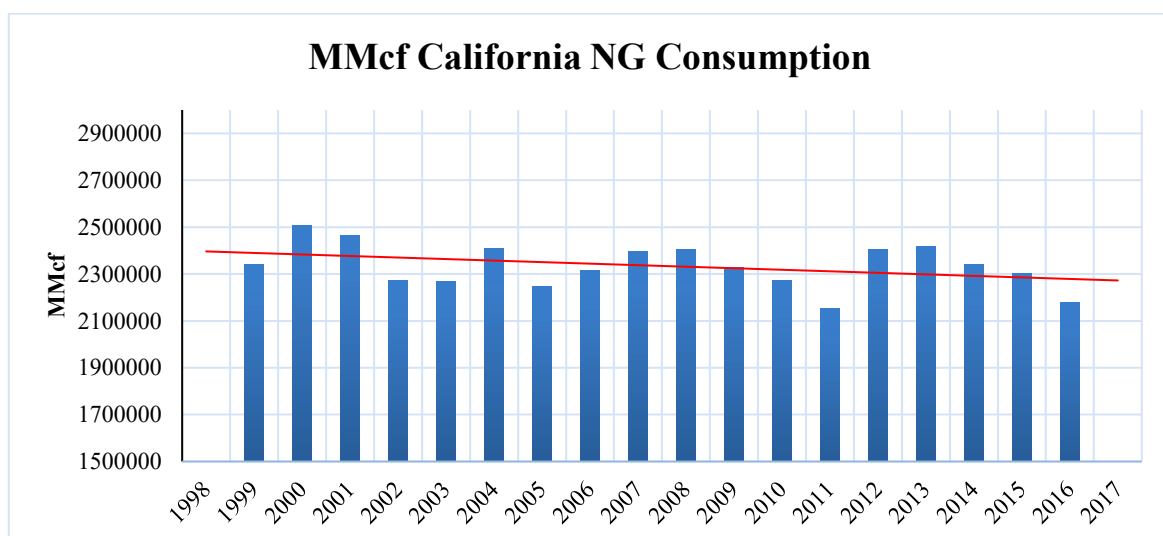


Figure 46 California natural gas consumption per 1997-2016,  $1 \text{ m}^3 = 35.3147 \text{ ft}^3$  [Source: U.S. EIA]

Despite the growth in population, with high efficiency technologies and implementation of low-carbon policies, in 2050 we assume a 100% reduction for power generation and a “frozen” consumption for residential, industrial and transportation sectors. With these hypotheses, the in-state future requirement of NG will be around 1.500.000 MMcf/yr. (-600.000/700.000 MMcf/yr. respect today demand) (42).

## 6.2 California curtailments and RES penetration

In April 2018, California solar and wind farms shut down or dialed back nearly 95,000 megawatt-hours of electricity, a new record, according to the California Independent System Operator, which manages the vast majority of the state’s electricity enough to power more than 30 million homes for an hour.

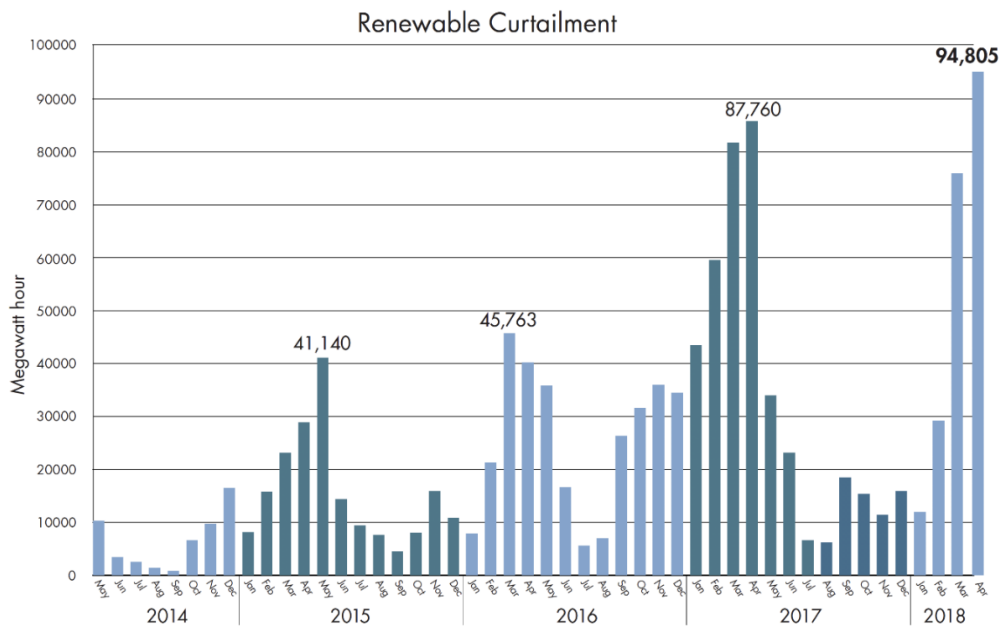


Figure 47 Curtailment totals by month (2016-2018) [CAISO]

This oversupply of solar is occurring because California has added vast amounts of renewable-energy generation in recent years, mainly to meet policy mandates requiring half the state’s electricity to come from carbon-free sources by 2030. With additional generation coming online in the next few years, the state is on pace to reach that target a decade ahead of schedule. This is excellent news for climate goals and reducing carbon emissions. But that success is also creating very real challenges, placing both economic and physical strains on the power system (43).

These limitations could discourage additional deployment of renewable energy, undermining broader efforts to overhaul the power sector. Indeed, this accounts partly for additional solar projects is already narrowing in California. Many regions and nations will experience similar growing pains as they ramp up renewable generation.

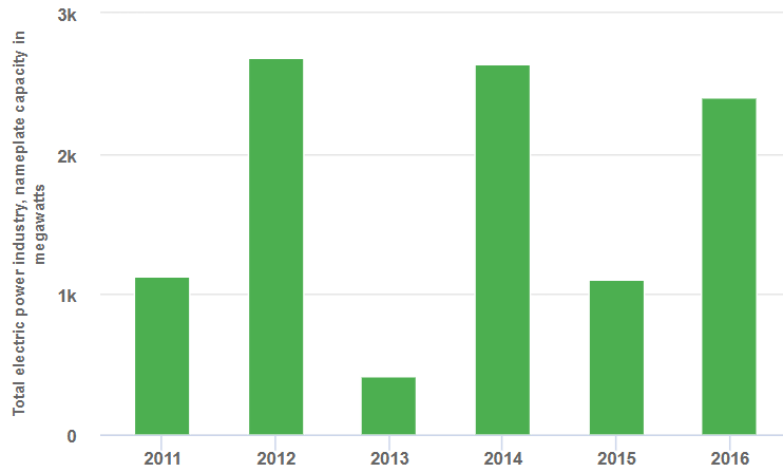


Figure 48 New clean and renewable energy capacity in California [Source: U.S. EIA]

California recently adopted rule requiring most new homes to include rooftop solar panels will further aggravate this issue, because it adds solar supply even as it reduces demand. As it stands, California’s system has limited ability to store that power, send it elsewhere. Significantly increasing the supply of renewable sources will place growing pressure on wholesale energy prices across the board, particularly squeezing the profits of inflexible generators like solar, wind, and nuclear. If solar provides 30 percent of the grid’s demands and wind supplies 10 percent, the prices for power from those sources will fall 39 percent in the New York market in 2030, and 27 percent in California.

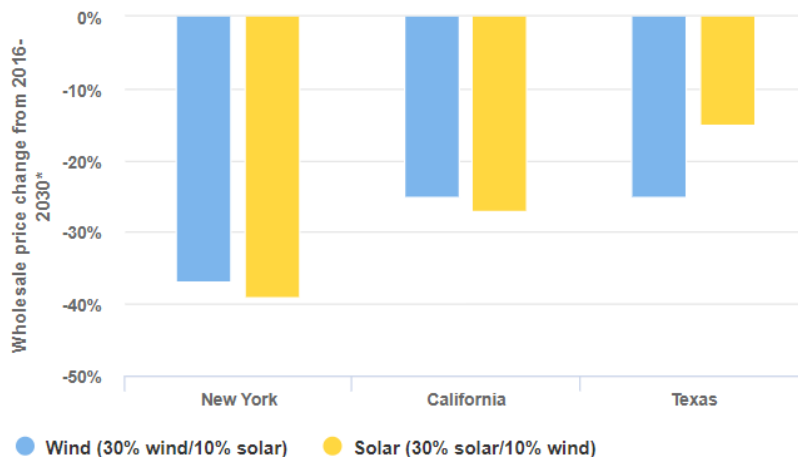


Figure 49 How increasing renewable penetration impacts wholesale electricity costs [Lawrence Berkeley National Laboratory]

### 5.3 Exploitation of oversupply for SNG generation

LBNL researches provide scenarios for the California future annual generation in 2030 (including curtailments). They assumed an aggressive increase in renewables, with a rump up of storage technologies and a rapidly falling in PV price.

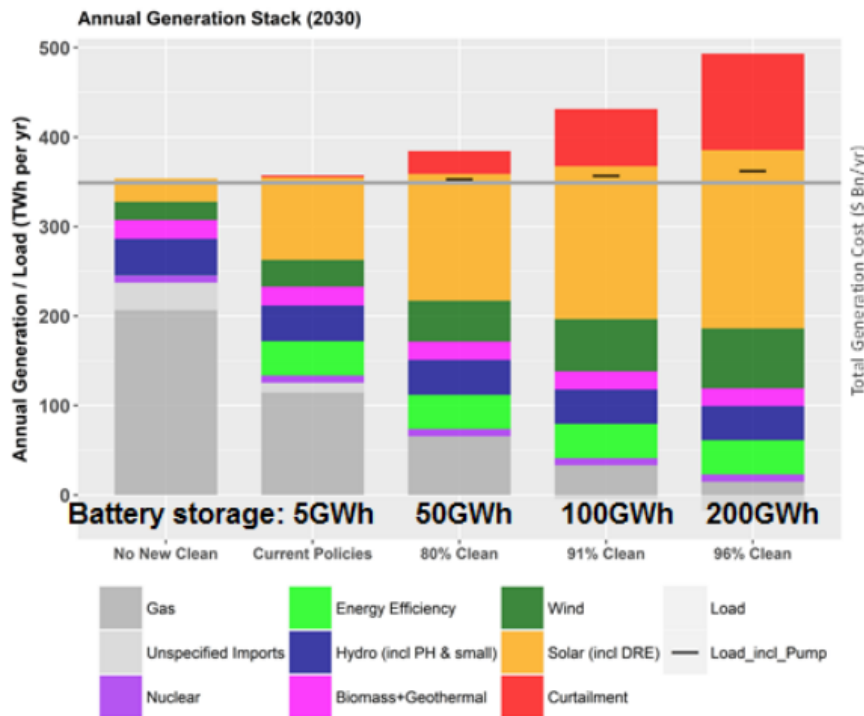


Figure 50 California scenario for future energy generation in 2030 [Wei et Al.]

In the more extreme case (96% clean), the curtailment in 2030 is 100 TWh/y. Taking this constant up to 2050, assuming to exploit all this energy as input in power to gas plants based on SOEC co-electrolysis and methanation, the SNG productivity can be calculated and compared to the NG demand. With reference to our model, the energy requirement previously calculated is 16.3 kWhel/kgSNG. The carbon dioxide and water requirement are respectively 2.72 kgCO<sub>2</sub>/kgSNG and 2.22 kgH<sub>2</sub>O/kgSNG. For the carbon source, in 2017 the California Air Resources Board estimates 411 million metric tons of CO<sub>2eq</sub> emission in the state. In accordance with the Executive Order S-3-05, we expect a 90% reduction in 2050, with total forecast emissions of 41 million metric tons. The cement industry for California accounts almost 8 million of metric ton of CO<sub>2eq</sub> emissions per year.

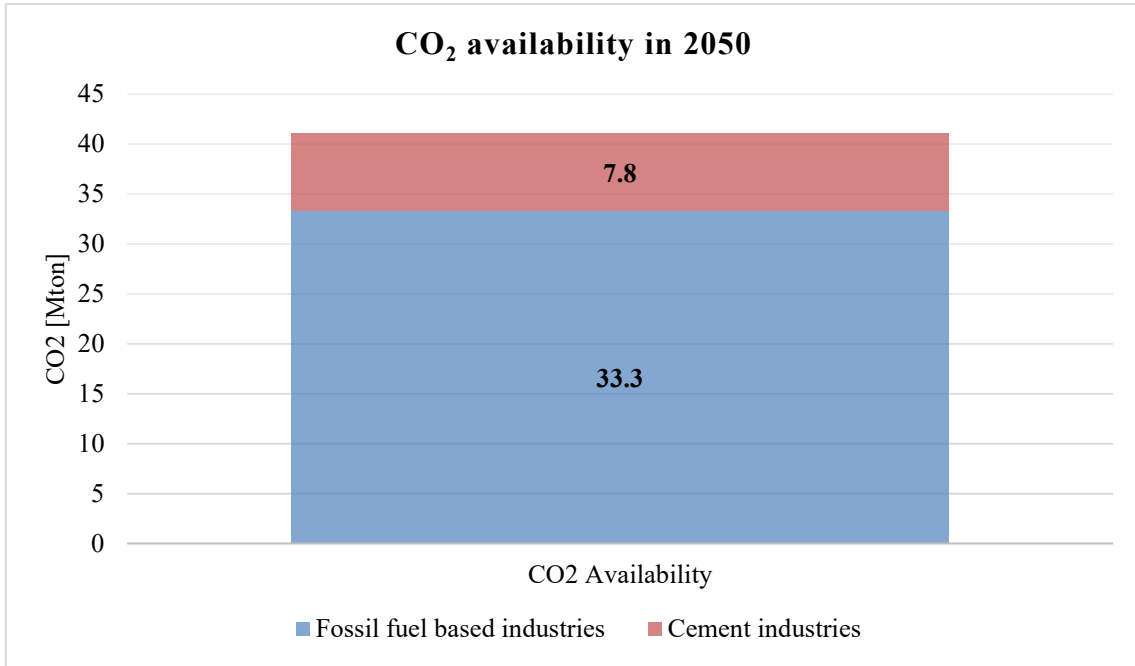


Figure 51 CO<sub>2</sub> availability in 2050

Table 33 Main assumptions for scenario in 2050

<b>Energy Input Availability [TWh/y]</b>	100
<b>H<sub>2</sub>O requirement [kgH<sub>2</sub>O/kgSNG]</b>	2.22
<b>CO<sub>2</sub> requirement [kgCO<sub>2</sub>/kgSNG]</b>	2.722

Table 34 Main output for scenario in 2050

<b>SNG productivity [Mton]</b>	6.1
<b>H<sub>2</sub>O requirement [Mton]</b>	13.6
<b>CO<sub>2</sub> requirement [Mton]</b>	16.7

Under the assumption of carbon capture and re-utilization system installations for both cement and fossil fuel based industries, the following results have been obtained:

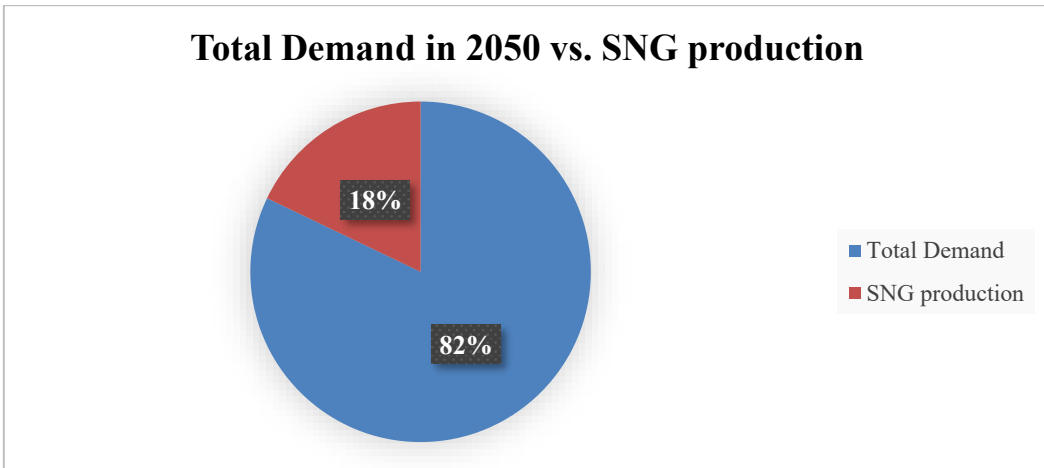


Figure 52 Main results for 2050 scenario, SNG offset of Total demand

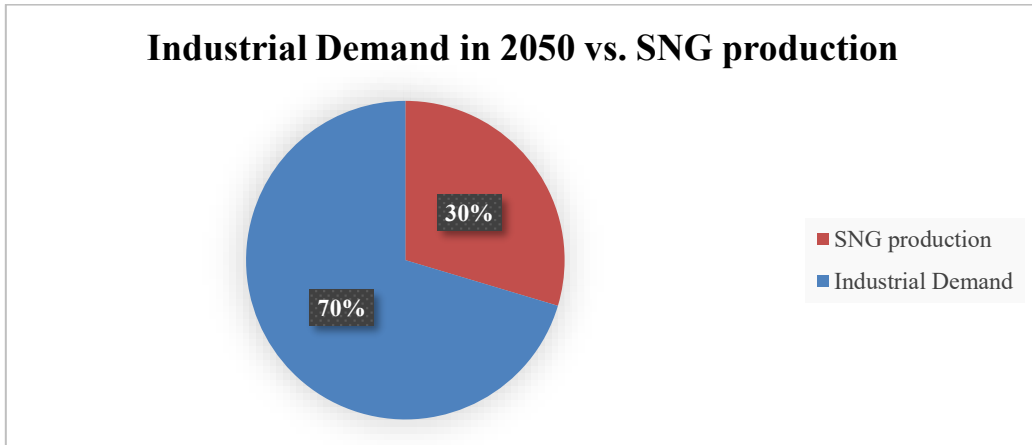


Figure 53 Main results for 2050 scenario, SNG offset of Industrial demand [if all SNG production is dedicated to this sector]

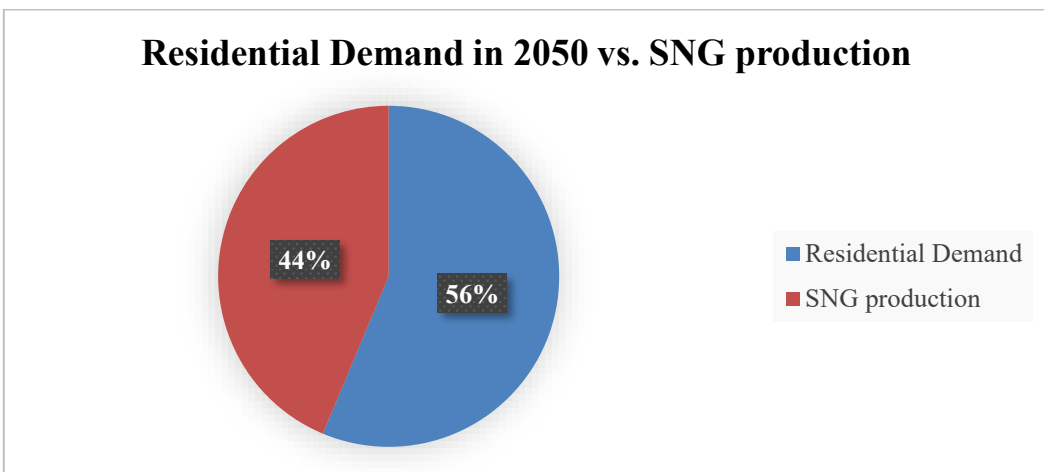


Figure 54 Main results for 2050 scenario, SNG offset of Residential demand [if all SNG production is dedicated to this sector]

The water needs could represent an issue, especially in desert areas or dry spell periods. A comparative analysis showed as is much more convenient, from a water consumption point of view, the SNG production via co-electrolysis respect than the shale gas one. This unconventional fuel is rapidly increasing as an available source of natural gas in the United States. Indeed, this country is the best producer of commercial shale gas in the world and it accounts almost for 40% on the overall gas supply (44).

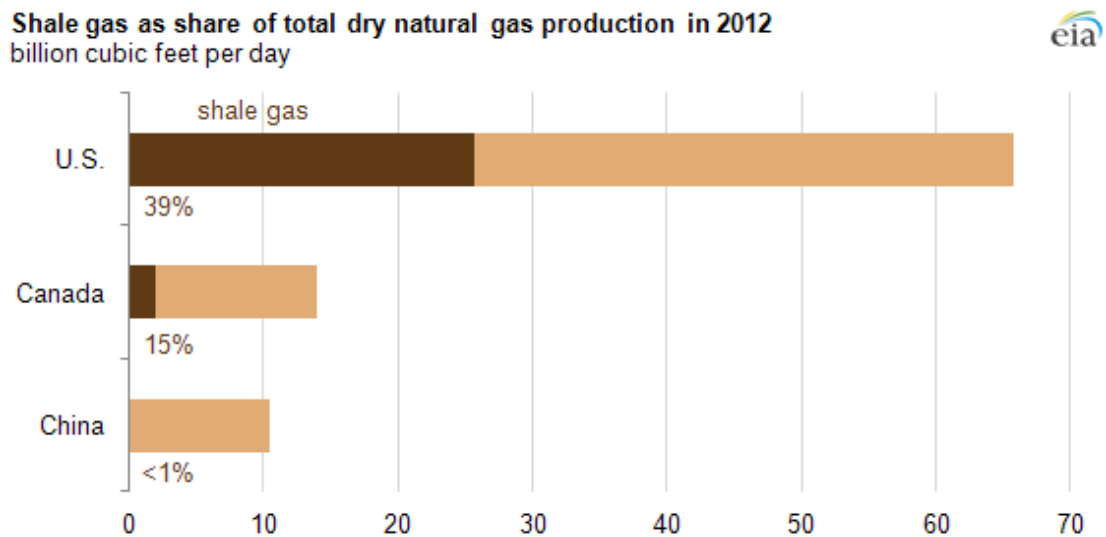


Figure 55 Shale gas as share of total dry NG production [Source: U.S. EIA]

Research (45) investigated the water needs for shale gas production. Considering all the processes involved, it accounts in average for  $10.41 \text{ l}_{\text{H}_2\text{O}}/\text{kg}_{\text{SHALEGAS}}$ , more than four times respect the electrochemical process of the developed model.

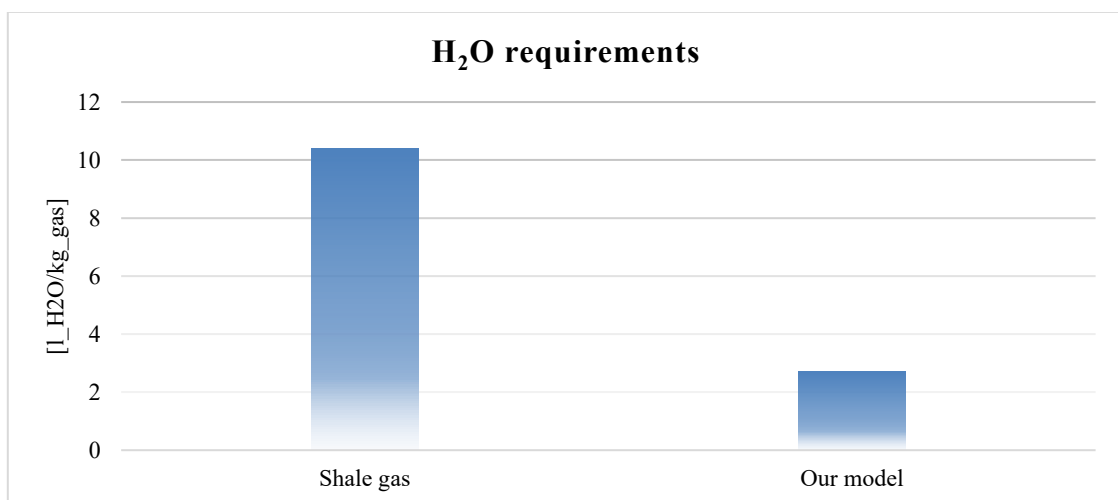


Figure 56 Water requirements: shale gas vs SNG

## 6. Conclusions

A plant for the production of synthetic natural gas using a solid oxide electrolyzer cell was designed and modeled meeting the quality requirements established in California for direct pipeline injection. The CO<sub>2</sub>, which together with H<sub>2</sub>O represents a key reactant in high temperature co-electrolysis, is recovered through carbon capture and re-utilization from the cement industry. A nearly perfectly matching thermal integration between the SOEC and the exothermic methanation section permits a minimization of the external energy requirement. In fact, the integrated process is characterized by an external input of 95 kW against an overall required thermal input of 663 kW by allowing an energy saving of 85.7% and bringing the overall plant efficiency from 53.7% to 80.6%. A detailed cost estimation of each plant section was provided, including an economical optimization of the heat exchanger network. The system cost based on CAPEX modeling was evaluated, showing a price between \$2000 and \$3000 per kW. Sensitivity analyses were performed to determine the synthetic natural gas LCOP with varying capacity factor and electricity input cost.

The reference case based on forecasts derived by CAISO (CF=20%) gives SNG prices at least 3 times more expensive respect the residential NG and 5 times respect the industrial NG. An increase of the CF up to 80% (with free electricity) or CF>80% (with very cheap electricity) is necessary to make the SNG cost equal to the residential NG market price in the state.

Despite might be difficult achieve these operating conditions, further researches and developments in SOEC technology could allow to reduce the investment cost with direct impact on the LCOP.

The implementation of this efficient storage system represents also an attractive method to achieve CO<sub>2</sub> reduction converting the exhaust carbon dioxide into working carbon, and could be a valuable assistance for renewable energy penetration and grid stabilization. The developed scenario for 2050 with the only exploitation of the otherwise curtailed power is estimated to meet almost 20% of the total in-state NG demand.

## References

1. 2011, U.S. Department of Energy. DOE/NETL. Cost Estimation Methodology for NETL Assessments of Power Plant Performance. Quality guidelines for energy system studies. [Online] 2011. <http://www.netl.doe.gov/energy-analyses/pubs/QGESSNETLCostEstMethod.pdf>.
2. Energy, U.S. Department of. DOE/NETL. Recommended Project Finance Structures for the Economic Analysis of Fossil-Based Energy Projects. [Online] 2011. <https://www.netl.doe.gov/energy-analyses/pubs/ProjFinanceStructures.pdf>.
3. Global CCS. Institute. Toward a common method of cost estimation for CO<sub>2</sub> capture and storage at fossil fuel power plants—CCS Costing Methods Task Force. [Online] 2013. <http://cdn.globalccsinstitute.com/sites/default/files/publications/85761/toward-common-method-cost-estimation-ccs-fossil-fuel-power-plants-white-paper.pdf>.
4. Agency, International Energy. IEA Greenhouse Gas R&D Programme. Criteria for technical and economic assessment of plants with low CO<sub>2</sub> emissions. Technical review. [Online] 2009. <http://cdn.globalccsinstitute.com/sites/default/files/publications/99086/criteria-technical-economic-assessment-plants-low-co2-emissions.pdf>.
5. EIA. [Online] <https://www.eia.gov/>.
6. Executive Order S-3-05. California Government, Office of Governor.
7. Syngastek. [Online] <http://syngastek.org/biocomposites/>.
8. J. Fuel Cell Sci. Technol. M. S. Sohal, J. E. O'Brien, C. M. Stoots, V. I. Sharma, B. Yildiz, A. Virkar. 2012.
9. Solid State Ionics. C. Graves, S. D. Ebbesen and M. Mogensen. 2011.
10. J. Electrochem. So. R. Knibbe, M. L. Traulsen, A. Hauch, S. D. Ebbesen and M. Mogensen. 2011.
11. Hydrogen Energy. X. Chen, L. Zhang, E. Liu and S. P. Jiang. 2011.
12. A. Hauch, S. D. Ebbesen, S. H. Jensen and M. Mogensen. 2008, J. Electrochem. Soc.
13. A. Hauch, S. H. Jensen, J. B. Bilde-Sorensen and M. Mogensen. 2007, J. Electrochem. Soc.
14. European Power to Gas. [Online] <http://europeanpowertogas.com/projects-in-europe/>.
15. CO<sub>2</sub> capture in the cement industry. D.J.Barker, S.A.Turnera, Napier-Moore, M. Clark, J.E.Davison. 2009.
16. [Online] [http://www.energy.ca.gov/maps/infrastructure/natural\\_gas.html](http://www.energy.ca.gov/maps/infrastructure/natural_gas.html).

17. [Online]  
(<https://www.arcgis.com/home/webmap/viewer.html?webmap=7213b586600e4ed1b468c5412aa6e502>).
18. CAISO, California Independent System Operator. [Online]  
[http://www.caiso.com/documents/jan22\\_2016explanationofdataassumptionsandanalyticalmet](http://www.caiso.com/documents/jan22_2016explanationofdataassumptionsandanalyticalmet).
19. Dynamis CO2 quality recommendations. E. de Visser, C. Hendriks, M. Barrio, M.J. Mølnvik, G. de Koeijer, S. Liljemark, Y. Le Gallo. 2008.
20. SoCalGas. [Online] <https://www.socalgas.com/regulatory/tariffs/tm2/pdf/30.pdf>.
21. SoCalGas. [Online] <https://www.socalgas.com/1443740736978/gas-quality-standards-one-sheet.pdf>.
22. TREMP, Haldor Topsøe. From solid fuels to Substitute Natural Gas (SNG) using. [Online]  
[http://www.topsoe.com/business\\_areas/gasification\\_based/](http://www.topsoe.com/business_areas/gasification_based/).
23. J. Jensen, J. Poulsen, N. Andersen,. From Coal to clean energy,Nitrogen+Syngas. [Online] 2011.  
[https://www.topsoe.com/business\\_areas/gasification\\_based/Processes/~~/media/PDF%20files/Gasification/topsoe\\_from\\_coal\\_to%20clean%20energy\\_nitrogen\\_syngas\\_march\\_april\\_2011.ashx](https://www.topsoe.com/business_areas/gasification_based/Processes/~~/media/PDF%20files/Gasification/topsoe_from_coal_to%20clean%20energy_nitrogen_syngas_march_april_2011.ashx).
24. Piovan, L. Progettare impianti a vapore. s.l. : Flaccovio Editore, 2010.
25. DOE/NETL. . Cost and Performance Baseline for Fossil Energy Plants. Volume 2:Coal to Synthetic natural Gas and Ammonia. Technical Report. [Online] [https://www.netl.doe.gov/energy-analyses/pubs/SNGAmmonia\\_FR\\_20110706.pdf](https://www.netl.doe.gov/energy-analyses/pubs/SNGAmmonia_FR_20110706.pdf).
26. Bell, K.J. Estimate S&T exchanger design fast,. s.l. : Oil Gas J. 4, 1978.
27. Fuel quality issues with biogas energy. An economic analysis for a stationary fuel cell system,. .D. Papadias, S. Ahmed, R. Kumar. s.l. : Energy 44 (2012) 257–277.
28. Kathryn E. Toghilla, Véronique Amstutz et Al. A dual circuit redox flow battery for hydrogen production. [Online] <http://nuweb9.neu.edu/mres/wp-content/uploads/2014/11/Kathryn-Toghill-presentation.pdf>.
29. [Online] <http://www.world-nuclear.org/information-library/facts-and-figures/heat-values-of-various-fuels.aspx>.
30. Renewable Power-to-Gas: A technological and economic review. Manuel Götz, Jonathan Lefebvre, Friedemann Mörs, AmyMcDaniel Kocha, Frank Graf. Siegfried Bajohr, Rainer Reimert, Thomas Kolbb. s.l. : Science Direct.
31. R. Turton, R. Bailie, W. Whiting, J. Shaeiwitz, D. Bhattacharyya. Analysis, Synthesis and Design of Chemical processes 4th ed. s.l. : Pearson Education International, 2013.
32. U.S. Department of Energy. A Total Cost of Ownership Model for Solid Oxide Fuel Cells in Combined Heat and Power and Power Only Applications. [Online]

[https://www.energy.gov/sites/prod/files/2016/06/f32/fcto\\_lbnl\\_total\\_cost\\_ownership\\_soft\\_systems.pdf](https://www.energy.gov/sites/prod/files/2016/06/f32/fcto_lbnl_total_cost_ownership_soft_systems.pdf).

33. U.S. Department of Energy. DOE/NETL. Cost and Performance Baseline for Fossil Energy Plants. Volume 2: Coal to Synthetic natural Gas and Ammonia. Technical Report. [Online] 2011. [https://www.netl.doe.gov/energy-analyses/pubs/SNGAmmonia\\_FR\\_20110706.pdf](https://www.netl.doe.gov/energy-analyses/pubs/SNGAmmonia_FR_20110706.pdf).

34. Energy, U.S. Department of. Analysis of integrated gasification fuel cell Plant Configurations. [Online] 2011. [https://www.netl.doe.gov/energy-analyses/pubs/IGFC\\_FR\\_20110225.pdf](https://www.netl.doe.gov/energy-analyses/pubs/IGFC_FR_20110225.pdf).

35. Syngas production via hightemperature co-electrolysis: an economic assesment. Q. Fu, C. Mabilat, M. Zahid, A. Brisse, L. Gautier. s.l. : Energy Environmental Science 3, 2010.

36. Production of Fischer–Tropsch liquid fuels from high temperature solid oxide co-electrolysis units. W.L. Becker, R.J. Brown, M. Penev, M. Melaina. s.l. : Energy 47, 2012.

37. Global CCS Institute. [Online] [https://hub.globalccsinstitute.com/publications/accelerating-uptake-ccs-industrial-use-captured-carbon-dioxide/2-co2-market#fnr\\_p02\\_001](https://hub.globalccsinstitute.com/publications/accelerating-uptake-ccs-industrial-use-captured-carbon-dioxide/2-co2-market#fnr_p02_001).

38. Consulting, SRI. Chemical Economics Handbook 2010. March 2010.

39. Sustainable hydrocarbon fuels by recycling CO<sub>2</sub> and H<sub>2</sub>O with renewable or nuclear energy. C. Graves, S. Ebbesen, M. Mogensen, K. Lackner. s.l. : Renewable Sustainable Energy Rev.15, 2011.

40. Topsoe, H2 Logic, Risø-DTU. Plan SOEC. R&D and commercialization roadmap for SOEC co eletrolysis. [Online] 2011. <http://www.hydrogenlink.net/download/reports/planSOEC-Report-May2011-FINAL.pdf>.

41. EIA. [Online] [https://www.eia.gov/dnav/ng/ng\\_pri\\_sum\\_dc\\_u\\_SCA\\_a.htm](https://www.eia.gov/dnav/ng/ng_pri_sum_dc_u_SCA_a.htm).

42. EIA. [Online] [https://www.eia.gov/dnav/ng/ng\\_cons\\_sum\\_dc\\_u\\_SCA\\_a.htm](https://www.eia.gov/dnav/ng/ng_cons_sum_dc_u_SCA_a.htm).

43. MIT. MIT Technology Review. [Online] [https://www.technologyreview.com/s/611188/california-is-throttling-back-record-levels-of-solarand-thats-bad-news-for-climate-goals/?utm\\_campaign=social\\_button&utm\\_source=facebook&utm\\_medium=social&utm\\_content=2018-07-22](https://www.technologyreview.com/s/611188/california-is-throttling-back-record-levels-of-solarand-thats-bad-news-for-climate-goals/?utm_campaign=social_button&utm_source=facebook&utm_medium=social&utm_content=2018-07-22).

44. EIA. [Online] <https://www.eia.gov/todayinenergy/detail.php?id=13491>.

45. Fractal characteristics of shales from a shale gas reservoir in the Sichuan Basin, China. Al., Yang et. 2014.

46. Government, California. [Online] <https://www.gov.ca.gov/news.php?id=18938>.

47. Al., Denholm et. Chart, Overgeneration from Solar Energy in California: A Field Guide to the Duck. [Online] 2015. <https://www.nrel.gov/docs/fy16osti/65023.pdf>.

48. Wordpress, Carbon Counter. [Online] <https://carboncounter.wordpress.com/2015/08/02/the-daily-cycle-of-wind-power-in-california/>.

49. Thermodynamic and economy analysis of solid oxide electrolyser system for syngas production. Al., Mahrokh Samavati et. 2017.
50. Stempien, Jen Powel. Fundamental aspects of solid oxide electrolyser cell modeling and the application for the system level analysis.
51. Hydrogen and synthetic fuel production using pressurized solid oxide electrolysis cells. S. Jensen, X. Sun, S. Ebbesen, R. Knibbe, M. Mogensen. s.l. : Int.J.Hydrogen Energy, 2010.
52. Berger, Ronald. Advancing Europe's energy systems: stationary fuel cell in distributed generation. A case study for the Fuel Cells and Hydrogen. [Online] 2015.  
[https://www.rolandberger.com/...pdf/roland\\_berger\\_fuel\\_cells\\_study\\_20150330.pdf](https://www.rolandberger.com/...pdf/roland_berger_fuel_cells_study_20150330.pdf).